



School of Civil Engineering and Surveying

Comparative Evaluation of the
In-Plane Shear Behaviour of
GFRP Composite Wall Systems
With and Without Window Openings

A dissertation submitted by

Saxon R. Xeros

In fulfilment of the requirement of

ENG4111/ENG4112 Research Project

Towards the degree of

Bachelor of Engineering (Honours) (Civil)

Submitted: October 2021

Abstract

The development of new construction methods and materials is of significant importance in the 21st Century, with the impacts of the construction industry on the environment, economy, and society a major issue. New construction methods such as modular construction may help to reduce these impacts, and research into alternative materials is also required to address the limitations of traditional building materials such as steel, concrete, and timber. Glass fibre reinforced polymer (GFRP) is a light-weight, strong, and durable material that is gaining interest in the construction industry as an alternative building material, and has high potential for use in modular construction. With advances in manufacturing of GFRP products, development of new structural systems is possible, including load bearing wall systems.

The objective of this study was to investigate the effect of sheathing and window openings on the in-plane shear behaviour of a GFRP wall system consisting of pultruded rectangular hollow section GFRP frame members with GFRP sheathing on each side, attached to the frame with structural adhesive. The hold-down arrangement consists of two M20 bolts passing through the bottom plate, with mechanical inserts. Three panels were subjected to in-plane shear loading until failure, with the panels being frame only, fully sheathed, and sheathed with a window opening. The deflection, failure, and strain behaviour was observed and analysed to assess the effects of sheathing and the presence of a window opening. A parametric study using finite element analysis (FEA) was then undertaken in Strand7, investigating how opening size affects the in-plane shear behaviour of the wall system.

The experimental and FEA results showed that sheathing added substantial stiffness to the wall system, and that openings resulted in stiffness reduction approximately proportional to the opening size. Failure of both sheathed panels was by splitting of the bottom plate at the hold-down. It was confirmed using FEA that opening size did not affect the load on the hold-down, and therefore in terms of strength, failure at the hold-down is unaffected by opening size. Other potential failure modes were explored, showing that for failure due to cracking at the corners of the opening occurs, larger openings result in a decrease in strength. These other failure modes also indicated the potential of significantly higher strengths than the hold-down failure mode observed in the experiment. It was also found that the presence and size of openings affects the development of stresses in the sheathing and affects the stress distribution in the vertical, compression stud, which may increase the potential for other failure modes.

Limitations of Use

University of Southern Queensland

School of Civil Engineering and Surveying

ENG4111/ENG4112 Research Project

Limitations of Use

The Council of the University of Southern Queensland, its School of Civil Engineering and Surveying, and the staff of the University of Southern Queensland, do not accept any responsibility for the truth, accuracy or completeness of material contained within or associated with this dissertation.

Persons using all or any part of this material do so at their own risk, and not at the risk of the Council of the University of Southern Queensland, its School of Civil Engineering and Surveying or the staff of the University of Southern Queensland.

This dissertation reports an educational exercise and has no purpose or validity beyond this exercise. The sole purpose of the course pair entitled “Research Project” is to contribute to the overall education within the student’s chosen degree program. This document, the associated hardware, software, drawings, and other material set out in the associated appendices should not be used for any other purpose: if they are so used, it is entirely at the risk of the user.

Certification of Dissertation

University of Southern Queensland

School of Civil Engineering and Surveying

ENG4111/ENG4112 Research Project

Certification of Dissertation

I certify that the ideas, designs and experimental work, finite element models, results, analyses, and conclusions set out in this dissertation are entirely my own effort, except where otherwise indicated and acknowledged.

I further certify that the work is original and has not been previously submitted for assessment in any other course or institution, except where specifically stated.

S.R.Xeros



Acknowledgments

I would like to give acknowledgement and thanks to all those who have contributed and helped me in completing both this project and my degree.

I thank my supervisor Professor Allan Manalo for the opportunity to work on this project, and for his guidance, support, and sharing of his expertise along the way.

I would also like to thank Mr. Arvind Sharda for this support and time spent discussing the project and answering my questions.

I thank Wagners Composite Technologies for provision of the specimens tested in this project.

I thank my employers for supporting me throughout the degree and giving me access to many resources and providing time for me to complete my study.

I also thank my colleagues, and in particular my manager, who has given many hours of his time throughout my degree to discuss ideas and helped me to learn a great deal that I otherwise may not have. These discussions have often been the highlights of my learning whilst studying.

I thank my friends who have given encouragement and support throughout my degree.

My family has been absolutely vital for me being able to complete both this project and degree, and I thank them for their love and support.

Finally, and most of all, I thank my wife Rhiannon for her love, belief, and support, for providing encouragement, gifts, and surprises to keep me motivated, for sacrificing so much time to allow me to study, for enduring through the difficult and trying times, and for being an unchanging and constant companion.

Contents

Abstract.....	i
Limitations of Use	ii
Certification of Dissertation.....	iii
Acknowledgments	iv
Contents	v
List of Figures.....	ix
List of Tables	xiii
Chapter 1 Introduction.....	1
1.1 Background and Problem Definition	1
1.2 Research Significance	3
1.3 Project Aims and Objectives	3
1.4 Expected Outcomes and Benefits.....	4
1.5 Limitations of Research.....	4
1.6 Structure of Dissertation	5
1.7 Summary.....	6
Chapter 2 Literature Review	7
2.1 Introduction.....	7
2.2 Importance of New Construction Technologies and Materials	7
2.3 Glass Fibre Reinforced Polymers	9
2.3.1 Overview.....	9
2.3.2 Beneficial Properties of GFRP.....	10
2.3.3 Applications of FRP in Civil Engineering	12
2.4 Light-Weight Shear Walls.....	14
2.4.1 Overview.....	14

2.4.2	Typical Light-Weight Shear Wall Materials and Construction	15
2.4.3	Typical In-Plane Shear Behaviour of Sheathed Shear Walls	15
2.5	Previous Research of Shear Walls	16
2.5.1	Shear Wall Materials	17
2.5.2	In-Plane Shear Test Methodology	17
2.5.3	Failure Modes of Shear Walls	21
2.5.4	Factors Affecting Shear Wall Strength and Stiffness	24
2.6	Finite Element Modelling of Shear Walls	27
2.6.1	Overview	27
2.6.2	Previous Modelling	28
2.6.3	Model Validation	30
2.7	Research Gap	30
Chapter 3	Experimental Methodology	32
3.1	Introduction	32
3.2	Specimen Details	32
3.2.1	General	32
3.2.2	Panel Naming Convention	32
3.2.3	Specimen Configurations	33
3.2.4	Specimen Preparation	35
3.3	Material and Section Properties	37
3.3.1	Pultruded GFRP RHS	37
3.3.2	GFRP Sheathing	39
3.3.3	GFRP Mechanical Bolt Insert	40
3.3.4	Structural Epoxy Adhesive	41
3.3.5	Bolts, Washers, Angle Brackets, and Rivets	41
3.4	Experimental Test Setup and Procedure	42
3.4.1	Setup and Instrumentation	42
3.4.2	Procedure	43
3.5	Project Safety and Timeline	44

3.6	Summary	44
Chapter 4 Experimental Results and Discussion45		
4.1	Introduction	45
4.2	Results and Observations	46
4.2.1	Panel FE – Frame Only Panel.....	46
4.2.2	Panel FSE – Fully Sheathed Panel.....	48
4.2.3	Panel FSO _{37.5E} – Sheathed with Window Opening.....	54
4.3	Analysis and Discussion	64
4.3.1	Introduction.....	64
4.3.2	Effect of Sheathing and Openings on In-Plane Shear Stiffness.....	64
4.3.3	Effect of Openings on In-Plane Shear Deflection Behaviour.....	66
4.3.4	Effect of Sheathing and Openings on Failure Behaviour and Strength.....	67
4.3.5	Effect of Sheathing and Openings on In-Plane Shear Ductility.....	71
4.3.6	Effect of Sheathing and Openings on Load-Strain Behaviour.....	72
4.4	Summary	73
Chapter 5 Finite Element Analysis and Parametric Investigation75		
5.1	Introduction	75
5.1.1	Strand7 Software.....	75
5.1.2	Linear Elastic Analysis.....	75
5.2	FEA and Parametric Investigation Methodology	75
5.3	Panel Naming Convention	76
5.4	Model Development	77
5.4.1	General.....	77
5.4.2	Frame Members.....	77
5.4.3	Hold-Down Bolts and Inserts.....	80
5.4.4	Angle Brackets and Rivets.....	82
5.4.5	Sheathing.....	83
5.4.6	Supports and Boundary Conditions.....	85
5.4.7	Applied Loads.....	85

5.5	Model Refinement	86
5.6	Model Validation and Results	88
5.6.1	General.....	88
5.6.2	Panels FE and FFE.....	89
5.6.3	Panels FSE and FSFE.....	91
5.6.4	Panels FSO _{37.5} E and FSO _{37.5} FE.....	94
5.7	Parametric Investigation	96
5.7.1	General.....	96
5.7.2	Panel Configurations.....	96
5.7.3	Effect of Opening Size on In-Plane Shear Stiffness.....	97
5.7.4	Effect of Openings on Hold-Down Reactions and Stress Concentrations.....	98
5.7.5	Effect of Opening Size on the Development of Stress Concentrations and Possible Alternate Failure Modes.....	99
5.7.6	Effect of Opening Size on Sheathing Tensile Stresses.....	104
5.7.7	Effect of Openings on Compression Stud Stresses.....	107
5.8	Summary	109
Chapter 6	Conclusions and Recommendations	111
6.1	Conclusions	111
6.1.1	Overview.....	111
6.1.2	Experimental Investigation of In-Plane Shear Behaviour.....	111
6.1.3	FEA Investigation of In-Plane Shear Behaviour.....	112
6.1.4	General Conclusions.....	113
6.2	Recommendations for Further Research	113
	References	116
	Appendix A: Project Specification	127
	Appendix B: Risk Assessment	128
	Appendix C: Project Timeline	131

List of Figures

Figure 2-1: Visual representation of a basic FRP (Shakir Abbood et al. 2021).....	10
Figure 2-2: Typical forces acting on and within a shear wall (Grossi, Sartori & Tomasi 2015b)	16
Figure 2-3: Typical deflection and deformation of a shear wall, including (a) rotation and uplift, (b) translation, and (c) shear (Casagrande et al. 2016)	16
Figure 2-4: In-plane shear test setup from ASTM E564-06 (ASTM International 2006)	19
Figure 2-5: (a) Nail pull-out of stud from bottom plate (Branco, Matos & Lourenço 2017) and (b) compression stud buckling (Branston, Chen, et al. 2006).....	22
Figure 2-6: Sheathing failure modes: (a) Diagonal tension crack in sheathing, and (b) buckling of compression stud (Manalo 2013).....	22
Figure 2-7: (a) Fastener edge pull out (Lafontaine et al. 2017) and (b) out-of-plane sheathing buckling (Grossi, Sartori & Tomasi 2015a).....	23
Figure 2-8: Influence of opening size on shear stiffness and strength for X-lam walls (Dujic et al. 2009)	25
Figure 3-1: Drawing of experimental panels and base connection detail	34
Figure 3-2: SS angle bracket and rivets	34
Figure 3-3: (a) Mechanical bolt insert (Wagners CFT Manufacturing Pty Ltd 2016) and (b) rectangular washers at hold-down nut	35
Figure 3-4: (a) Strain gauge on stud and (b) strain gauges on sheathing	36
Figure 3-5: Strain gauge and load application locations	36
Figure 3-6: Dye on panel for DIC camera	37
Figure 3-7: RHS dimensions and section properties (Wagners 2021).....	38
Figure 3-8: (a) Fibre stacking sequence for the pultruded GFRP RHS profiles (Hizam et al. 2019) and (b) typical pultruded GFRP sections produced by WCFT (Wagners CFT Manufacturing Pty Ltd 2016)	38
Figure 3-9: Images of (a) the overall test setup, (b) a panel attached to the support beam, (c) the hydraulic jack and load cell, and (d) the string pot for measuring horizontal deflection.....	43
Figure 4-1: Load application locations	45
Figure 4-2: Load-deflection behaviour of panel FE.....	46
Figure 4-3: (a)-(b) Deformed shape of panel FE during and after loading, and (c)-(d) opening of joint between vertical stud and bottom plate and top plate	47
Figure 4-4: Load and strain behaviour of panel FE	48
Figure 4-5: Panel FSE installed in testing frame	49

Figure 4-6: Load and horizontal deflection behaviour at top of panel FSE.....	50
Figure 4-7: Failure of the RHS bottom plate at left-hand hold down, with (a)-(b) longitudinal splitting, (c) bending deformation, and (d) gapping between bottom plate and vertical stud, for panel FSE.....	51
Figure 4-8: Additional failure mechanisms at left-hand hold-down include (a) slight washer embedment and (b) failure of the insert, for panel FSE	52
Figure 4-9: Cracking and slight gapping of the right-hand hold-down insert, for panel FSE.....	52
Figure 4-10: Minor crushing of right-hand vertical stud, for panel FSE	53
Figure 4-11: Load and strain behaviour of panel FSE	54
Figure 4-12: (a) Global deflection and (b) uplift of panel FSO _{37.5E}	55
Figure 4-13: Load and horizontal deflection behaviour at top of panel FSO _{37.5E}	56
Figure 4-14: Points of measurement by DIC camera of deflection of opening corners.....	56
Figure 4-15: Load and horizontal deflection behaviour at the corners of the opening and top of panel FSO _{37.5E}	57
Figure 4-16: Load and vertical deflection behaviour of opening corners of panel FSO _{37.5E}	59
Figure 4-17: Failure of the RHS bottom plate at left-hand hold down, with (a)-(b) longitudinal splitting, (c) bending deformation, and (d) gapping between bottom plate and vertical stud, for panel FSO _{37.5E}	60
Figure 4-18: Deformation of the bottom wall of bottom plate was higher on side of loading, visible both (a) during and (b) after loading, for panel FSO _{37.5E}	60
Figure 4-19: Failure mechanisms at left-hand side hold-down included (a) washer failure and (b) insert failure, for panel FSO _{37.5E}	61
Figure 4-20: (a) Minor cracking of the right-hand hold-down insert and (b) minor crushing at base of right-hand vertical stud, for panel FSO _{37.5E}	61
Figure 4-21: Load and strain behaviour of panel FSO _{37.5E}	63
Figure 4-22: Load and strain behaviour of sheathing of panel FSO _{37.5E}	63
Figure 4-23: Global stiffnesses of experimental panels	65
Figure 4-24: Behaviour of a theoretical panel in (a) pure in-plane shear deformation and (b) pure clockwise rotation	66
Figure 4-25: Deformed shape of panel FSO _{37.5E} opening at various loads	67
Figure 4-26: Consistent failure mode of splitting of bottom plate for panels (a) FSE and (b) FSO _{37.5E}	69
Figure 4-27: Rigid bottom plate hold-down reaction theory, indicating linearly proportional loads on left and right-hand hold-downs	71
Figure 4-28: Combined frame load-strain behaviour for sheathed panels	72
Figure 4-29: Combined sheathing load-strain behaviour for sheathed panels	73
Figure 5-1: Frame material properties in Strand7	78
Figure 5-2: Image of (a) full frame and (b) gap between vertical and horizontal members in Strand7	78

Figure 5-3: Point Contact Type 1 property sheet	79
Figure 5-4: Images showing (a) the location of frame-to-frame Point Contacts and (b) joint deformation at this location	79
Figure 5-5: Hold-down bolt properties in Strand7	80
Figure 5-6: Point Contact Type 2 property sheet	81
Figure 5-7: Images of (a) the bottom wall of RHS to bolt shank Point Contact and (b) top wall and washer Point Contacts in Strand7	81
Figure 5-8: Mechanical bolt insert material properties in Strand7	82
Figure 5-9: Bolt insert Point Contact (a) property sheet and (b) image of Point Contacts on insert	82
Figure 5-10: Property sheets for (a) SS angle bracket and (b) aluminium rivets in Strand7	83
Figure 5-11: Angle bracket attachment and Point Contacts	83
Figure 5-12: Sheathing material properties in Strand7	84
Figure 5-13: Sheathing-to-frame connection and sheathing offset in Strand7	84
Figure 5-14: FEM support conditions in Strand7	85
Figure 5-15: Applied load and insert	86
Figure 5-16: Refined mesh locations for frame members at (a) the hold-downs and (b) joint between top plate and stud	87
Figure 5-17: Refined mesh locations for frame and sheathing	88
Figure 5-18: Joint deformation of panel FFE, noting moment connection behaviour of top left and pinned connection behaviour at top right	90
Figure 5-19: Stress concentrations at angle bracket in both (a) tension and (b) compression indicating possible yielding of the bracket	90
Figure 5-20: Uplift along base and deformation of bottom plate at hold-down of panel FSFE	92
Figure 5-21: RHS wall deflection at the hold-down in Strand7	92
Figure 5-22: Transverse stress concentrations on the underside of the bottom plate at the left-hand hold-down on both the (a) outer surface and (b) inner surface, indicating likely failure of RHS bottom plate, for Panel FSFE	93
Figure 5-23: Deformed shape of panel FSO ₃₇ FE (with five times exaggeration)	95
Figure 5-24: Transverse stress concentrations on the underside of the bottom plate at the left-hand hold-down on both the (a) outer surface and (b) inner surface, indicating likely failure of RHS bottom plate, for Panel FSO ₃₇ FE	95
Figure 5-25: Drawings of panels used in parametric investigation	97
Figure 5-26: Relationship between opening size and normalised global stiffness	98
Figure 5-27: Possible alternate failure modes shown in FEM, including (a) longitudinal tension failure at the left hold down, (b) longitudinal compression failure at the base of the right stud, and (c) shear failure at the top corners of the opening	102
Figure 5-28: Graph of loads at onset of potential failure modes	103

Figure 5-29: Sheathing tensile stress distribution and plot along diagonal for panels (a)-(b) FSO _{12.5} FE, (c)-(d) FSO ₂₅ FE, (e)-(f) FSO _{37.5} FE, (g)-(h) FSO ₅₀ FE, and (i)-(j) FSO _{56.25} FE	107
Figure 5-30: Stress distribution within right-hand compression stud on both outer and inner walls of the RHS, for panels (a) FSE-5.5, (b) FSO _{12.5} FE, (c) FSO ₂₅ FE, (d) FSO _{37.5} FE, (e) FSO ₅₀ FE, and (f) FSO _{56.25} FE.....	108

List of Tables

Table 3-1: Experimental panel naming convention	32
Table 3-2: Mechanical properties of the GFRP RHS profile	39
Table 3-3: Mechanical properties of GFRP sheathing	40
Table 3-4: Techniglu-HP R26 epoxy adhesive mechanical properties (Manalo & Aravinthan 2012).....	41
Table 3-5: M20 class 8.8 SS bolt properties (Hizam et al. 2019)	41
Table 3-6: SS angle bracket and washer material properties	41
Table 4-1: Global stiffnesses of experimental panels	65
Table 4-2: Ductility ratio of experimental panels	72
Table 5-1: FEM panel naming convention	76
Table 5-2: Applied load pressures for FEM.....	86
Table 5-3: Comparison of FEA results and experimental data for panels FE and FFE.....	89
Table 5-4: Comparison of FEA results and experimental data for panels FSE and FSFE	91
Table 5-5: Comparison of FEA results and experimental data for panels FSO _{37.5} E and FS O _{37.5} FE....	94
Table 5-6: FEM panel naming convention for parametric study	97
Table 5-7: Deflection and calculated global stiffness of all panels with an applied load of 5.5 kN.....	98
Table 5-8: Hold-down reactions for all panels with an applied load of 5.5 kN	99
Table 5-9: Loads at onset of possible alternate failure modes	103

Chapter 1 Introduction

1.1 Background and Problem Definition

Owing to its large consumption of resources, production of waste, and subsequent impacts on the environment (Ajayi et al. 2015), the construction industry is faced with a range of challenges in the 21st Century. The social impacts of construction-related activities are also considerable, including health risks and disruption to services (Mara, Haghani & Harryson 2014; Wang et al. 2016). In addition, construction projects are demanding economically, particularly the rehabilitation or renewal of existing infrastructure that is no longer serviceable (Mara, Haghani & Harryson 2014; Wang et al. 2016). With some experts suggesting over-population is imminent (Dovers & Butler 2015) as the population continues to grow, these challenges are of increasing concern. To address some of these challenges, new technologies such as modular construction are being developed to reduce the negative environmental, social and economic impacts of construction (Tam et al. 2007; Mao et al. 2013; Cao et al. 2015; El-Abidi & Ghazali 2015; Asamoah et al. 2016). Traditional materials such as timber, concrete, and steel show limitations in addressing the challenges faced, particularly their weight and lack of durability due to rot and corrosion. The development of new construction materials is therefore considered of significant interest, with the potential to address some challenges that may otherwise remain unresolved.

Fibre reinforced polymers (FRP) are a class of composite materials in which extremely strong fibres, such as glass or carbon, are combined with a polymer matrix to form a very strong, light, and durable material (Gand, Chan & Mottram 2013). Of these, glass fibre reinforced polymer (GFRP) is particularly attractive due to a strength-to-weight ratio far greater than steel (Gand, Chan & Mottram 2013; Wagners CFT Manufacturing Pty Ltd 2016; Ahmed et al. 2020) and a relatively low cost when compared to other fibres such as carbon, basalt and Aramid. Being non-corrosive and durable in many environments, it requires little maintenance and has a long potential service life (Wang et al. 2015). It is also electromagnetically neutral, an advantageous property in the electrical, imaging, and computer industries (Bakis et al. 2002). GFRPs are also very versatile through the various manufacturing processes by which they can be made and by the adjustability of their constituents and properties (Van Den Einde, Zhao & Seible 2003). It is noted that FRP materials have some potential challenges, such

as high cost, susceptibility to high-temperatures, low elastic modulus, smaller body of industry knowledge and experience, and environmental challenges with respect to recycling. Regardless, a variety of industries have utilised FRP for many years, and applications within the civil industry are being explored, largely where FRP's light-weight, strength, and durable nature are beneficial (Hollaway 2010; Gand, Chan & Mottram 2013; Wagners 2021).

In the context of modular buildings, light-weight load bearing walls are considered advantageous due to the reduction in superstructure weight that can be achieved as compared to a structural frame with columns, rafters, and beams. Predominantly, light-weight shear walls are constructed of timber or light-gauge steel framed walls with a structural sheathing such as plywood (Branston, Chen, et al. 2006; Standards Australia 2013), with the sheathing carrying the lateral, in-plane loads. Extensive research has been undertaken on light-weight shear walls with timber or steel frames and a variety of traditional sheathing materials; however, apart from research by Manalo (2013) that tested walls with a rigid polyurethane foam frame and manganese oxide sheathing, very limited investigation into the use of novel or new materials in this application has been undertaken. Owing to its properties, GFRP has great potential as a suitable material for light-weight shear walls.

Previous studies have shown that the behaviour, failure modes, strength, and stiffness of walls are affected by a variety of factors, including the sheathing material and thickness (Manalo 2013; Grossi, Sartori & Tomasi 2015b, 2015a), sheathing-to-frame connection (Liew, Duffield & Gad 2002; Branston, Chen, et al. 2006; Peck, Rogers & Serrette 2012; Manalo 2013; Memari & Solnosky 2014; Grossi, Sartori & Tomasi 2015b, 2015a; Xiao, Li & Wang 2015; Lafontaine et al. 2017), and the method of hold-down to the ground (Richard et al. 2002; Lebeda et al. 2005; Dujic, Klobcar & Zarnic 2009; Grossi, Sartori & Tomasi 2015b, 2015a; Lafontaine et al. 2017). These are therefore critical aspects to consider in developing a wall system composed of any new material. However, in addition to these, openings in shear walls have also been shown to have impacts on the behaviour of shear walls, including its stiffness, strength, and failure mode. The overall size of the opening was found to be a major factor (Dujic, Klobcar & Zarnic 2009; Grossi, Sartori & Tomasi 2015b, 2015a; Shahnewaz et al. 2017), as was aspect ratio and location of the openings within the wall panel (Abdullah et al. 2017; Shahnewaz et al. 2017; Husain, Eisa & Hegazy 2019). Further, Kozem Šilih and Premrov (2012), Grossi, Sartori and Tomasi (2015b, 2015a), and Anil et al. (2016) found that openings can result in stress concentrations leading to the primary failure of the wall. Both Abdullah et al. (2017) and Husain, Eisa and Hegazy (2019) noted that the strength and failure behaviour of the wall may be affected by the presence, size, shape, and location of openings. Investigation of how openings impact the in-plane behaviour of a wall is therefore important when developing a new wall system.

Research and development of a GFRP wall system is of interest and benefit to the industry to explore the benefits of these novel materials in light-weight shear wall applications. A GFRP wall system needs

to be evaluated and its behaviour, strengths, and constraints understood. This project aims to investigate the behaviour of a wall system composed of pultruded GFRP rectangular hollow section (RHS) frame members with a GFRP sheathing, including consideration of how openings within the sheathing impact its behaviour. Experimental testing will be undertaken on full scale specimens, followed by a numerical finite element analysis (FEA) parametric study to further understand how openings affect the wall system's behaviour.

1.2 Research Significance

Very limited investigation of the use of GFRP materials as structural members in building structures and load bearing walls has been undertaken to date, yet the strength, light-weight, durability, and other characteristics of GFRP could be of significant benefit in these applications. In the context of load bearing framed and sheathed walls, codes and guidelines for GFRP are non-existent. This research will help reduce the gap in knowledge and research in this area, by providing an understanding of how framed and sheathed GFRP walls behave when subject to in-plane loads. Aspects such as the performance of GFRP sheathing as a load bearing panel, the performance of adhesive as a sheathing-to-frame connection, and the performance of bolted hold-down mechanisms for thin-walled GFRP members will be considered, which will provide useful information for the potential ongoing development of similar walls systems. The results of this project will also provide understanding of the effect of openings on the in-plane shear behaviour of GFRP walls, and in particular how openings may affect the stiffness, strength, and failure mechanisms of the GFRP wall system. As such, this project will provide valuable contributions to understanding the performance of GFRP wall systems, informing the ongoing development of the system and potentially its eventual use in the industry.

1.3 Project Aims and Objectives

The aim of this research is to understand the in-plane shear behaviour of a light-weight GFRP sheathed wall system with and without window openings. The panels are all single panel walls, 2.4 m high by 0.6 m wide and with two bolted hold-downs through the bottom plate. The unsheathed panel consists of two vertical studs and a top and bottom plate. Sheathed panels have sheeting on both sides and have the same frame, except for additional horizontal members provided at the top and bottom of openings. The panels were tested under a static, monotonic loading setup and procedure, with the experimental testing undertaken to obtain real-world data and information on the failure mechanisms and in-plane shear behaviour of walls with and without sheathing and openings. Using this information, finite element modelling was undertaken, enabling a broader study of how opening size influences the wall's behaviour. It is considered that a deeper understanding of the behaviour and critical constraints of a GFRP wall system will direct future research in this area.

To achieve these aims, the following objectives were developed.

1. To experimentally investigate the in-plane shear behaviour of full-scale GFRP composite wall systems.
2. To evaluate the effect of sheathing and windowing openings on the in-plane shear behaviour of composite wall systems.
3. To numerically verify the in-plane shear behaviour of composite wall systems with window openings and undertake a parametric study.

1.4 Expected Outcomes and Benefits

GFRP framed and sheathed wall systems have not been developed at the time of this research, despite the potential benefits of using GFRP in such an application. This project aims to fill this research gap and provide a better understanding of the potential benefits and limitations of a GFRP wall system and how openings influence its behaviour. The expected outcomes of this research are as follows:

- To generate experimental data of the in-plane shear behaviour of a GFRP framed and sheathed wall system.
- To analyse experimental data and provide comparison between panels with and without sheathing and openings, and to compare with research undertaken previously on similar light-weight wall system constructed of different materials.
- To develop finite element models (FEMs) of the GFRP wall system that reflect the experimental testing and data.
- Through a parametric investigation using FEA, to develop an understanding of the impact openings on the in-plane shear behaviour of the GFRP wall system.
- To determine key constraints or weak components of the GFRP wall system which can inform future research on the wall system.

1.5 Limitations of Research

Whilst this project aims to develop useful and relevant information with respect to the in-plane shear behaviour of framed and sheathed light-weight walls constructed of GFRP rectangular hollow section profile frame members with GFRP sheathing, it is restricted in a number of ways. Some limitations of this project are as follows:

- Only investigation of the behaviour of single panel walls will be undertaken, with all panels of the same overall dimensions.
- A single type of sheathing material, thickness, and adhesive is used.
- A single type and size of frame member is used
- Alternative hold-down arrangements and configurations are not considered.
- Only static, monotonic testing loading will be utilised.
- Vertical restraints and compression loads are not utilised in this testing.
- Durability, temperature effects, and fatigue of the proposed wall system are not investigated.

1.6 Structure of Dissertation

Chapter 1: Introduction: an overview of the project is provided, including background to the need for and benefit of the proposed research, a description of the proposed experimental and FEA work, and an outline of the project aims, objectives, and limitations.

Chapter 2: Literature Review a detailed review of the available literature is provided, relating to the properties of GFRP, type and construction of light-weight shear walls, and previous experimental testing and FEA of shear walls. This chapter will establish the gap in research which this project aims to address.

Chapter 3: Experimental Methodology: a detailed outline of the experimental methodology used is provided, including specimen configuration, details of material properties, and test set up and procedure.

Chapter 4: Experimental Results and Discussion: results and observations from experimental testing is outlined for each panel, noting deflection, failure, and strain behaviour. Then, discussion and comparison between results is provided, noting how sheathing and openings effect these results.

Chapter 5: Finite Element Analysis and Parametric Investigation: a description of the FEMs developed is provided, including element types and boundary conditions. An outline of model validation with experimental data is then given, followed by a parametric study of the effect of opening size on the in-plane shear behaviour of the panels.

Chapter 6: Conclusions and Recommendations: an outline of key findings from both the experimental testing and FEA is provided, along with recommendations for areas of potential future research of this GFRP wall system.

1.7 Summary

The development of a GFRP wall system may aid in addressing some of the challenges faced by the construction industry, largely due to GFRP's light-weight, high-strength, and durable nature. By undertaking both experimental testing and finite-element modelling, this project aims to contribute to the development of this wall system by investigating its in-plane shear behaviour, and to assess how openings affect the wall's performance. To outline the need and benefit of this research in greater detail, a detailed literature review has been undertaken. This review considers existing research on light-weight shear walls and the use of GFRPs in the construction industry, and identifies the need for further research in this area. It also establishes the methods of testing and highlights critical aspects of shear wall behaviour that are to be assessed in the investigation undertaken.

Chapter 2 Literature Review

2.1 Introduction

To establish the motivations for this research, this chapter first discusses the importance of and need for the development of new construction technologies and materials in order to meet the challenges currently facing the construction industry. It then provides background information on fibre reinforced polymers, in particular on the beneficial properties of modern glass FRP materials and products. Review of current applications of FRP in the construction industry and areas of research and development is also provided. This will identify potential applications in which FRP has not been utilised, revealing how FRP can not only aid in addressing the challenges facing the industry, but may also provide new opportunities. Further, a brief history of composite load bearing walls will be established, with a focus on shear walls. A review of previous experimental testing and finite element modelling of shear walls will then establish the basis of testing and investigation undertaken as a part of this research project. In doing the above, this literature review will identify the gap in research and knowledge on light-frame sheathed shear walls constructed of GFRP, both with and without window openings, showing how this project will extend the knowledge base of GFRP as a construction material and benefit the broader industry.

2.2 Importance of New Construction Technologies and Materials

The construction industry faces a variety of challenges as the needs of society change. These challenges include environmental and sustainability issues, negative impacts on society due to construction works, increased demands owing to a growing population, and changes and advances in other industries with which the construction industry must keep up. These challenges affect every part of the supply chain, from resource extraction, transportation, design, fabrication and construction, intended use, and demolition. To address these challenges, new materials and construction methods can be developed.

According to Ajayi et al. (2015), the construction industry is responsible for consumption of approximately half of global extracted natural resource, the production of over a third of landfill waste, and the production of over a third of global CO₂. These are considerable factors contributing to the damage of many ecosystems and environments. Many studies suggest that earth's ability to support our current and indeed growing resource usage and waste production is limited, with some suggesting the earth's population may be at or close to a sustainable limit (Dovers & Butler 2015).

Social impacts of the industry are also a matter for consideration, particularly health risks associated with pollution and waste, as well disruptions to transportation and use of infrastructure during construction works, and of course social impacts resulting from environmental issues such as climate change (Mara, Haghani & Harryson 2014; Wang et al. 2016).

Whilst the construction industry employs a very large number of people and is a major part of many economies, there are aspects of the industry that are detrimental from an economic point of view. During construction projects or maintenance and rehabilitation of existing infrastructure, a reduction in productivity from the surrounding districts can occur. This is due to time losses such as traffic interruptions and downtime for businesses directly affected by the works. Additionally, maintenance costs themselves can be significant, and whether the costs are borne by taxpayers or private developers, improvements such as extending the design life of structure are desirable (Mara, Haghani & Harryson 2014; Wang et al. 2016).

Resource use in construction is a function of both the sheer quantity of development projects underway, as well as the efficiency of material use within individual projects. Increasing the service life and periods between which the structures and materials need to be repaired or replaced during the design stage is one way to reduce material use and construction costs. Another approach is efficiency through reduction in size and material requirements of individual components, which is also achieved during the design phase. Reduction in other costs such as transportation, and heavy machinery and equipment requirements can also be achieved in design by specification of lighter and more manageable materials and components. It can therefore be seen that development of new and alternative building technologies and materials can help achieve more environmentally, economically, and socially sustainable construction.

One growing trend aimed at reducing some of the negative impacts of construction is modular or prefabricated construction (El-Abidi & Ghazali 2015). In modular construction, significant parts of a structure are constructed in a controlled, off-site environment, often indoors in a dedicated facility. These modules are then transported to the site and assembled and lifted into place to form the whole structure. Common smaller examples of prefabrication include precast concrete panels, pits, manholes, culverts, and pipes. Large scale modular construction involves whole rooms and sections of buildings, including structural components and many of the final finishes and services, being constructed off-site. Motivations and potential advantages of adopting modular construction include improved quality control, reduced construction costs, reductions in waste and improved environmental aspects, reduced construction time, and improved construction process efficiency (Tam et al. 2007; Mao et al. 2013; Cao et al. 2015; El-Abidi & Ghazali 2015; Asamoah et al. 2016). With these potential benefits, ongoing development of modular systems is therefore worthwhile.

In modular construction, due to the need to transport large portions of structure and lift them into place, material strengths and weight are critical. The development of strong, light-weight structures could therefore be of significant benefit. Whilst traditional materials such as timber, steel, and concrete have performed well for many years and their mechanical and durability characteristics are well understood within the industry, these materials have limitations. Firstly, they are heavy, have relatively low strength-to-weight ratios, and are therefore not conducive to light-weight structures. This places limitations on how they can be constructed, transported, and demolished. Additionally, their corrosivity and lack of durability in many environments limits their design life, and the cost, time, and resources required to repair or replace these materials is significant. The environmental impacts of these materials are also of concern, in particular the emission production in the manufacture of steel and concrete (Syngros, Balaras & Koubogiannis 2017). With the challenges facing the industry in the 21st Century, the limitations of traditional materials are likely to amplify. Development of new building materials without the limitations associated with more traditional materials is therefore an area of significant interest as they may be able to contribute to solving a number of the challenges currently facing the industry.

2.3 Glass Fibre Reinforced Polymers

2.3.1 Overview

To appreciate the potential benefits of fibre reinforced polymers, an understanding of the material is required. Composite materials consist of different materials combined together to produce a final material with enhanced properties (Gand, Chan & Mottram 2013). Fibre reinforced polymers (FRP) are one such composite material, consisting of strong, thin fibres in a polymer-based matrix (PlasticsEurope n.d.), as depicted in Figure 2-1. In FRP, the fibres are the primary load bearing component whilst the solid matrix forms the shape of the FRP object, protects the fibres from the surrounding environment, and acts to transfer applied forces to and between the fibres. The fibres themselves are typically made of very strong and stiff materials such as glass (GFRP), carbon (CFRP), aramid (AFRP), and basalt (BFRP), although other fibre types exist (Gand, Chan & Mottram 2013; Shakir Abbood et al. 2021; Hamakareem n.d.). The matrix is typically a thermosetting polymeric material such as epoxy resin, vinyl ester, or polyester resin (Gudonis et al. 2013; Shakir Abbood et al. 2021; PlasticsEurope n.d.). The focus of this paper will be on glass fibre reinforced polymers (GFRP) largely due to their lower relative cost compared to FRPs with other fibres. It is noted, however, that many properties of GFRP are shared by other FRP products.

In contrast with steel, most FRPs have multi-layered orthotropic properties, with different mechanical properties in each orthogonal direction. This is due to the layup and direction of the long fibres, which provide the main strength to the composite. As such, the behaviour of FRPs under load can be sensitive

to different loading conditions. This is of note when considering joints where loading conditions are variable and less uniform (Hizam et al. 2019).

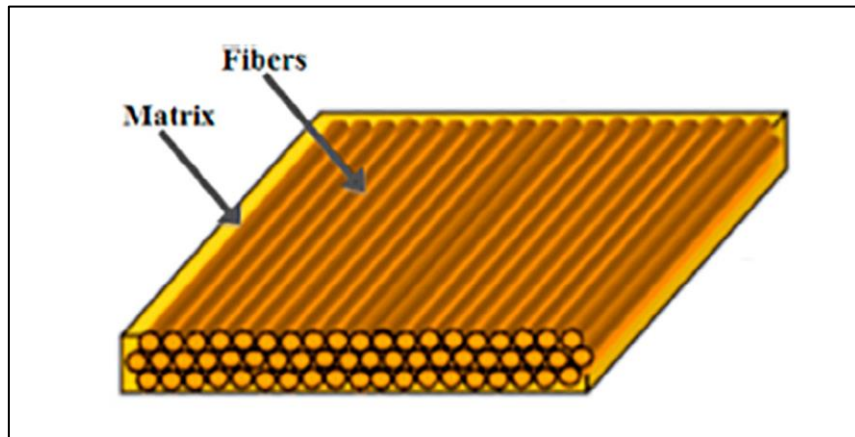


Figure 2-1: Visual representation of a basic FRP (Shakir Abbood et al. 2021)

2.3.2 Beneficial Properties of GFRP

GFRP materials have a range of properties that make them potentially advantageous and useful in the construction industry. In general GFRPs are light-weight, have very high strength-to-weight ratios, are resistant to many forms of corrosion, require low amounts of maintenance, are electromagnetically neutral, and are adaptable in terms of shape and other properties as they can be produced by a variety of different manufacturing processes (Van Den Einde, Zhao & Seible 2003; Gand, Chan & Mottram 2013; Guades, Aravinthan & Islam 2014; Ascione, Lamberti & Razaqpur 2015; Shakir Abbood et al. 2021). These aspects are explored in more detail below.

2.3.2.1 High Strength-to-Weight Ratio

GFRP materials typically have very high strength-to-weight ratios when compared to traditional materials such as timber, steel, and concrete. GFRP densities are typically in the range of 1.25-2.5 gm/cm³ and tensile strengths can be in the range of 483-4580 MPa. Compared to a typical steel density of 7.85 gm/cm³ and tensile strengths of 483-690 MPa (Gand, Chan & Mottram 2013; Wagners CFT Manufacturing Pty Ltd 2016; Ahmed et al. 2020), this can result in significantly higher tensile strength-to-weight ratios. Compressive, shear, and flexural strength-to-weight ratios are also very high in comparison with traditional materials. Studies undertaken comparing GFRP hollow power poles to standard timber poles concluded that the GFRP poles were able to withstand similar loads but weighed a third of the weight (Gand, Chan & Mottram 2013). This characteristic provides potential practical benefits including reduction in foundation and column costs for bridges and other elevated structures, longer unsupported spans, reduction in transportation time and costs, and speedier construction due to easier handling (Van Den Einde, Zhao & Seible 2003; Gand, Chan & Mottram 2013). For modular construction, these properties of obvious benefit with respect to transportation and lifting.

2.3.2.2 Corrosion Resistance and Durability

Another key motivation cited for the use of GFRP materials is their high corrosion resistant properties in comparison to traditional materials (Zaman, Gutub & Wafa 2013; Satasivam & Bai 2014; Liu, Zwingmann & Schlaich 2015; Ferdous, Bai, et al. 2018; Shakir Abbood et al. 2021). This is largely due to the constituent materials of FRPs being insusceptible to electrochemical corrosion (Wang et al. 2015). In harsh environments where structures are subject to moisture and chemicals, materials such as timber and steel are prone to degradation in the form of rot and rust and frequently require repairs or replacement of those components. This is notably the case in steel reinforced concrete, with steel corrosion the leading cause of deterioration of concrete structures (Portland Cement Association 2002). Considerable research into use of FRP reinforcement in concrete structures continues to be undertaken for this reason (Gudonis et al. 2013; Al-Rubaye 2018; Krall & Polak 2019; Alajarmeh 2020). Due to their non-corrosive nature, FRP materials and products may require very limited maintenance, reducing impacts such as cost for monitoring and repair, disruptions to users during maintenance, and improved safety. It is noted, however, by Wang et al. (2015), Bazli, Ashrafi and Oskouei (2016) and Al-Sabagh et al. (2017) that ongoing research into the effects of long-term exposure of FRP to harsh environments is required to better understand its performance in such conditions, particularly for structural applications.

2.3.2.3 Electromagnetic Neutrality

Being non-metallic, GFRP is also electromagnetically neutral, as compared to steel and other metals whose limitations are frequently exposed in the electrical, communications, computing, and medical imaging industries (Bakis et al. 2002; Gand, Chan & Mottram 2013; Gudonis et al. 2013; Zaman, Gutub & Wafa 2013). Other noteworthy benefits include safety from electrocution due to GFRP's non-conductive nature. FRP therefore has potential benefits in specialised applications.

2.3.2.4 Adaptability and Manufacturing Processes

GFRP is very versatile and adaptable due to the variety of manufacturing methods and processes by which it can be produced, enabling it take a number of different shapes and forms with different characteristics suited to various applications (Van Den Einde, Zhao & Seible 2003). Manufacturing processes and techniques included hand and spray layup, vacuum bag moulding, resin injection and resin infusion, compression moulding, pultrusion, and injection moulding. Each technique enables particular properties suited to the desired application to be achieved (Rajak et al. 2019). Additionally, the strength characteristics of GFRPs can also be altered by adjustments to the type, length, number of, and orientation of the fibres, and by use of different matrix materials (Van Den Einde, Zhao & Seible 2003).

For civil engineering applications and with respect to this research project, the pultrusion manufacturing process is of particular interest. Pultrusion is an automated process for the production of long,

continuous profiles, achieved by pulling continuous fibres injected with a resin through a heated die. The heat causes a chemical reaction to occur in the resin which subsequently hardens, after which the profile exits the die, cools, and solidifies (Wagners CFT Manufacturing Pty Ltd 2016; Hizam et al. 2019). A variety of shapes of different sizes are able to be produced by this process, including rectangular and circular hollow sections, angles, channels, and I-, T-, and L-beams. Pultrusion enables relatively economical production of sections which typically exhibit improved axial strengths, torsional rigidity, ability to withstand out-of-plane forces, and higher strength and stiffness in the minor axis compared to sections produced by other processes such as moulding or filament winding (Gand, Chan & Mottram 2013; Hizam et al. 2019).

Relatively recent developments in pultrusion manufacturing include the development of sections with multi-direction glass fibre reinforcement. Due to the multi-directional configuration of the fibres, the overall structural and mechanical performance is improved (Bakis et al. 2002). Guades, Aravinthan and Islam (2014) and Al-saadi, Aravinthan and Lokuge (2019) both undertook research to investigate the mechanical properties of pultruded hollow GFRP sections produced by Wagners Composite Fibre Technology (WCFT), based in Toowoomba, Australia. These studies showed that the presence of the $\pm 45^\circ$ fibres reduced outright tensile strength due to a reduction in fibres aligned in the axial direction of the section, but improved overall structural performance, particularly in terms of flexural and shear properties. This improvement widens potential applications for such sections in flexural and shear type loading conditions.

2.3.3 Applications of FRP in Civil Engineering

Owing to their various mechanical and durability properties, FRP materials have been used in a wide variety of industries and applications for decades, notably the aerospace (Soutis 2005), boating and marine (Rubino et al. 2020), automotive (Stewart 2011), and wind energy industries (Mishnaevsky et al. 2017). The use of FRP materials in these industries has been motivated by its unique properties outlined above. In civil engineering applications, motivations for use of FRP are much the same. According to Hollaway (2010), early civil engineering applications primarily consisted of non- or semi-loading bearing panels whose light weight and adaptable shapes was of benefit. During the 1970's, designers sought to develop structural applications of FRP, particularly to replace traditional materials in harsh environments. The development of automated pultrusion manufacturing enabled the large-scale production of structural members which heralded in wider applications of FRP in civil engineering. Currently, use of FRP in civil engineering includes some reasonably established applications, and a variety of applications subject to ongoing research.

A key area of application for FRP in structural applications has been in elevated structures, where its light-weight, high-strength, corrosion resistance, and ease of installation have been of benefit. For example, FRP bridge decks have been used on traditional bridge superstructures, with the decking

typically being of pultruded FRP sections. The light-weight decking has either ensured the existing supporting structure did not require upgrading, or the new structure could be made smaller and more economical (Bakis et al. 2002; Hollaway 2010; Mara, Haghani & Harryson 2014). Studies have indicated that such approaches can achieve lower life-cycle costs than traditional deck systems such as reinforced concrete, largely due to longer service lives, as well as comparatively lower social and environmental impacts (Mara, Haghani & Harryson 2014). A number of all-FRP composite bridge structures have also been constructed, with FRP's long-service life, ease of installation, low maintenance, and light-weight and non-corrosive properties of benefit (Hollaway 2010; Gand, Chan & Mottram 2013; Wagners 2021). Use of FRP pultruded sections in marine, flood prone and caustic environments has been undertaken, owing to the non-corrosive nature of the material. Examples include wharves, pontoons, jetties, and viewing platforms (Gand, Chan & Mottram 2013; Wagners 2021).

Due to steel reinforcement's high-weight and susceptibility to corrosion, use of FRP reinforcement in RC structures has gained attention, with its strength, non-corrosive, electromagnetic neutrality characteristics being major motivations for this application (Hollaway 2010; Zaman, Gutub & Wafa 2013; Alajarmeh 2020). According to Bakis et al. (2002), applications include reinforcement in bridges, suspended slabs and decks, on-ground pavements, seafront structures, piles and piers, and pre-stressed structures.

FRP materials have also been used to strengthen and rehabilitate existing structures, particularly reinforced concrete beams, slabs, and columns (Bakis et al. 2002; Hollaway 2010; Attari, Amziane & Chemrouk 2012; Zaman, Gutub & Wafa 2013). For example, FRP sheets or strips can be bonded to an existing RC structure either at surface level, or FRP bars can be installed in shallow grooves in the case of Near Surface Mounted (NSM) systems. These would be placed in locations and orientations of high flexural and shear stresses to overcome the existing structure's strength deficiencies, or wrapped around an existing column to improve confinement issues (Hollaway 2010). In these applications, FRP's high strength-to-weight ratio and ability to bond and easily conform to the shape of existing structures have been advantageous.

Use of FRP in situations benefitting from its electromagnetic neutrality have included power infrastructure such as poles and using pultruded GFRP SHS tube cross-arms, and due to GFRP's poor flammability, a reduction in pole-top fires could be achieved (Gand, Chan & Mottram 2013; Guades, Aravinthan & Islam 2014). Additional applications include in magnetic imaging applications and the electronics and computer industries (Gand, Chan & Mottram 2013).

Hybrid structural systems have also been developed, with both FRP and traditional construction materials. Examples include use of composite shell systems (CSS), where FRP shells are filled with concrete; the FRP shell provides formwork and longitudinal and circumferential confinement

reinforcement, and the concrete provides compressive strength and stability. This technology poses reasonable economic viability. Tests on CSS structures undertaken by the University of California, San Diego (UCSD) gave positive results (Van Den Einde, Zhao & Seible 2003; Hollaway 2010; Gand, Chan & Mottram 2013).

Some areas of research and development include use of GFRP hollow profiles in retaining walls, with potential applications being retaining walls in marine environments such as sea walls where traditional materials are subject to corrosion (Ferdous, Almutairi, et al. 2018; Ferdous, Bai, et al. 2018). Research into use of FRP composite railway sleepers has also been undertaken (Ferdous et al. 2015). Furthermore, use of FRP in sandwich structures is another area of ongoing research, with the mechanical behaviour of a sandwich structure considered to potentially overcome some of the mechanical limitations of FRP (Manalo, Aravinthan & Karunasena 2010; Manalo & Aravinthan 2012; Manalo, Aravinthan & Karunasena 2013; Ferdous, Manalo, et al. 2018).

Sharda et al. (2021) presented findings of axial compressive behaviour of modular walls constructed of a GFRP frame and sheathing in research that this project accompanies. Apart from that paper, at the time of this research, very limited study on the use of FRP materials as structural components in load bearing walls or in modular building applications had been undertaken. Further investigation in this area is therefore considered advantageous to the industry.

2.4 Light-Weight Shear Walls

2.4.1 Overview

In the absence of a structural frame where trusses, rafters, beams, and columns carry and transfer loads to a structure's foundations, load bearing walls may carry vertical and horizontal loads. A variety of load bearing wall types exist, including heavy walls such as reinforced concrete or double brick masonry, and lighter timber or steel framed walls with thin sheathing applied to the sides. A load bearing wall that is designed to carry lateral, in-plane loading is called a shear wall. These walls are tied to roof and flooring structures which act as diaphragms and enable transfer of horizontal loads to the walls (Grossi, Sartori & Tomasi 2015b; Branco, Matos & Lourenço 2017). In comparison with structural framing, a key advantage of load bearing wall construction is the overall lighter weight that can be achieved by the use of smaller and lighter components and materials. This higher strength-to-weight ratio allows construction to be achieved largely by hand, reduces the overall weight of the superstructure, and subsequently reduces size of the substructure. A light-weight load-bearing wall is also of obvious benefit in the context of modular construction, as it will reduce transportation and lifting difficulties and costs. In addition, load bearing walls also create the required partitions between rooms and to also enclose the building. In contrast, with structural framing, light-weight, non-structural walls are still

required to achieve this purpose, adding additional weight. Development of shear walls with light-weight yet strong materials can therefore be seen to be of benefit.

2.4.2 Typical Light-Weight Shear Wall Materials and Construction

The frame members of traditional light-weight load bearing walls are typically slender rectangular timber members which are nailed at their joints, resulting in an essentially pin-jointed structure. As a consequence, the frame itself is capable of carrying vertical loads but not lateral, in-plane forces (Grossi, Sartori & Tomasi 2015b). Typically, vertical members are called studs, the top horizontal member is called the top plate, the bottom vertical member is called the bottom plate, and any intermediate horizontal members are called noggings (Standards Australia 2013). In-plane loads are carried by bracing, which is typically thin-sheeting fixed to one or both sides of the wall with nails or screws. Metal diagonal straps are another form of bracing (Standards Australia 2013). A variety of structural sheathing materials are typically used, including timber board lining, plywood, hardboard, and oriented strand board (OSB). Non-structural sheathing includes plasterboard or gypsum wall board (Standards Australia 2013; Xiao, Li & Wang 2015; Lafontaine et al. 2017). Steel framing is also used in light-weight load bearing walls, with the construction similar in terms of thin frame members and a form of sheet or strap bracing (Branston, Boudreault, et al. 2006). Benefits of steel compared to timber have been cited as higher strength-to-weight ratio of frame members, improved ductility, improved durability, and fire and pest resistant properties (Khaliq & Moghis 2017; Buckley 2020). Whilst steel framing may be beneficial in high loading scenarios, such as mid-rise buildings in seismic areas (Peck, Rogers & Serrette 2012; Khaliq & Moghis 2017), steel framing is typically more costly, corrosive in coastal areas, and has a larger environmental footprint than timber (Buckley 2020). Use of GFRP in shear walls has not been previously undertaken.

The method of hold-down of the wall to the underlying floor varies. In AS 1684.2 – *Residential timber-framed construction, Part 2: Non-Cyclonic Areas* (Standards Australia 2013), lower capacity shear walls may be fixed to the floor with nominal nail fixing through the bottom plate, whilst higher capacity walls require stronger hold-downs. The type of hold-down depends on the expected loads, and should be sized so as to not result in failure of the wall.

2.4.3 Typical In-Plane Shear Behaviour of Sheathed Shear Walls

Figure 2-2 below shows the typical force distribution in a sheathed shear wall. Part (a) indicates a horizontal, in-plane load applied to the wall panel, as well as a vertical load such as from an upper floor. Part (b) indicates how the loads are transferred through the frame to the hold-downs and supports via a moment-couple, and part (c) indicates how the lateral load results in shear forces within the sheathing which transfer to the frame at its edges and points of fixation. It is noted that if the lateral load is applied on the left-hand side of the wall and is large enough to overcome the stabilising moment created by the

vertical load, the left-hand stud and hold-down will be primarily in tension, and the right-hand stud would primarily be in compression (Casagrande et al. 2016). The shear stress within the sheathing tends to elongate the bottom-left to top-right diagonal sheathing panel, resulting in tensile forces in the direction of that diagonal, whilst compressive forces would be experienced in the direction of the top-left to bottom-right diagonal.

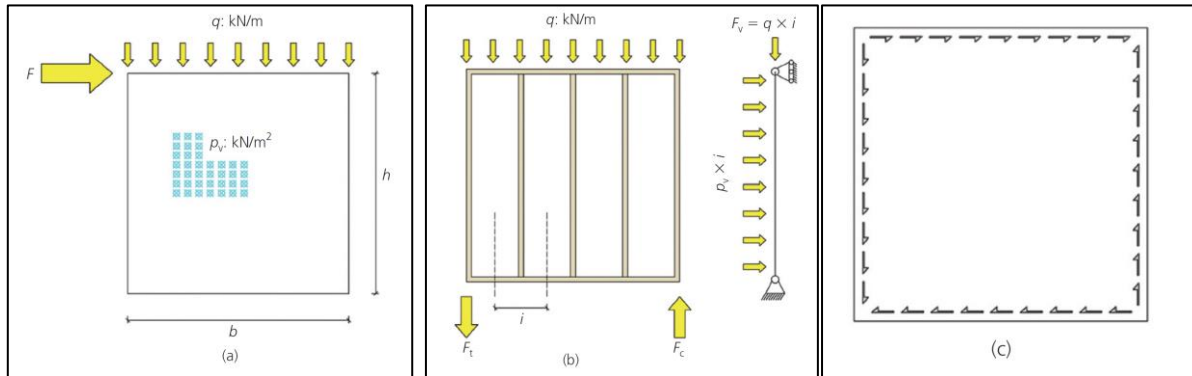


Figure 2-2: Typical forces acting on and within a shear wall (Grossi, Sartori & Tomasi 2015b)

As a result of the lateral load, a shear wall may deflect or deform in one or a combination of the ways shown in Figure 2-3, which are (a) rotation and uplift, (b) translation, and (c) shear deformation. In addition, panels may begin to bend as a cantilevered beam, particularly beams with large height-to-width ratios.

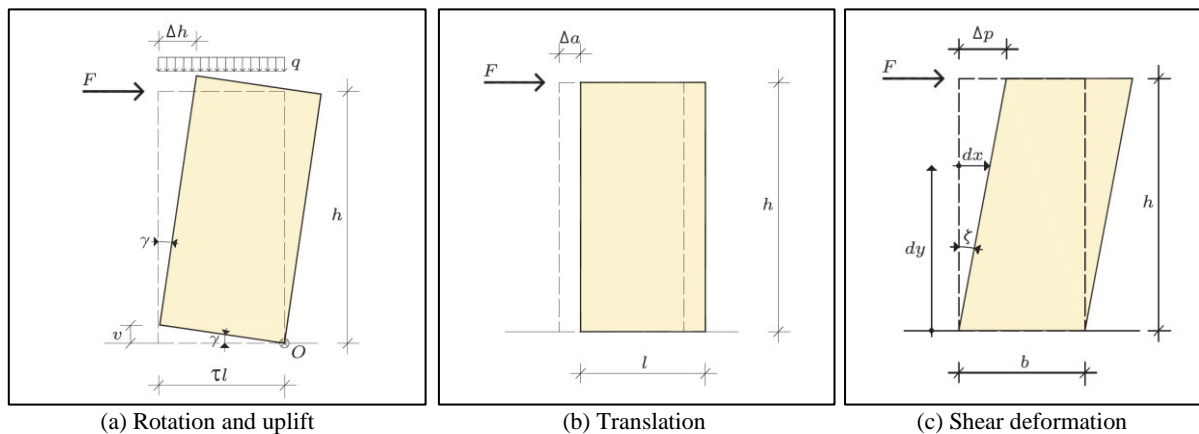


Figure 2-3: Typical deflection and deformation of a shear wall, including (a) rotation and uplift, (b) translation, and (c) shear (Casagrande et al. 2016)

2.5 Previous Research of Shear Walls

There has been substantial research into the behaviour of shear walls, and experimental testing of shear walls is a well-established practice. Numerical, computational research using FEM has also been undertaken. By reviewing previous research, it is possible to better understand the expected behaviour of light-weight shear walls, possible failure modes, the influence of various parameters on the behaviour of the walls, and in particular how these aspects affect the failure mode, strength, and stiffness of shear walls. This will also help establish the gap in research, and will inform the objectives of this project.

2.5.1 Shear Wall Materials

To establish the current state of research in terms of material types used in shear walls, a review of previous testing and investigation has been undertaken. This will establish the gap in research relating to the use of GFRP in these applications.

With respect to frame materials, the majority of investigation has been undertaken on timber framed walls, including but not limited to Liew, Duffield and Gad (2002), Richard et al. (2002), Memari and Solnosky (2014), Grossi, Sartori and Tomasi (2015b, 2015a), Xiao, Li and Wang (2015), Casagrande et al. (2016), Branco, Matos and Lourenço (2017), and Lafontaine et al. (2017). Light-gauge steel framed walls have also been investigated, by Branston, Boudreault, et al. (2006), Peck, Rogers and Serrette (2012), and Khaliq and Moghis (2017), amongst others. Solid, cross-laminated timber walls have been investigated by Dujic, Klobcar and Zarnic (2009), Casagrande et al. (2016), and Shahnewaz et al. (2017) to name a few. No investigation of GFRP frame members for shear walls has been undertaken previously.

Various sheathing materials have been used and tested. Gypsum wall board, or drywall, on shear walls has been tested by Liew, Duffield and Gad (2002), Peck, Rogers and Serrette (2012), Memari and Solnosky (2014), and Lafontaine et al. (2017), whilst Grossi, Sartori and Tomasi (2015b, 2015a) tested gypsum fibre board (GFB) sheathing, and Khaliq and Moghis (2017) undertook testing on walls with fibre cement board (FCB). OSB sheathing has been tested by Richard et al. (2002), Branston, Chen, et al. (2006), Grossi, Sartori and Tomasi (2015b, 2015a), Abdullah et al. (2017), and Branco, Matos and Lourenço (2017), whilst Branston, Chen, et al. (2006) also undertook testing on plywood sheathed walls. Xiao, Li and Wang (2015) undertook testing on walls with ply-bamboo sheathing. Use of GFRP sheathing has not been previously investigated.

Investigation of other novel materials in shear wall applications has been limited. Manalo (2013) investigated the behaviour of prefabricated walls with rigid polyurethane foam (PUF) frame members with manganese oxide (MgO) sheathing. Wu (2009) tested the in-plane shear behaviour of developing composite construction of glass fibre reinforced gypsum (GFRG) panels filled with concrete, and Husain, Eisa and Hegazy (2019) undertook FEM on reinforced concrete walls with openings that were retrofitted with CFRP laminates. Again, it is evident that no research into GFRP shear wall systems has been undertaken.

2.5.2 In-Plane Shear Test Methodology

To develop a methodology to test the proposed GFRP wall system, a review of testing procedures and setups is important. This will help ensure any testing undertaken produces useful and reliable results. The following sections outline some accepted methods and procedures of testing of shear walls.

2.5.2.1 Standardized Test Procedures

Setup and procedures for methods of testing in-plane shear behaviour of walls are outlined in both ASTM E564-06 (ASTM International 2006) and ASTM E72-15 (ASTM International 2015). E72-15 is specifically designed for testing of the sheathing and sheathing-to-framing attachment; use of a 1:1 aspect ratio and full overturning restraint help to achieve this end. In contrast, E564-06 is designed to evaluate the shear resistance of a framed wall panel and therefore the exact construction of the panel itself and its method of hold-down are not explicitly defined. Whilst the methods differ slightly, both outline static load tests where the resistance of a framed wall panel is evaluated by fixing the subject panel to a rigid support and applying a load at the top of wall that is in the plane of the wall and parallel to the rigid support. The test procedures can be used to estimate the panel strength and stiffness and are therefore relevant to this project. Key aspects of the setup and procedure are as follows:

- The panel shall be suitably anchored to the rigid support and laterally supported at its top with rollers to restrict out-of-plane displacement.
- The panel should be free to deflect without being obstructed by any devices or the loading support frame itself.
- The panel shall be loaded at its top, along its plane, and parallel with the rigid support. The load should be applied directly to the panel.
- The load shall be applied in stages, progressing until the ultimate load is reached.
 - In both Standards, loads are to be applied to a set level, released, and then re-applied to the next set level.
- Continuous data measurements should be made of the following:
 - Applied load
 - Horizontal displacement of the top plate
 - Horizontal displacement of the bottom plate (base slip)
 - Vertical displacement of the bottom plate on the side of load application
 - Vertical displacement of the bottom plate on the opposite side to the load application
 - E564-06 specifies measurement of the diagonal elongation
- Notes of any visible failures and displacements should be made during and after the test

The setup described in E564-06 is shown in Figure 2-4 below.

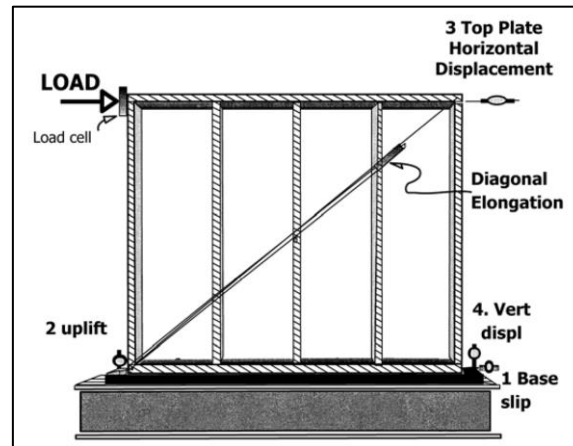


Figure 2-4: In-plane shear test setup from ASTM E564-06 (ASTM International 2006)

A key difference between the two procedures is that E564-06 specifies that a vertical, gravity load may be applied to the top of the panel to simulate upper floor or roof loads on the wall, whilst E72-15 does not include a vertical load or restraint. Whilst these vertical loads will impact the results, they are not necessary to obtain useful data and information. It is noted that testing undertaken within the literature includes cases both with and without applied vertical loads.

2.5.2.2 Monotonic and Cyclic Tests

When considering in-plane shear testing of walls, both monotonic and cyclic methods can be used. Monotonic testing involves applying an increased load in one direction until failure, such as the procedures outlined in ASTM E564-06 and E72-15. Cyclic testing typically involves loading the wall in both directions, at a specific rate and to specific loads. Both van de Lindt (2004) and Branco, Matos and Lourenço (2017) noted that cyclic tests provide additional information on energy dissipation and behaviour of the wall after repeated loading. Different failure modes may also be expected between monotonic and cyclic testing (van de Lindt 2004). It is also noted by van de Lindt (2004) that research suggests monotonically loaded walls may exhibit higher load bearing capacities than walls subject to cyclic loading. Regardless, it is accepted that monotonic tests can still be used to assess the maximum force, the stiffness, the elastic and ultimate displacements, and the ductility of a wall, and hence useful information and data is still able to be obtained (ASTM International 2006, 2015; Branco, Matos & Lourenço 2017).

2.5.2.3 Setup and Procedures Utilised in Previous Experimental Testing

Procedures that have been utilised by researchers vary depending on the objectives of the research. Manalo (2013) tested composite walls composed of PUF frame members and MgO sheathing to investigate how these materials performed as a composite wall, and to assess the influence of different anchor types on the wall behaviour. The method was similar to the static, monotonic ASTM E564-06 method, including a single point of load application, and uplift restraint to simulate connection to adjacent walls and continuity of the top plates. Similarly, Lebeda et al. (2005) undertook monotonic and cyclic testing on timber framed walls with OSB sheathing, however no vertical load or restraints

were used. Casagrande et al. (2016) tested two panels separated by a pinned-beam to simulate the effect of the upper floor, with no vertical loads and the horizontal load applied directly to the first panel.

Dujic, Klobcar and Zarnic (2009) undertook cyclic shear testing with a constant vertical load applied on panels constructed of cross-laminated solid timber (X-lam or CLT) to investigate the influence of openings on panel behaviour. The horizontal load was applied at one location directly to the panel. Vasconcelos et al. (2013) used a similar setup and cyclic procedure with constant vertical loads to test traditional timber walls and the influence of vertical pre-compression levels on the cyclic behaviour of the walls. Similarly, Grossi, Sartori and Tomasi (2015b) undertook monotonic and cyclic testing with applied vertical loads on timber framed walls, investigating the influence of different sheathing materials, presence of openings, hold-down anchors, and sheathing nail spacings.

Liew, Duffield and Gad (2002) undertook testing of timber framed walls with plasterboard sheathing to evaluate the influence of supplementary restrains on the wall behaviour, such as connections to adjacent walls and the ceiling. To simulate these restrains, vertical restrains were used on one panel whilst end blocks were used on another. To simulate possible real-world conditions, the panels were first pulled 8 mm in one direction, pushed in the opposite direction by 8 mm, and then pulled in the first direction until failure occurred, in an attempt to simulate permissible drift in accordance with the serviceability limit state.

In investigating timber frame walls with ply-bamboo sheathing, Xiao, Li and Wang (2015) utilised a setup where the horizontal load was applied to a beam placed on top of the panel. The applied load was therefore distributed across the width of the wall, in contrast to other methodologies where the load is applied at a single point. Both monotonic and cyclic testing was undertaken. Lafontaine et al. (2017) used a similar setup with a load distribution beam and a monotonic and cyclic procedure whilst investigating timber framed panels with gypsum sheathing. Likewise Branco, Matos and Lourenço (2017) utilised a distribution beam and monotonic and cyclic testing on timber framed walls with OSB sheathing to investigate sheathing and base fixation influence on the wall behaviour. A similar setup with a load distribution beam was used by Khaliq and Moghis (2017), who undertook monotonic testing of a cold-formed light-gauge steel framed panel with fibre cement board sheathing infilled with expanded polystyrene foam concrete. Branston, Boudreault, et al. (2006) also used a load distribution beam to undertake monotonic and cyclic testing on a light-gauge steel framed wall with various sheathing types.

Richard et al. (2002) investigated the effect of hold-downs, panel shape, nail density, longer nails with washers and supplementary bracing on timber walls sheathed with OSB. In this set up, the top plate was restrained by a rigid frame, whilst the base was fixed to a shaking table that moved parallel to the length of the wall. Both monotonic and cyclic testing was undertaken.

Another approach was utilised by Memari and Solnosky (2014) to investigate the effect of sheathing joint compound on behaviour of the a timber framed wall with drywall sheathing. In the test a horizontal loading frame was used. The wall panel was fixed at its effective base and slid on rollers when loaded in a cyclic manner.

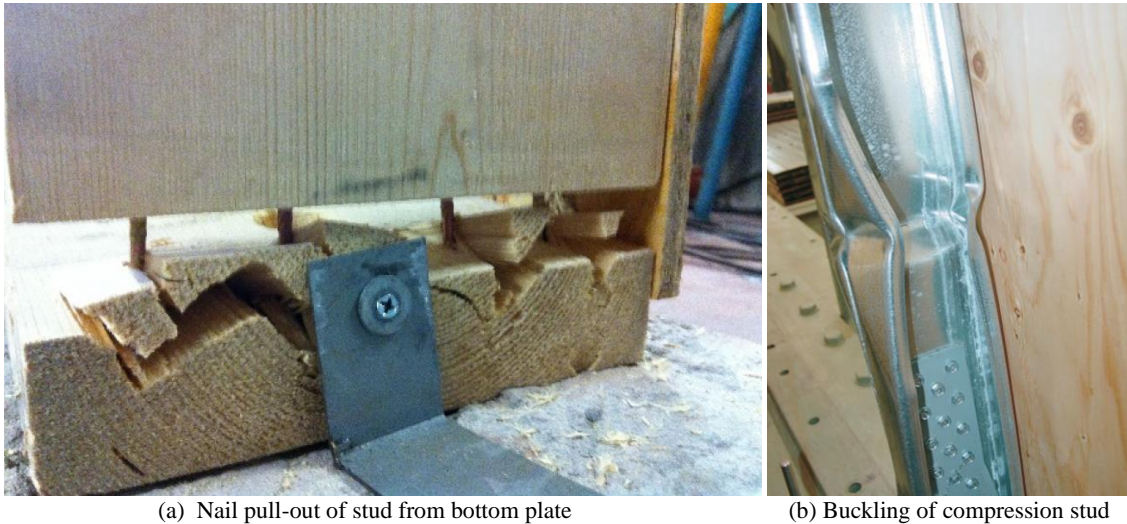
Reviewing previous setups and procedures has shown that various arrangements can be utilised to obtain useful information and data, and both monotonic and cyclic testing are suitable for testing in-plane shear behaviour of walls. Methods similar to those outlined in ASTM E564-06 and E72-15 are often used, with some utilising vertical restraint or a compressive load, and others not. Use of similar methods to those in the literature and standards is considered acceptable.

2.5.3 Failure Modes of Shear Walls

A review of the major failure modes experienced in previous experimental testing will help to establish a basis for analysis of any experimental testing undertaken as a part of this project. Previous research has shown that shear walls can fail in a number of ways, depending on the strength of individual components. The following sections outline some key failure modes for shear walls.

2.5.3.1 Frame Failure

Failure of the frame can occur in a number of ways. Timber frames with nailed connections and without sheathing exhibited limited strength and stiffness, and failed by opening joints between horizontal and vertical frame members, as found by Richard et al. (2002). For sheathed panels, if the sheathing and sheathing-to-frame connection is suitably strong, the frame itself may become the critical, weakest component of the structure and may subsequently fail. Branco, Matos and Lourenço (2017) found that timber frame walls with OSB sheathing tended to fail by nail pull-out of the vertical studs from the bottom plate, as shown in Figure 2-5(a). Lafontaine et al. (2017) noted a similar failure when GWB sheathing with decreased fastener spacing was used. Notably, the improved sheathing-to-frame connection strength resulted in a change in failure mode compared to frames with sparser spacing. Denser spacing resulted in pull out of stud end nails, increased the hold-down deflection, and crushing of the bottom plate by the anchor bolt. Similar findings by Branston, Chen, et al. (2006) showed that for walls with plywood and OSB sheathing, dense sheathing-to-frame fastener spacing resulted in buckling of the compression stud, as shown in Figure 2-5(b).



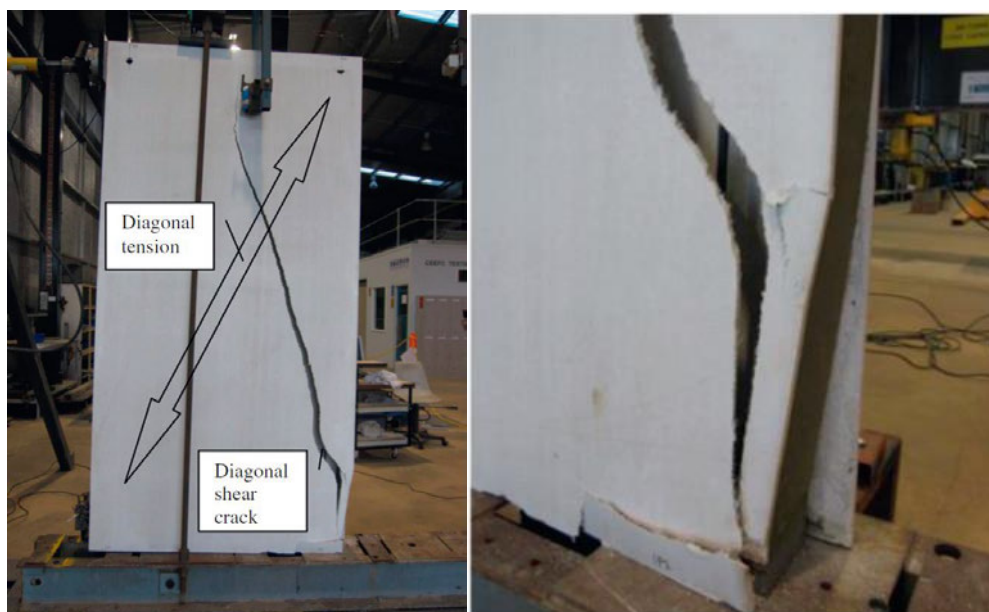
(a) Nail pull-out of stud from bottom plate

(b) Buckling of compression stud

Figure 2-5: (a) Nail pull-out of stud from bottom plate (Branco, Matos & Lourenço 2017) and (b) compression stud buckling (Branston, Chen, et al. 2006)

2.5.3.2 Sheathing Failure

Shear wall sheathing may fail in a number of ways. For walls with strong sheathing-to-frame connection, diagonal tension cracking of the sheathing may occur, as was noted by Manalo (2013). Following failure of the sheathing, the compression stud buckled, resulting in final failure of the wall. These failure modes are shown in Figure 2-6, and are an example of how one failure mode leads to a secondary failure mode, prior to final failure of the wall. In this case, the MgO sheathing was found to be the weakest component of the wall, and structural bonding of the sheathing to the frame performed satisfactorily. Richard et al. (2002) also found that sheathing tension failure occurred on timber framed walls with OSB sheathing, as well as buckling failure of the sheathing itself.



(a) Diagonal tension cracking

(b) Buckling of compression stud

Figure 2-6: Sheathing failure modes: (a) Diagonal tension crack in sheathing, and (b) buckling of compression stud (Manalo 2013)

Failure of the sheathing-to-frame connection is another failure mode found in the literature. For walls bonded to the frame, as opposed to fixed with nails or screws, debonding of the sheathing from the frame may occur. This can cause significant loss of load carrying capacity, as was found by Manalo (2013), who also noted that that sheathing-on-sheathing bearing pressure of adjacent wall panels can contribute to debonding of the sheathing. Walls with nailed sheathing-to-frame connection have also been found to fail at the connections. Ply-bamboo sheathing on a timber frame tested by Xiao, Li and Wang (2015) showed that different types of fasteners will fail in different ways, be it due to head pull through, or bending or tension failure of the fastener. Lafontaine et al. (2017) found similar results with GFB sheathing on a timber frame, where fastener failure dominated either through bending or rupture of the screws, or by edge pull through, as shown in Figure 2-7(a). They also noted that fastener rupture often occurred after a significant number of other fasteners had pulled through and load was transferred to the remaining fasteners. This is another example of the primary failure leading to a secondary failure mode. Liew, Duffield and Gad (2002), Branston, Chen, et al. (2006), Peck, Rogers and Serrette (2012), Memari and Solnosky (2014), and Abdullah et al. (2017) also noted edge tear-out of fasteners through various sheathing material types. Similarly, Grossi, Sartori and Tomasi (2015b, 2015a) found that GFB panels with larger fastener spacing failed by sheathing-to-frame failure. They also noted out-of-plane buckling of GFB sheathing, shown in Figure 2-7(b), which was accompanied by failure of the sheathing-to-frame connection.



(a) Fastener edge pull out

(b) Out-of-plane sheathing buckling

Figure 2-7: (a) Fastener edge pull out (Lafontaine et al. 2017) and (b) out-of-plane sheathing buckling (Grossi, Sartori & Tomasi 2015a)

2.5.3.3 Hold-Down Failure

Failure of the hold-down can also occur, if the sheathing and sheathing-to-frame connection is adequately strong. Deflection of the hold-down and crushing of the timber bottom plate at the hold-down anchor bolt were noted by Lafontaine et al. (2017). Richard et al. (2002) noted failure of a hold-

down when reduced fastener spacing was used. Dujic, Klobcar and Zarnic (2009) tested solid X-lam walls and found that the anchors exhibited deformation during loading and were the governing element in these walls. Overall, it is considered that within previous experimental testing on light-framed shear walls, hold-down failure is relatively uncommon but can occur if they are the weakest component of the wall system.

It was noted by Liew, Duffield and Gad (2002) that testing standalone walls does not necessarily accurately reflect conditions or behaviour of walls if they were installed as part of a complete structure. This is of particular relevance in consideration of hold-downs and resistance to overturning. Walls in structures would have a vertical load from roof or floors above which help resist overturning, as would connection to adjacent walls and to the ceiling itself. If no vertical loads are applied there is increased likelihood of the hold-down failure being the primary failure mode. This should be considered when testing standalone walls, particularly if hold-down failure occurs.

2.5.3.4 Preferred Failure Modes

In considering the various failure modes, preference is generally given to modes of failure that are ductile as this is considered safer as warning of a structures potential failure is given, enabling potential occupants to evacuate if need be. In sheathed shear walls, failure of the frame or hold-downs is generally brittle and not considered preferable. Rather, failure of the sheathing-to-frame connections is preferred as this is generally a more ductile failure mode (Liew, Duffield & Gad 2002; Richard et al. 2002; Branco, Matos & Lourenço 2017). It was noted by Liew, Duffield and Gad (2002) that in Australia bracing panels are not glued, due to the potential brittle failure of the glue and questionable life-span of the glue. As such, the overall strength of the sheathing-to-frame connection system should be considered to ensure a ductile failure behaviour. This may mean reducing fastener spacing or the strength of the bonding agent.

2.5.4 Factors Affecting Shear Wall Strength and Stiffness

A review of the literature provides an understanding of the factors that influence the strength and stiffness of light-weight sheathed shear walls. This understanding will help inform this project's investigation and analysis. Key factors that influence the strength of the walls are discussed below.

2.5.4.1 Influence of Openings on Shear Walls

The presence of an opening in a shear wall will reduce the strength and stiffness of the wall, as shown in studies by Dujic, Klobcar and Zarnic (2009), Grossi, Sartori and Tomasi (2015b, 2015a), Abdullah et al. (2017), Shahnewaz et al. (2017), and Husain, Eisa and Hegazy (2019). Additionally, these studies have shown that the size, shape and location of the opening will affect the change in strength and stiffness.

Dujic, Klobcar and Zarnic (2009) found that solid X-lam walls with openings up to about 30% of the total wall area had relatively small influence on load-bearing capacity, but did have notable impact on shear stiffness which reduced by approximately 50% with a 30% opening, as shown in Figure 2-8. This was shown both in the numerical modelling, and also in the experimental tests where a ratio of opening of 0.41 showed minimal change in shear strength, but notable shear resistance loss. A similar study by Shahnewaz et al. (2017) using FEM investigated the stiffness reduction of solid X-lam walls due to openings of various sizes and aspect ratios. This study found that the ratio of opening to total wall area, the maximum aspect ratio of the opening to wall and the aspect ratio of the opening can have a significant impact on the stiffness of the CLT walls. The study showed that a wall with 50% window had up to an 86% reduction in stiffness. Testing undertaken by Grossi, Sartori and Tomasi (2015b, 2015a) on timber walls with sheathing showed that an opening area of about 16% of the panel area reduced the wall stiffness by approximately 17%, compared to the same panel with no opening. In the test, a diagonal crack near the corner of the opening was noted, indicating that openings can result in stress concentrations and subsequent failure of the wall. Anil et al. (2016) also found that the presence of openings resulted in failure at the corner of the openings, and that openings reduced the strength and stiffness of the panels. An experimental and FEM investigation on timber walls with OSB sheathing by Abdullah et al. (2017) showed that walls with the narrowest opening resisted the highest load, and the wall with the largest opening resisted the lowest load. Husain, Eisa and Hegazy (2019) undertook FEM of reinforced concrete shear walls with openings, and found that openings reduced the strength and stiffness of the walls. It also found that the position of openings impacted the wall behaviour, with walls with ordered opening, such as one opening directly above another, failed in a more brittle manner than walls with staggered openings.

It is therefore well established that the presence, size, and arrangement of openings are an important consideration in the strength and stiffness of shear walls.

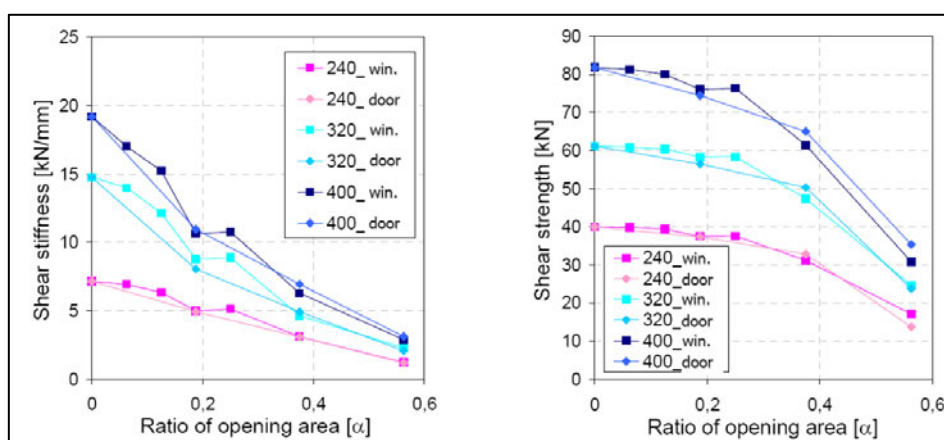


Figure 2-8: Influence of opening size on shear stiffness and strength for X-lam walls (Dujic et al. 2009)

2.5.4.2 Influence of Hold-Downs

The type, strength, and arrangement of the hold-downs has also been shown to affect the structural behaviour of shear walls particularly in stiffer walls where hold-down failure may be the governing factor in terms of strength (Richard et al. 2002; Dujic, Klobcar & Zarnic 2009; Lafontaine et al. 2017). However, Grossi, Sartori and Tomasi (2015b, 2015a) found that the horizontal capacity of the walls tested was only influenced by the hold-down method when the wall failure mechanism was associated with the hold-down. In particular, when minimal uplift of the wall occurred, the stiffness did not appear to alter due to the hold-down. Somewhat in contrast, placement of hold-downs was shown by Lebeda et al. (2005) to significantly affect the behaviour of shear walls, with misplaced hold-downs causing a reduction in strength and stiffness. Study by Richard et al. (2002) on timber frame walls with OSB sheathing found that using four hold-downs as compared to two did not significantly increase strength and marginally increased stiffness; however, the resultant brittle behaviour was undesirable. This demonstrates how the hold-downs can be a significant factor in the behaviour of the wall, and will inform analysis of the wall system investigated in this project.

2.5.4.3 Influence of Sheathing Material Properties and Thickness

In light-weight, sheathed walls, the lateral load is carried by the sheathing, with minimal contribution in lateral strength and stiffness provided by the frame. It is therefore obvious that the sheathing plays a significant part in the wall's overall structural behaviour, a fact established within design standards and reflected in the literature. For example, AS 1684.2 – *Residential timber-framed construction, Part 2: Non-Cyclonic Areas* (Standards Australia 2013) specifies stress grades and thicknesses for plywood sheathing, with higher stress grades requiring thinner sheathing panels. The material's strength properties and thickness are therefore key aspects in the behaviour the wall, as was shown by Grossi, Sartori and Tomasi (2015b, 2015a) where walls with GFB sheathing were significantly weaker and less stiff than those sheathed with OSB. Manalo (2013) also demonstrated that the failure of a shear wall may be governed by the strength of the sheathing. Investigation into shear wall materials should therefore consider the properties and thickness of the sheathing and how these will impact the wall's behaviour.

2.5.4.4 Influence of Sheathing-to-Frame Connection

A number of studies have shown that the primary failure mode of sheathed shear walls may be due to failure of the sheathing-to-frame connection system, including Liew, Duffield and Gad (2002), Branston, Chen, et al. (2006), Peck, Rogers and Serrette (2012), Manalo (2013), Memari and Solnosky (2014), Grossi, Sartori and Tomasi (2015b, 2015a), Xiao, Li and Wang (2015), and Lafontaine et al. (2017). In the case of bonded connections, debonding of the sheathing from the frame may occur, whilst for fasteners pulling through the sheathing material is the likely failure mechanism. In addition, bending of the fastener and hole enlargement may occur, which may not cause failure but will reduce the

stiffness of the wall. Xiao, Li and Wang (2015) also noted that the type of fasteners, in particular their stiffness and strength, can affect the stiffness and ductility of the wall.

2.5.4.5 Influence of Sheathing-to-Sheathing Joints

Joints between sheathing sheets have been shown to influence the strength of walls in shear. A study by Memari and Solnosky (2014) on walls with gypsum wall board (GWB) used two different compounds to finish the joints between the sheets. The study showed that a cement-based product increased strength significantly compared with a standard joint compound, and resulted in a different failure mechanism of the walls with the cement compound resulting in sheathing screw tear out and no failure at the sheet joints.

2.5.4.6 Panel Size and Configuration

The size and aspect ratio of a panel can affect its in-plane behaviour. Manalo (2013) found that in comparison with single panel walls, two panel walls exhibited a failure load almost double that of single panel walls, whilst deflections were similar. This indicated that the two panel walls act compositely in resisting the applied loads (Manalo 2013). It was also observed that the sheathing of adjacent panels did bear against each other, leading to debonding from the frame and reduction in load carrying capacity. Anil et al. (2016) tested walls of different aspect ratios and found that the strength, stiffness, and displacement ductility increase with aspect ratio.

2.5.4.7 Presence of Vertical Loads

The presence of vertical, compressive loads alters the moment resisting reactions that develop at the support and hold-downs. Vasconcelos et al. (2013) noted a low vertical compression load resulted in predominantly rocking behaviour, whilst higher vertical compression resulted in shear deformation of the wall. Similarly, Grossi, Sartori and Tomasi (2015b, 2015a) found that increasing the vertical load resulted in a reduction in racking and therefore reduction in load on the hold-down. Overall, they found that the load-carrying capacity increased with vertical load, and that the influence of failure mechanisms not associated with the hold-down were more prevalent with higher vertical loads. Vertical loads can therefore reduce the potential for hold-down failure due to uplift, but will result in higher shear forces being developed within the panel itself.

2.6 Finite Element Modelling of Shear Walls

2.6.1 Overview

Experimental studies are often limited by the cost and time associated with making and testing physical specimens, a limitation for the research as many variables and arrangements are not able to be tested. Numerical investigations such as finite element modelling (FEM) enable further investigation to be undertaken, reducing the need to make and test additional specimens (Richard et al. 2002). This enables

a more extensive study to be complete, where the effect of changes to various parameters can be analysed in short periods of time and at comparatively low costs. In the context of this project, FEM will enable a much deeper understanding of the GFRP wall system than would otherwise be possible. FEM of shear walls has been undertaken by a variety of researchers, and a review of these will help inform the FEM and parametric investigation to be undertaken within this project.

2.6.2 Previous Modelling

A large amount of previous modelling of shear walls had been undertaken, and a review of this will inform the development of the FEMs for this project. Abdullah et al. (2017) undertook experimental testing and FEM on timber frames with OSB sheathing on both sides, with the sheathing nailed to the timber frame. The software used was ANSYS (version 14), and walls with and without openings were investigated. To model frame members the Beam188 element was used, which has six degrees of freedom at each node, including translations and rotations in the X, Y, and Z directions. These beams were modelled as non-linear materials with orthotropic and elasto-plastic properties. The sheathing was modelled as shells, specifically Shell181 elements which have four nodes and six degrees of freedom at each node. Nails, including between frame members and for the sheathing-to-frame fastening, were modelled as spring elements. In ANSYS, the Combin14 element provides unidirectional tension-compression behaviour, with three degrees of freedom being translations in the Y, Y and Z directions. Supports were modelled as fixed-supports with no translational or rotational movement.

Similarly, Richard et al. (2002) modelled timber walls with OSB sheathing where the frame was modelled using two-node elastic beam elements, and the sheathing was modelled with four node elastic orthotropic plate elements. The nailed frame connections were modelled as perfect hinges, as it was noted that these connections are a relatively weak connection. Frame-to-sheathing connection was modelled by force transformation between nodes on the frame and sheathing. The bolted hold-downs were modelled by an element that linked a fixed node on the 'ground' to the node of the corresponding vertical beam. Stiffness parameters were specified to represent the hold-down stiffness.

In slight contrast, Szczepański and Migda (2020) undertook FEM on a pine wood frame with OSB sheathing and a polyurethane (PU) foam, using the RFEM software. In this case the timber frame was modelled using shell elements with the dimensions of the timber members and orthotropic linear elastic 2D material properties. The OSB sheathing was modelled using two shell elements, one each side, which also had orthotropic linear elastic 2D material properties. The PU foam was modelled using a shell element, modelled as an isotropic linear elastic 2D material. The structure's supports were modelled as node supports, acting as hinges at the base of each vertical frame member. This was considered to somewhat represent the hold-down bolts used on the actual panel.

Oktavianus et al. (2018) undertook modelling of closed panel composite timber (CPCT) wall systems with OSB boards stiffened with timber and steel studs using Abaqus 6.13 software. The studs and OSB wall were modelled using a 3D deformable 8-node linear brick element with orthotropic material properties. Both nails and adhesive were used to connect the OSB to the studs, with nails modelled using 3D deformable two-node beam elements embedded into the stud and the wall. The adhesive was modelled by defining a cohesive interaction between the stud and the OSB wall.

To model solid CLT walls, Dujic, Klobcar and Zarnic (2009) used SAP2000 software. The CLT walls were modelled as homogeneous orthotropic membrane elements. Longitudinal springs were used to simulate the anchor behaviour which were absolutely stiff in the direction of the foundation (downward), but allow free movement away from the foundation. Friction between the walls and the foundation was also modelled, with the anchor springs only engaging once the friction force exceeds a certain value. Shahnewaz et al. (2017) also modelled CLT walls, using ANSYS software. In this case the CLT panel was modelled using twenty node solid elements (SOLID186). The glue between the layers of lamellas was modelled using contact elements, with a friction coefficient of 1 used to account for its rigidity. Connection to the ground was modelled using linear spring elements with a specified stiffness.

In terms of modelling of GFRP materials, both Guades, Aravinthan and Islam (2014) and Al-saadi, Aravinthan and Lokuge (2019) investigated the material behaviour and characteristics of GFRP hollow sections using FEA in Strand7. Detailed models of the RHS were developed and Plate elements with laminate properties were used with good results. Sharda et al. (2021) modelled GFRP sheathed wall panels with GFRP RHS frame members in compression using Abaqus, where the RHS frame and sheathing were modelled using 3D deformable shell elements with orthotropic material properties. A tie interaction was used to model the adhesive connection between the frame and sheathing. Tie interactions link separate surfaces together to prevent relative motion between them and in effect create a perfect connection. A mechanical fastener connection was used to model the rivetted SS angle brackets connecting to the RHS frame. Hizam et al. (2019) also modelled GFRP sections in a bolted truss system, using ANSYS 18.2 Workbench software. The models were of the bolted connections only, with the focus on the failure mechanism of these connections. The GFRP was modelled as an orthotropic, linear elastic material using a solid element, SOLID186. This element type was also used to model the SS bolt and mechanical inserts placed at the bolt locations. To model the bolt-frame contact, contact elements CONTA174 and TARGE170 were used which prevent penetration of two surfaces into each other and enable load transfer between two surfaces. Similarly, Ferdous, Bai, et al. (2018) used ANSYS to model thin walled, concrete filled GFRP retaining structures, where a SOLID186 element with orthotropic material properties was also used to model the GFRP. Modelling of GFRP shear walls has not been undertaken at the time of this project.

As can be seen in the above, the choice of element type for frame and sheathing members has varied depending on the material, type of member, and desired results. However, where thin plate member deformation and stress analysis is required, plate or shell type elements are typically required in lieu of beam type members. Use of orthotropic material properties for plate elements is also possible, in contrast with beam elements. Frame-to-sheathing connection has been modelled in a variety of ways; however, for a strong adhesive bond, a 'perfect' connection may be acceptable, which prevents relative movement between frame and sheathing (Shahnewaz et al. 2017; Sharda et al. 2021). It is noted that this is only suitable if the frame-to-sheathing connection was not a point of failure or significant deformation. Bolts, rivets, and nails are often modelled using a form of a beam type element, where the properties of the mechanical fastener, such as diameter and modulus, are used to connect adjacent nodes (Oktavianus et al. 2018; Sharda et al. 2021). Where accurate representation of bolt bearing against a thin wall is required, detailed modelling of the interaction between the bolt and frame was undertaken to produce accurate stress and deformation patterns at the bolt (Hizam et al. 2019).

2.6.3 Model Validation

A critical step in the development of numerical models of structures is the recreation of experimental results in the software, as noted by Szczepański and Migda (2020). This calibration and validation is to ensure that the numerical model is developed to realistically represent the actual world, and to avoid major errors in modelling. It is considered that numerical models are only reliable if appropriate validation with experimental work is undertaken (Dujic, Klobcar & Zarnic 2009). Validation involves determining and setting correct material properties, appropriate boundary conditions and constraints, appropriately representing the structure's components and connections, and specifying correct loading conditions. The model is then run and adjustments made to obtain results reflective of the experimental results. Comparison of the load-deflection curves between the FEM and experimental tests is a common method of validating numerical models (Richard et al. 2002; Dujic, Klobcar & Zarnic 2009; Manalo & Aravinthan 2012; Abdullah et al. 2017; Lafontaine et al. 2017; Oktavianus et al. 2018; Husain, Eisa & Hegazy 2019; Szczepański & Migda 2020). However, Ferdous, Manalo, et al. (2018) compared not only the load-deflection curve, but also failure mode, ultimate load, and load-strain behaviour to validate their FEM of a sandwich beam structure, indicating that depending on what is being analysed within the FEM, additional calibration may be appropriate.

2.7 Research Gap

As has been demonstrated in this chapter, new technologies and materials are required to continue to address the challenges facing the construction industry in the 21st Century. In the context of building structures, modular construction is one major trend that has the potential to address some of these challenges. Within modular construction, structural components must be light-weight and strong to

enable transportation and lifting into place. This is a challenge with traditional building materials such as timber, steel, and concrete due to their relatively low strength-to-weight ratios and susceptibility to corrosion; therefore, exploration of new materials may be required. GFRP is a strong and versatile material, with high resistance to corrosion and a variety of other benefits that could contribute toward addressing some of the current challenges in the industry. However, although FRP materials have been used in a few retrofitting and repair applications, and a limited number of FRP structures have been constructed, at this stage there is very limited use or research of GFRP as structural components in buildings. This is certainly true in the context of light-weight load bearing walls, and in particular shear walls. Additionally, no research into the effect of openings on in-plane shear behaviour of walls constructed of GFRP composite materials has been undertaken.

Due to the potential benefits of a GFRP based shear wall, not only in modular construction but also industry wide, a GFRP wall system consisting of a frame constructed of pultruded GFRP RHS members with GFRP sheathing on both sides has been developed. This wall system has not been fully tested and analysed in terms of its in-plane shear behaviour and the effect of openings on this behaviour. The main motivation of this research is therefore to test and investigate the structural behaviour of the prefabricated GFRP wall systems with and without window openings under in-plane shear, as is outlined in the following chapters.

Chapter 3 Experimental Methodology

3.1 Introduction

It has been established that development of the use of materials such as GFRP in civil applications may help to address some of the limitations in using conventional construction materials, aid in reducing the negative impacts of the industry on, and herald in new opportunities and possibilities. In the context of structural components in prefabricated construction, GFRP has particularly high potential. Research and investigation of GFRP for use as structural components exists, but very limited study of its use in structural wall applications has been undertaken. As this project aims to undertake an experimental and numerical investigation of shear walls constructed of GFRP, the following chapter outlines the experimental methodology used to undertake this research. Details of the test specimen configurations, material properties, and experimental test setup, instrumentation, and procedure will be provided.

3.2 Specimen Details

3.2.1 General

Three specimen panels were prepared for testing. Each specimen consisted of a GFRP frame, and two panels were sheathed on both sides with GFRP sheeting. One panel was fully sheathed, whilst the other had an opening to simulate a window. Further details are provided in the following sections.

3.2.2 Panel Naming Convention

The naming convention used for this project is as follows. The panels are designated FSO_pX, where F stands for frame, and S stands for sheathing. O indicates an opening, and the subscript p indicates the size of the opening as a percentage of the total panel area. X indicates if the panel was an experimental specimen (E) or a finite element model (FE). A summary of the experimental panels is provided in Table 3-1 below.

Table 3-1: Experimental panel naming convention

NAME	SHEATHING	OPENING (% of total panel area)
FE	No sheathing	N/A
FSE	Sheathed on both sides	No opening
FSO _{37.5} E	Sheathed on both sides	37.5%

3.2.3 Specimen Configurations

3.2.3.1 Panels

Three experimental specimens were manufactured by Wagners Composite Fibre Technologies and were delivered to the University of Southern Queensland (USQ) for the experimental tests. The experimental specimens share overall dimensions of 0.6 m wide by 2.4 m high. The height was chosen to reflect typical ceiling heights, and the width was chosen to allow two panel configurations to be tested within the same testing frame (not included as a part of this project). The three experimental panels are shown in Figure 3-1, and a description of each panel follows.

The frame only wall, panel FE, consisted of two vertical 100x75x5 mm GFRP rectangular hollow section studs, each 2.4 m long and continuous from top to bottom of the wall. Top and bottom plates were provided between the studs, each being 450 mm long. The frame members were connected with 35x35x75 mm by 4 mm thick SS angle brackets, which were riveted to the panel using six aluminium 5 mm pin diameter and 12 mm long rivets, as shown in Figure 3-2.

The fully sheathed specimen, panel FSE, was identical to the panel FE but with sheathing applied to both sides for the full width and height, except for a 10 mm offset along the base of the wall to prevent the sheathing bearing directly against the ground. The sheathing was bonded to the frame using Techniglu-HP R26 structural epoxy adhesive. Adhesive was applied between the sheathing and frame on all touching faces.

Panel FSO_{37.5}E was similar to FSE but had a 1200 mm high opening located 900 mm from the base of the wall, extending the full width between the vertical studs, with the area of the opening being 37.5% of the total panel area. Horizontal noggings were provided at the top and bottom of the opening, both of which were attached with angle brackets to the vertical studs.

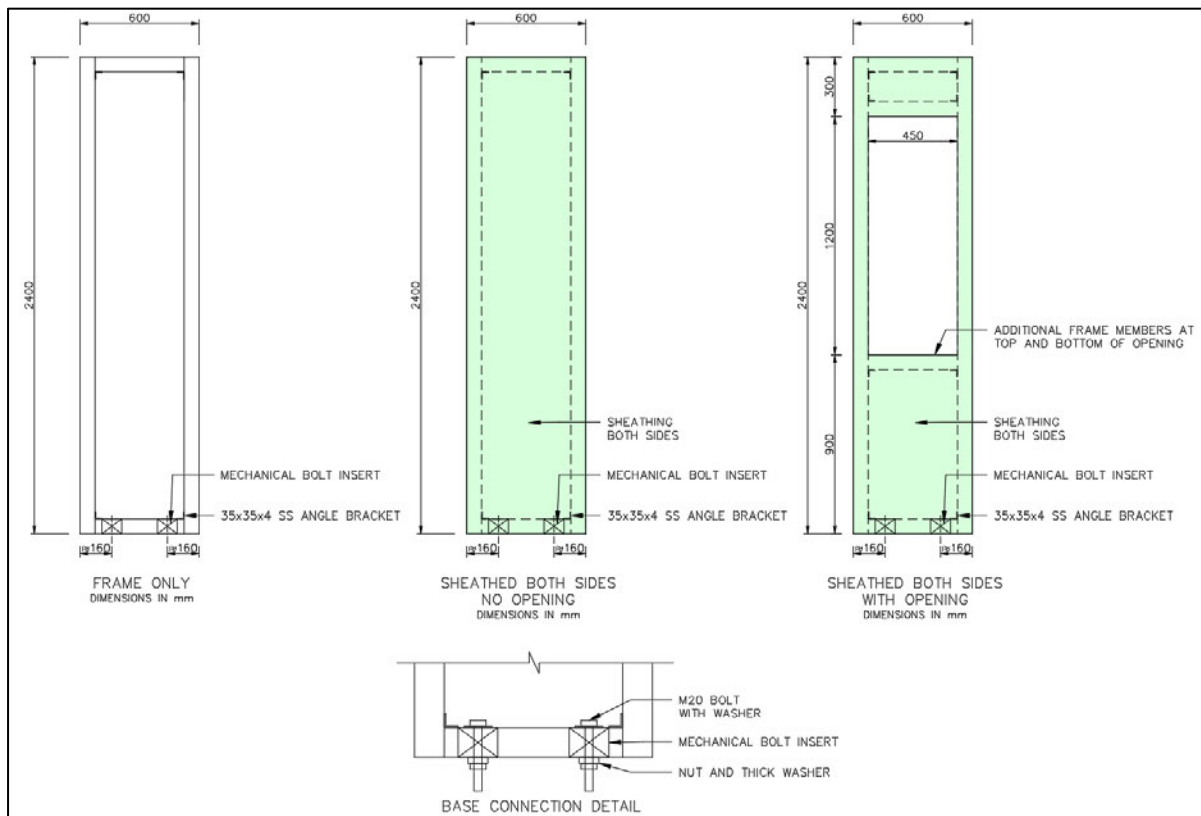


Figure 3-1: Drawing of experimental panels and base connection detail



Figure 3-2: SS angle bracket and rivets

3.2.3.2 Hold-Downs

Hold-downs for all panels consisted of two SS M20 bolts passing through the bottom plate, centred approximately 160mm in from the outside edges of the panel. Mechanical bolt inserts made of moulded thermoplastic with short-fibre glass reinforcement, shown in Figure 3-3(a), were installed inside the RHS at the two hold-down locations. These inserts improve the strength and stiffness of the joint by enabling improved load distribution (Hizam, Karunasena & Manalo 2013; Hizam et al. 2019). Each hold-down had a 2 mm thick SS circular washer with a diameter of 37 mm at the bolt head, and a 20mm thick rectangular washer at the nut, as shown in Figure 3-3(b). In contrast to Hizam et al. (2019), no adhesive was placed between the insert and frame.

This hold-down configuration is reflective of basic hold-downs for light-weight shear walls, such as those specified in AS 1684, and is similar to those used by Manalo (2013).



(a) Mechanical bolt insert

(b) Rectangular washers at hold-down nut

Figure 3-3: (a) Mechanical bolt insert (Wagners CFT Manufacturing Pty Ltd 2016) and (b) rectangular washers at hold-down nut

3.2.4 Specimen Preparation

Final preparation of the specimens for testing included application of strain gauges and preparation for use of data measurement devices.

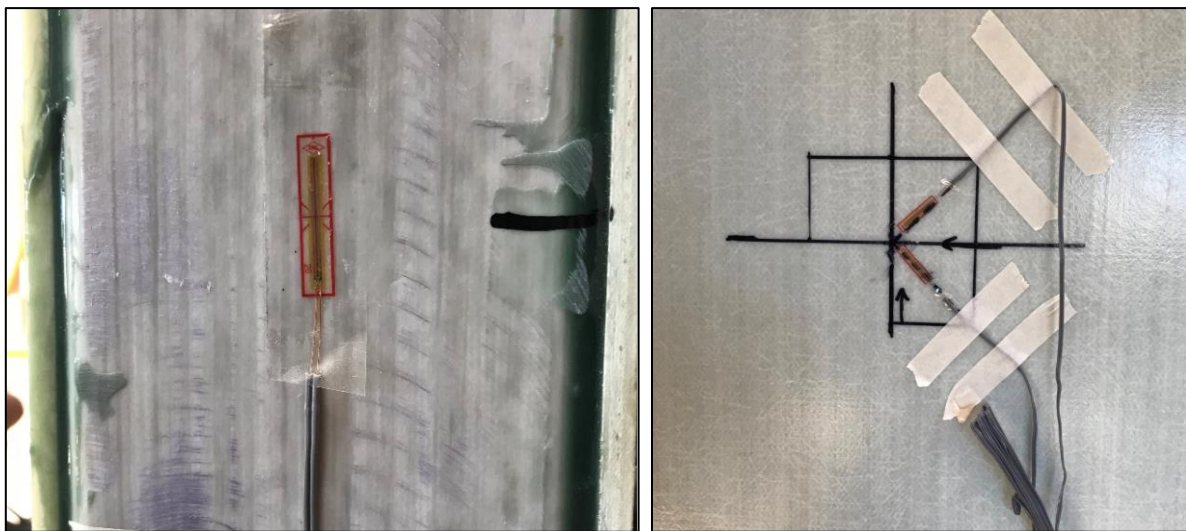
3.2.4.1 Strain Gauge Locations

Polyester foil strain gauges, 20 mm long, were installed by cleaning the surface of the panel with acetone and applying a strong glue, in accordance with the manufacturer's requirements. Strain gauges were installed at the following locations:

- Panel FE:
 - One each on the outside of and parallel with both vertical studs at the midpoint of the stud
 - One on the top and at the midpoint of the top plate, parallel with the top plate
- Panel FSE:
 - One each on the outside of and parallel with both vertical studs at the midpoint of the stud
 - Two on the face of one side of the sheathing, located at the centre of the sheathing, and angled at $\pm 45^\circ$
- Panel FSO_{37.5E}:
 - One each on the outside of and parallel with both vertical studs at the midpoint of the stud

- One on the outside of and parallel with vertical stud on the loaded side of the panel and aligned with the base of the opening
- Two on the face of one side of the sheathing, located at the centre of the sheathing below the opening, and angled at $\pm 45^\circ$

A typical strain gauge on a vertical stud is shown in Figure 3-4(a), and strain gauges installed at $\pm 45^\circ$ on the sheathing are shown in Figure 3-4(b). The locations of all strain gauges and load application are shown in Figure 3-5.



(a) Strain gauge on stud
 (b) Strain gauges on sheathing
Figure 3-4: (a) Strain gauge on stud and (b) strain gauges on sheathing

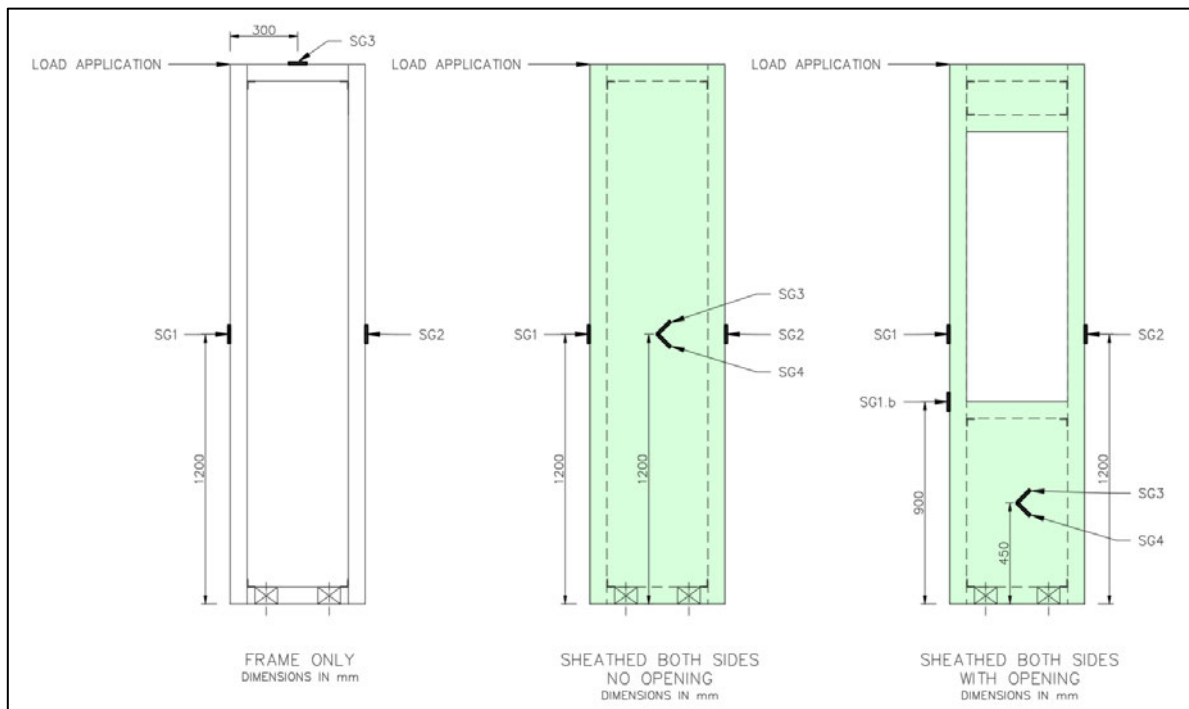


Figure 3-5: Strain gauge and load application locations

3.2.4.2 DIC Camera

In addition to the strain gauges, a Digital Image Correlation (DIC) camera was used to measure the vertical and horizontal deflection of the corners of the opening for panel FSO_{37.5E}. Preparation of the panel for this was undertaken by suitably trained personnel at USQ. The basic process involved applying a dye in a spotted pattern to the panels, setting the camera up at a suitable distance from the specimen, and calibrating the camera based on a gauged length. The spotted pattern, shown in Figure 3-6 below, enables the camera to clearly detect and measure movement of the panel.

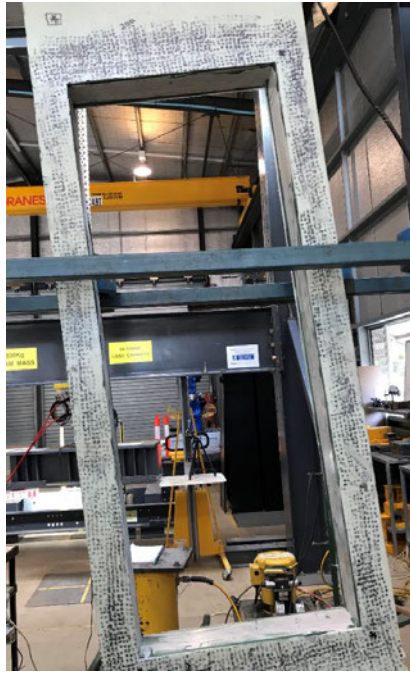


Figure 3-6: Dye on panel for DIC camera

3.3 Material and Section Properties

The material and section properties used in the construction of the panels are outlined below.

3.3.1 Pultruded GFRP RHS

The pultruded RHS members were produced by Wagners Composite Fibre Technologies (WCFT), and consisted of 100x75mm profiles with 5 mm wall thicknesses (product code STR-VRHS-100x75x5). The GFRP composition consists of electrical-corrosion resistant (ECR) type glass fibres in a vinyl ester resin matrix, with a grade designation of WCFT Grade GV36-S (Wagners CFT Manufacturing Pty Ltd 2016). A thermoplastic non-woven surface veil is provided which provides a smooth finish and UV protection. The RHS dimensions and section properties are provided in Figure 3-7 below.

PRODUCT CODE		DIMENSIONS									
STR-VRHS-100x75x5	WCFT	100	x	75	x	5.0	RHS	10.0	4.75	3.21	0.333

SECTION PROPERTIES								
Gross Section Area A_g	About x-axis			About y-axis			Torsion Constant J	Torsion Modulus C
	I_x	Z_x	r_x	I_y	Z_y	r_y		
mm ²	10 ⁶ mm ⁴	10 ³ mm ³	mm	10 ⁶ mm ⁴	10 ³ mm ³	mm	10 ⁶ mm ⁴	10 ³ mm ³
1580	2.14	42.8	36.8	1.37	36.5	29.4	2.76	59.2

Figure 3-7: RHS dimensions and section properties (Wagners 2021)

The RHS profiles were the same as used by Hizam et al. (2019), who undertook testing to determine properties of the sections. The glass fibres consist of five layers of continuous fibres laid in a multi-directional pattern. The stacking sequence is shown in Figure 3-8(a) ($0^\circ / +45^\circ / 0^\circ / -45^\circ / 0^\circ$), noting that higher percentage of longitudinal fibres results in a high tensile strength and elastic modulus (Hizam et al. 2019). Fibre weight and volume fraction are 81.5% and 65% respectively based on a burn-out test performed by Hizam et al. (2019). This differs slightly from the values provided by WCFT, which are 77.4% and 57.7% respectively (Wagners CFT Manufacturing Pty Ltd 2016). The density of the material is assumed to be 2,030 kg/mm³ (Hizam et al. 2019). A photo of typical pultruded GFRP sections produced by WCFT is shown in Figure 3-8(b).

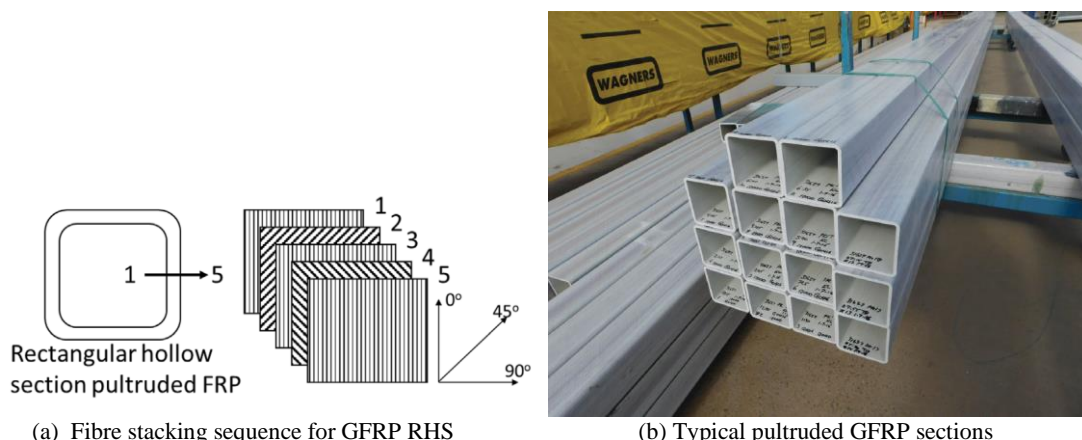


Figure 3-8: (a) Fibre stacking sequence for the pultruded GFRP RHS profiles (Hizam et al. 2019) and (b) typical pultruded GFRP sections produced by WCFT (Wagners CFT Manufacturing Pty Ltd 2016)

The mechanical properties for the RHS profiles were characterised previously by Hizam et al. (2019) using coupon testing, with the properties shown in Table 3-2 below.

Table 3-2: Mechanical properties of the GFRP RHS profile

PROPERTY	SYMBOL	VALUE
Tensile stress, longitudinal	f_{Lt} (MPa)	686.43
Tensile elastic modulus, longitudinal	E_{Lt} (GPa)	42.92
Poisson's ratio, longitudinal	ν_L	0.3
Tensile stress, transverse	f_{Tt} (MPa)	46.84
Tensile elastic modulus, transverse	E_{Tt} (GPa)	12.19
Poisson's ratio, transverse	ν_T	0.15
Compressive stress, longitudinal	f_{Lc} (MPa)	543.83
Compressive elastic modulus, longitudinal	E_{Lc} (GPa)	39.59
Compressive stress, transverse	f_{Tc} (MPa)	147.7
Compressive elastic modulus, transverse	E_{Tc} (GPa)	14.76
In-plane shear, strength	f_{Lv} (MPa)	88.95
In-plane shear, elastic modulus	G_L (GPa)	5.42
Pin bearing strength (plain)	$f_{br,plain}$ (MPa)	260
Pin bearing strength (thread)	$f_{br,thread}$ (MPa)	185

3.3.2 GFRP Sheathing

The GFRP sheathing consisted of 6 mm thick sheets of E-glass fibres in a vinyl ester matrix. Based on testing undertaken at USQ, the sheets consist of multi-directional fibres in five layers, with 75% of the fibres in the longitudinal (0°) direction and a fibre weight fraction of 69.91%. The sequencing consisted of Chopped Strand Mat (CSM) in the outer and middle layers, and 0° longitudinal fibres in between (CSM / 0° / CSM / 0° / CSM). Similar sheet material tested by Sharda et al. (2021) showed that the additional longitudinal fibres give significantly enhanced tensile and compressive mechanical properties in that direction. The density of the material is assumed to be 2,030 kg/mm³.

The mechanical properties of the sheathing are provided in Table 3-3 below. Compressive properties were unavailable; however, based on the ratio of tensile to compressive stresses for the pultrude GFRP RHS material, estimates on the values are made, with the longitudinal compressive stress estimated at 80% of the magnitude of longitudinal tensile stress, and the transverse compressive stress estimated as three (3) times the magnitude of the transverse tensile stress.

A shear modulus was also not provided. Equation 3.1 was used to estimate the shear modulus, noting that the material is a linear elastic material and therefore Hooke's law can be applied.

$$G = \frac{1}{2} \frac{E}{1 + \nu}$$

Equation 3.1

Where: E = Tensile elastic modulus

ν = Poisson's ratio

A modulus E of 11.78 GPa and a Poisson's ratio ν of 0.13 were used, giving an in-plane shear modulus of 5.212 GPa. This is comparative with the shear modulus value of the GFRP RHS provided by Hizam et al. (2019) and is considered a reasonable value. It is noted that Summerscales (2000) suggested that for orthotropic materials, such as long fibre CFRP and GFRP materials, the shear modulus can be based off both the longitudinal E_{Lt} and transverse E_{Tt} elastic moduli and respective Poisson's ratios ν_L and ν_T . The equation offered by Summerscales (2000) was found to return high values of shear modulus compared to those found by Hizam et al. (2019). As such, for this paper, the lower value estimated by Equation 3.1 has been used.

Table 3-3: Mechanical properties of GFRP sheathing

PROPERTY	SYMBOL	VALUE
Tensile stress, longitudinal	f_{Lt} (MPa)	541.43
Tensile elastic modulus, longitudinal	E_{Lt} (GPa)	34.37
Poisson's ratio, longitudinal	ν_L	0.27
Tensile stress, transverse	f_{Tt} (MPa)	40.81
Tensile elastic modulus, transverse	E_{Tt} (GPa)	11.78
Poisson's ratio, transverse	ν_T	0.13
<i>Compressive stress, longitudinal (estimated)</i>	f_{Lc} (MPa)	433*
<i>Compressive stress, transverse (estimated)</i>	f_{Tc} (MPa)	122*
In-plane shear, strength	f_{Lv} (MPa)	72
In-plane shear, elastic modulus	G_L (GPa)	5.212

*Indicates estimated stresses based on the ratios of tensile to compressive stresses for the pultruded GFRP RHS material

3.3.3 GFRP Mechanical Bolt Insert

The mechanical bolt inserts are produced by WCFT (product code ACC-INST-100x75xM20) and are anti-crush inserts placed inside the RHS with a 22 mm diameter hole designed for M20 bolts. As tested by Hizam et al. (2019), the inserts consist of a moulded thermoplastic alloy (TPA) matrix with approximately 49.35% short glass fibres. The inserts are designed to provide additional strength and load transfer at bolt locations, and are also pest resistant (Wagners CFT Manufacturing Pty Ltd 2016). In contrast with Hizam et al. (2019), no adhesive was applied between the insert and the inside of the RHS for this testing. No mechanical properties data was available for this project.

3.3.4 Structural Epoxy Adhesive

Techniglu-HP R26 structural epoxy resin adhesive with H26 hardener was used to bond the sheeting to the frame, with the adhesive similar to that used by Manalo and Aravinthan (2012) and Hizam et al. (2019). The mechanical properties of the adhesive are shown Table 3-4.

Table 3-4: Techniglu-HP R26 epoxy adhesive mechanical properties (Manalo & Aravinthan 2012)

Property	Symbol	Value	Test method
Tensile strength	f_t	34.1 MPa	ISO 527-2
Tensile Modulus	E_t	2409 MPa	ISO 527-2
Lap shear strength	f_v	11.9 MPa	ASTM D3161
Heat deflection temperature	HDT	85 °C	ISO 75

3.3.5 Bolts, Washers, Angle Brackets, and Rivets

Stainless steel M20 bolts, nuts, and washers were installed as hold-downs for the panels. The bolts were class 8.8 high-tensile SS shanked bolts, the properties of which are provided in Table 3-5. Standard washers for M20 bolts were used.

Table 3-5: M20 class 8.8 SS bolt properties (Hizam et al. 2019)

Items	Specification
Property class:	8.8 (M20)
Minor diameter, Dc:	19.67 mm
Area of root of thread:	225 mm ²
Pitch, P:	2.50 mm
Minimum tensile strength:	830 MPa
Proof strength:	600 MPa
Minimum yield strength:	660 MPa
Minimum shear stress ^a :	514.6 MPa
Min. breaking load in single shear (Thread):	117 kN
Minimum bolt tension ^b :	145 kN

^a Ultimate shear stress equals 62% of ultimate tensile strength.
^b Full tightening.

The stainless steel (SS) brackets were 35x35x75 mm and 4 mm thick angle brackets, riveted to the RHS frame members. The washers and brackets are Grade 304 stainless steel, with the material properties shown in Table 3-6 (Australian Stainless Steel Development Association 2020). Aluminium rivets of 4.8 mm diameter were used. The aluminium is assumed to have an elastic modulus of 69 GPa (Austral Wright Metals 2015).

Table 3-6: SS angle bracket and washer material properties

PROPERTY	VALUE
Tensile strength (MPa)	515
Yield stress (MPa)	205
Elastic modulus (GPa)	193
Density (kg/mm ³)	5.212

3.4 Experimental Test Setup and Procedure

3.4.1 Setup and Instrumentation

The experimental setup utilised, shown in Figure 3-9, is reflective of methods outlined in both ASTM E564-06 and E72-15 and of methods used by previous researchers, including Lebeda et al. (2005), Dujic, Klobcar and Zarnic (2009), Manalo (2013), Vasconcelos et al. (2013), and Grossi, Sartori and Tomasi (2015b). No vertical restraints or compressive load were utilised, and load application was at a single point on the panels, not through a load distribution beam.

The testing frame consisted of two large vertical steel columns well over 2.4 m high, with approximately 1.8 m clearance between flanges. A large steel beam was fixed at the base of the columns to form the base support for the panels. This beam had flange thicknesses of approximately 20 mm, and due to its weight and strength, was considered suitable as a rigid support for the panels. The panels were bolted to the flange of this beam by the two hold-downs, with the bolts snug tightened with a wrench. It is noted that a specific tightening torque could not be achieved due to inaccessibility of the nut with the available torque wrench. As such, care was taken not to overtighten the hold-downs. It is considered that as the hold-down bolt was not expected to be loaded near its capacity and lateral sliding was limited to the diameter of the hold-down hole, the data would not be significantly different to if a specific tightening torque was achieved.

Load was applied by a manually operated 100 kN hydraulic jack with a 150 mm shaft stroke, mounted horizontally to the testing frame columns. A load cell was attached to the jack to allow continuous measurement of the applied load. A string pot potentiometer was used to measure horizontal deflection at the top of the panel on the opposite side to the load application. As mentioned earlier, a DIC camera was also used to measure deflection of the corners of the opening for panel FSO_{37.5E}. All measurements were recorded by dedicated computer systems which recorded load, deflection, and strain data in 0.1 second timesteps or smaller. A video camera was also set up facing directly toward the front of each panel to allow for future analysis of the panel deflection and audible cracking that was heard, and cameras were used to take high-quality still pictures.



(a) Overall test setup

(b) Panel attached to support beam

(c) Hydraulic jack and load cell

(d) String pot measuring horizontal deflection

Figure 3-9: Images of (a) the overall test setup, (b) a panel attached to the support beam, (c) the hydraulic jack and load cell, and (d) the string pot for measuring horizontal deflection

3.4.2 Procedure

The procedure used was determined based on available equipment and suited the desired outcomes of gaining understanding of the overall behaviour of GFRP shear walls subject to in-plane loads. It follows a basic static, monotonic loading similar to ASTM E564-06 and E72-15, noting that a computerized loading rate was not possible due to equipment availability. Loading and unloading during the test was also not undertaken. The procedure used is outlined below.

- Ensure there is contact between load cell and panel by pumping the jack slowly to close any gap, without applying load to the panel
- Commence data recording on all computers simultaneously
- Manually activate the jack at a steady, manageable rate without stopping or unloading

- Continue to apply load to the wall as it deflects
 - As the wall deflects, record the load at which audible cracks are heard
 - Record the load at which any notable changes to the wall behaviour occur
- Apply the load through to final failure of the wall, indicated by a loss of load even as the jack continues to extend. Continue to activate the jack until the end of the its stroke
- End data recording
- Make observations of the wall in its deformed state
- Remove the load and note any residual deformations or damage
- Remove panel from the testing frame
- Undertake further inspections of any damage and deformations

3.5 Project Safety and Timeline

To ensure suitable risk assessment and safety was maintained throughout the project, a Risk Management Plan was undertaken and is provided in Appendix B. Similarly, a preliminary Project Timeline was developed to help ensure the project was completed within the time constraints, and is provided in Appendix C.

3.6 Summary

Based on well-established testing methods, the project's experimental testing methodology has been outlined, with three panels to be tested using a monotonic loading procedure and test set up. Undertaking the steps outlined in this chapter will provide data and observational results that can be used to understand the behaviour of the wall system and how sheathing and openings affect its behaviour.

Chapter 4 Experimental Results and Discussion

4.1 Introduction

To assess the performance of the GFRP composite wall system under in-plane shear loads, an experimental program utilising a monotonic loading procedure has been developed and presented in Chapter 3. This chapter presents the results and observations of the experimental tests on the sheathed composite wall panels with window openings. As a control specimen, the behaviour of the frame only was also investigated and is presented as well. The results and observations include the load-deflection behaviour, the propagation and final failure of the tested walls, and strain in different components of the wall panels. Then, analysis and discussion of the results is provided, comparing panel behaviour and allowing deductions of relevant parameters relating to shear wall behaviour to be made, such as stiffness, failure mode, and ductility. For the purposes of this paper, the left-hand side of panels corresponds to the side of load application, as shown in Figure 4-1 below.

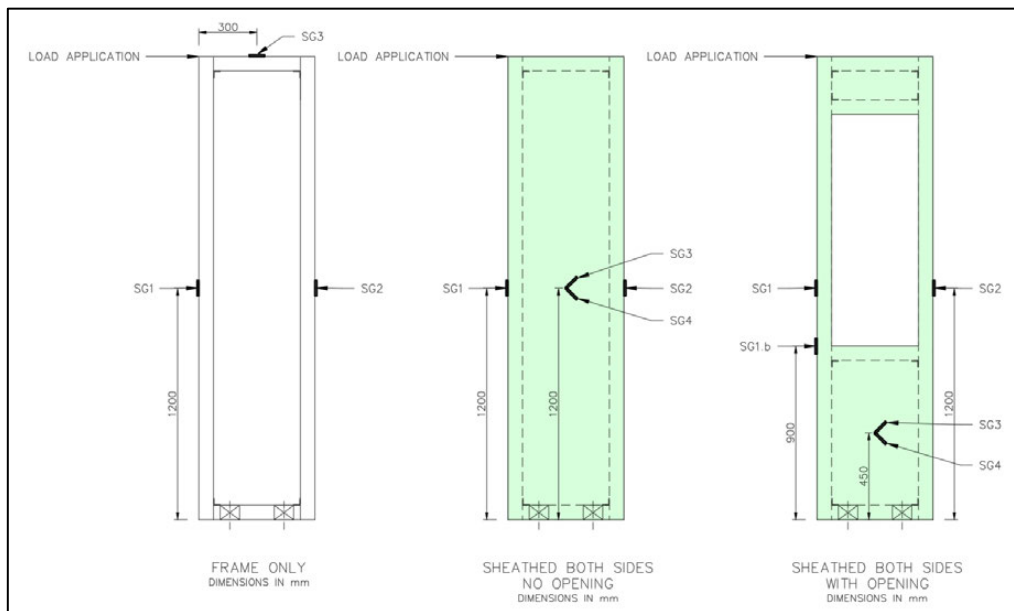


Figure 4-1: Load application locations

4.2 Results and Observations

4.2.1 Panel FE – Frame Only Panel

4.2.1.1 Load-Deflection Behaviour

The horizontal deflection of panel FE was measured at the top right-hand side, with the load-deflection behaviour shown in Figure 4-2. Under in-plane shear loading, panel FE deformed in shear with no noticeable rotation or uplift of the bottom plate. The deflection appeared to be elastic and linear, with low stiffness apparent. At a peak load of 469 N, deflection was 117 mm, after which the load was released. Once the load was completely removed, deflection remained at 32 mm. Whilst audible cracking occurred during the test, the cracking cannot be correlated with any particular change in the load-deflection behaviour of the panels or with any noticeable damage to the panel.

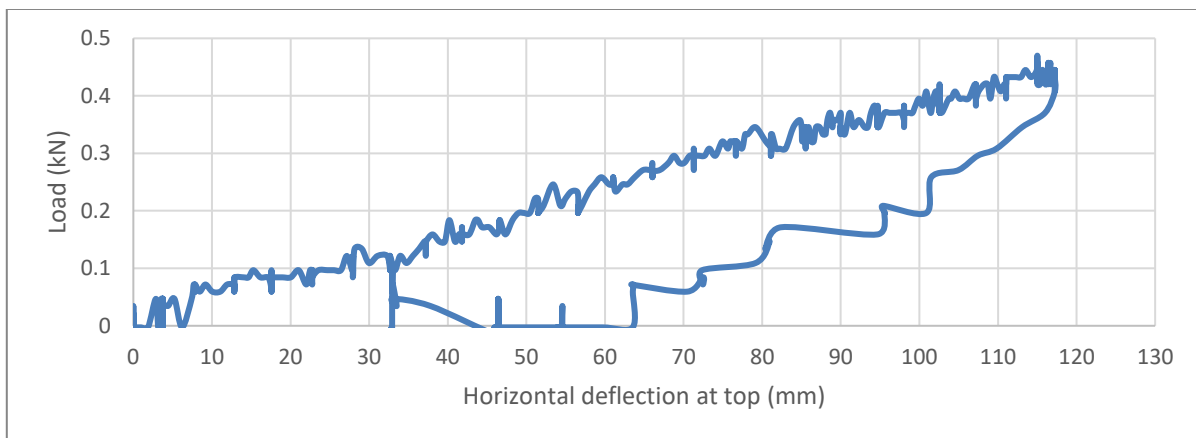


Figure 4-2: Load-deflection behaviour of panel FE

It is noted that the load-deflection curve does not produce a smooth, constant line, even though the overall behaviour is relatively linear and consistent. The irregularities are potentially due to a number of factors, including:

- The load magnitudes are low and therefore susceptible to small interferences
- The manual operation of the jack not allow for a constant rate of load application
- Slight stiction of the jack shaft, causing slight build-up of the load without deflection until the stiction was overcome, noting again the low load magnitudes

Whatever the cause, these irregularities are not considered significant given the overall consistent linear behaviour shown.

4.2.1.2 Failure Behaviour

Whilst audible cracking was exhibited as the load and deflection of panel FE increased, no major failure occurred during the testing. The hold-downs did not show signs of damage, and the riveted joints

showed no visible signs of pull out or bearing failure of the rivets against the walls of the RHS. However, upon release of the load, the panel remained slightly deformed and did not regain its original shape, as shown in Figure 4-3(a) and (b). This correlates with the residual deformation measured at 32 mm and noted in Section 4.2.1.1. During the testing, slight opening of the joint between vertical studs and the bottom plate and top plate occurred, as shown Figure 4-3(c) and (d). This indicates deformation of the SS brackets occurred and that there may have been some minor plastic deformation of the bracket, contributing toward the residual deformation of the whole panel after the load was removed.

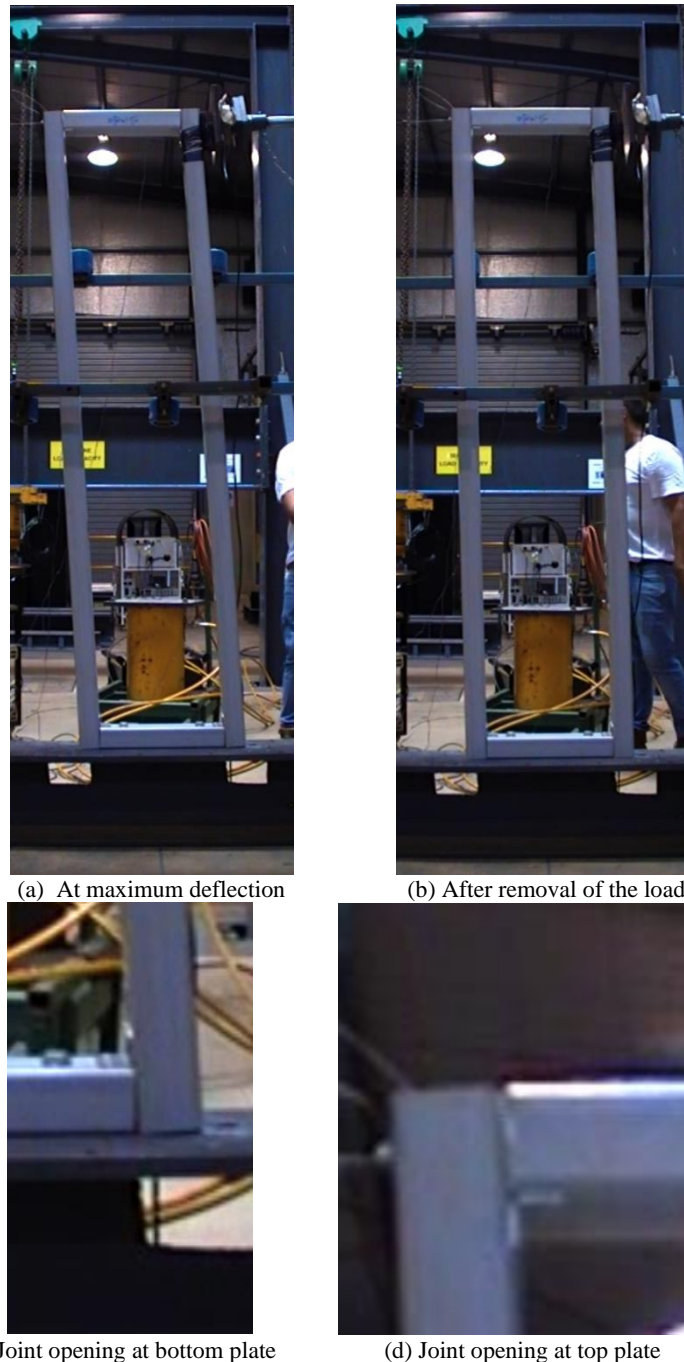


Figure 4-3: (a)-(b) Deformed shape of panel FE during and after loading, and (c)-(d) opening of joint between vertical stud and bottom plate and top plate

4.2.1.3 Load-Strain Behaviour

The load-strain behaviour of panel FE is shown in Figure 4-4. Upon loading, the left-hand side stud went into initial tension to a load of approximately 96 N and a maximum strain of 8.8 microstrain. After this, relatively linear behaviour occurred and strain reversed into compression to a peak load of 469 N and strain of -112.7 microstrain. The right-hand side stud remained in compression at all times and also showed relatively linear behaviour to a peak strain of -172.9 microstrain. The top plate showed minimal initial strain to a load of about 100 N, followed by linear compressive behaviour to a peak strain of -107.3 microstrain. Peak strain in all gauges occurred at the maximum deflection of 117 mm.

The compressive strain values measured in the left-hand stud indicate that this stud was in reverse curvature bending; that is, the outside face of the stud being compressed and the inside face of the stud being extended. This phenomenon indicates possible moment connections between the vertical and horizontal studs, noting that the loads applied to the wall were relatively low and any moment connection may not act as such if higher loads were to be applied. This will be further considered in a later chapter with reference to FEA of the panel.

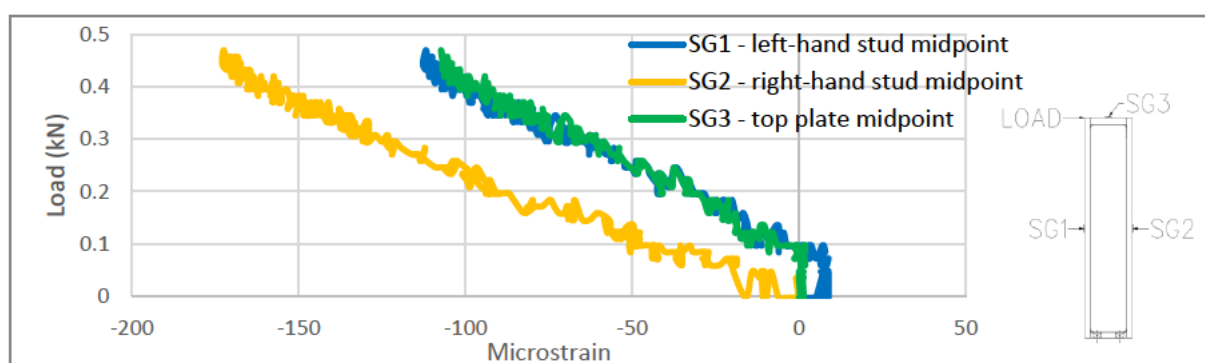


Figure 4-4: Load and strain behaviour of panel FE

The irregularities in the load-strain data are similar to that of the load-deflection data as discussed in Section 4.2.1.1, are not considered a significant factor.

4.2.2 Panel FSE – Fully Sheathed Panel

4.2.2.1 Load-Deflection Behaviour

The horizontal deflection of panel FSE was measured at the top right-hand corner, and is shown in Figure 4-5 below. Under in-plane shear loading panel FSE rotated around a point of rotation at the base of the right-hand vertical stud, and there was no significant sliding of the bottom plate. Uplift of the bottom plate occurred, highest at the left-hand end of the bottom plate on the same side as the load application. The bottom plate remained relatively straight and exhibited no visible signs of bending, with the amount of uplift appearing to linearly increase from the point of rotation to the left-hand corner. The wall continued to deflect until ultimate failure.



Figure 4-5: Panel FSE installed in testing frame

The load-horizontal deflection is shown in Figure 4-6. When loaded, the panel exhibited initial non-linear behaviour to a load of approximately 2.5 kN and a deflection of 8mm. After this, elastic linear deflection and stiffness was exhibited to a load of approximately 6.5 kN and a deflection of 26 mm. At the load of 6.5 kN a loud crack was heard and slight curvature of the load-deflection graph is shown, with decreasing stiffness as the load increased. This is considered the yield point of the panel. This loud crack may have been due to initial cracking and splitting of the wall of the RHS bottom plate or cracking of the bolt insert at the hold-down, both of which occurred in this panel and are shown in Figure 4-7 and Figure 4-8. After this, a reduction in stiffness was exhibited, shown by a decrease in the gradient of the load-deflection curve. The panel continued to show relatively linear behaviour between 7 kN and 8.7 kN. A number of loud cracks occurred at approximately 8-9 kN, which are also reflected by drops in load on the graph. The most notable of these cracks occurred at approximately 8.7 kN and a deflection of 49 mm. These loud cracking noises are considered to have been due to propagation of cracks in wall of the RHS bottom plate or the hold-down insert. After this point, the panel continued to resist load until failure at an ultimate load of approximately 11.6 kN and deflection of 80 mm, with stiffness remaining relatively linear during this final loading phase. Cracking continued to occur throughout this loading period, with a loud crack occurring between 9.5-10 kN. After peak load, the panel appeared to

lose load carrying capacity, shown by the downward slope on the graph. It is noted that during this test the hydraulic jack ran out of stroke at approximately 92mm.

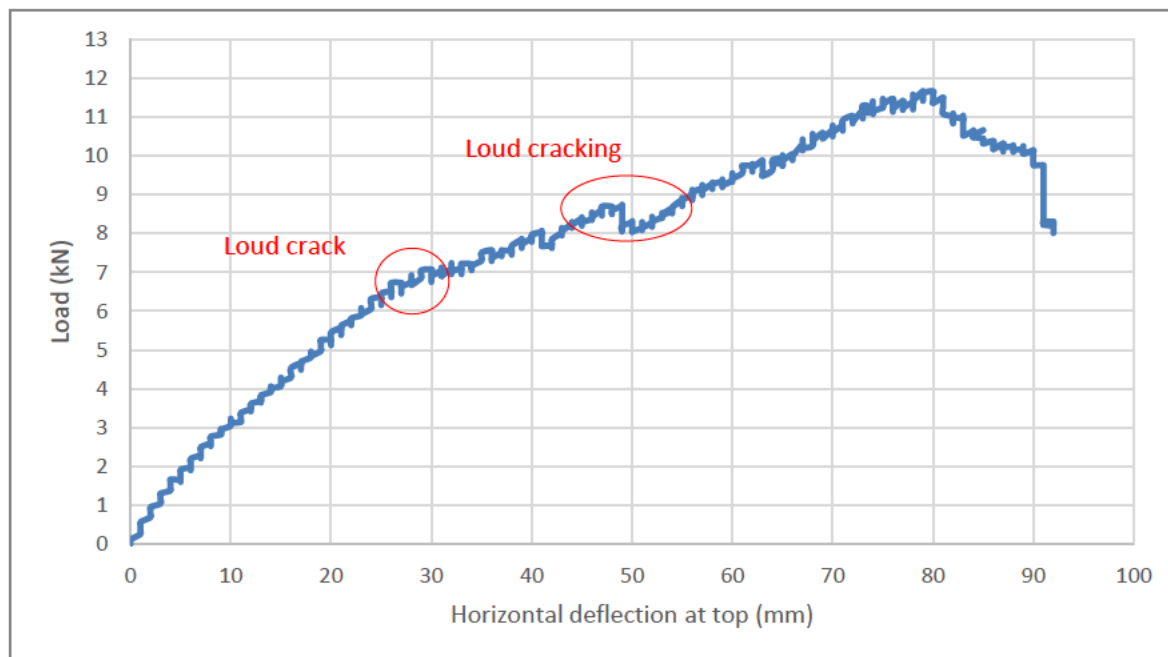


Figure 4-6: Load and horizontal deflection behaviour at top of panel FSE

4.2.2.2 Failure Behaviour

As noted previously, primary failure occurred at a load of 6.5 kN when audible cracking was heard. It is considered that this primary failure is associated with longitudinal cracks that developed in the bottom wall of the RHS bottom plate on both sides of the left-hand hold-down, as shown in Figure 4-7(a) and (b). This is a transverse failure of the bottom plate wall, indicating the development of high transverse tensile stresses in the section. At this location, the bottom wall of the bottom plate RHS section was subject to local outward bending, creating an apex in the centre of the wall in-line with the hold-down, shown in Figure 4-7(c) and (d). This bending caused tensile stress development on the outer surface of wall of the RHS, contributing to the transverse crack formation. At the wall-shank interface, minor crushing of the RHS wall against the hold-down also occurred, indicating horizontal load transfer from the wall to the bolt shank. The friction that resulted at this interface would have created a resisting, downward force when combined with the observed vertical uplift of the bottom plate. This frictional force is therefore considered to have contributed to the bending of the wall of the RHS, the development of transverse stresses, and subsequently toward the primary failure of the wall.

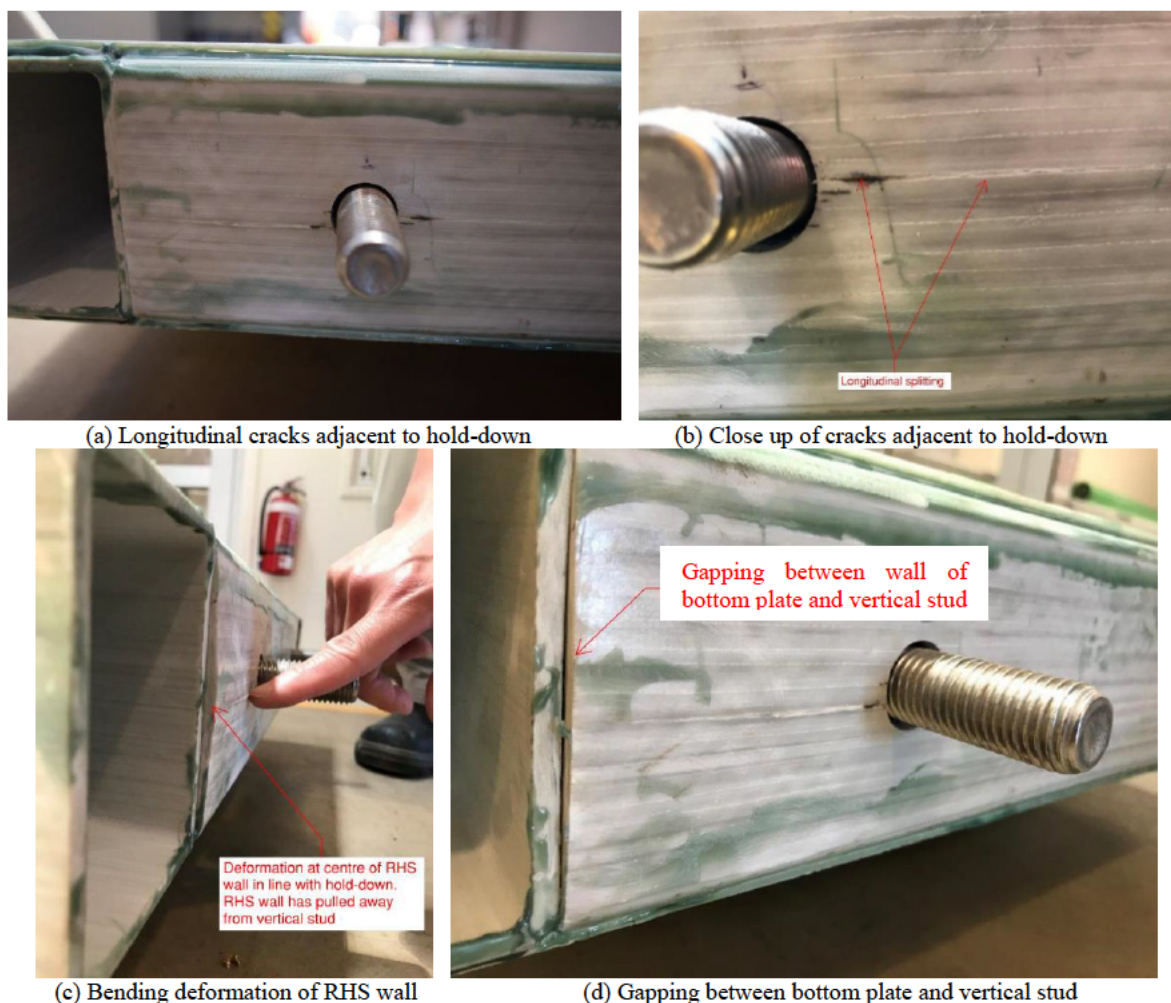
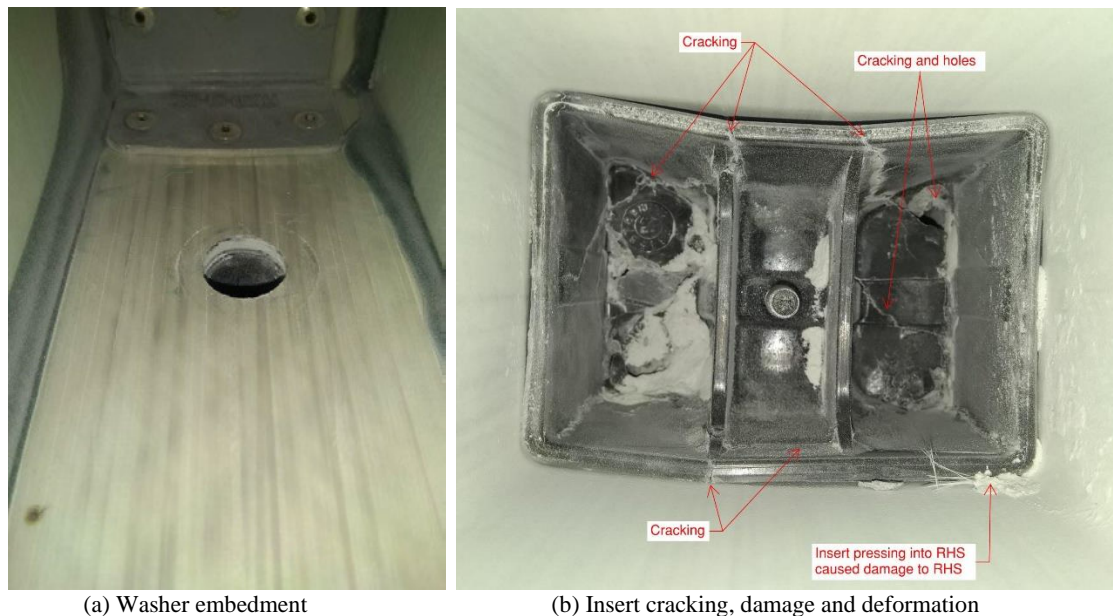


Figure 4-7: Failure of the RHS bottom plate at left-hand hold down, with (a)-(b) longitudinal splitting, (c) bending deformation, and (d) gapping between bottom plate and vertical stud, for panel FSE

Additional failure mechanisms at the left-hand hold-down include slight indentation of the bolt washer into the RHS, shown in Figure 4-8(a). The top wall of the bottom plate also showed signs of inward, concave deformation and the insert at this location had considerable cracking and fractures and remained deformed, see Figure 4-8(b). The cracking of the insert would have contributed toward the audible cracking heard during the testing. Residual deformation also shows that the top wall of the bottom plate deflected inwards and the bottom wall deflected outwards. More inward deformation at the top was noted than downward deformation on the bottom; this is to be somewhat expected as the washer and hold-down bolt are loading directly at the top of the RHS and causing deformation. Conversely, the bottom of the RHS is loaded through the insert which would aid in distributing the load across the width of the RHS, noting that deformation of the RHS at the base would also require deformation of the insert itself.



(a) Washer embedment (b) Insert cracking, damage and deformation
Figure 4-8: Additional failure mechanisms at left-hand hold-down include (a) slight washer embedment and (b) failure of the insert, for panel FSE

The right-hand hold-down washer showed minimal signs of deformation or damage; this is expected as this hold-down was under considerably less load than the left-hand hold-down. However, the insert at the right-hand hold-down had begun to crack, and slight deformation had begun to occur, with gapping remaining around the edges of the insert, see Figure 4-9.

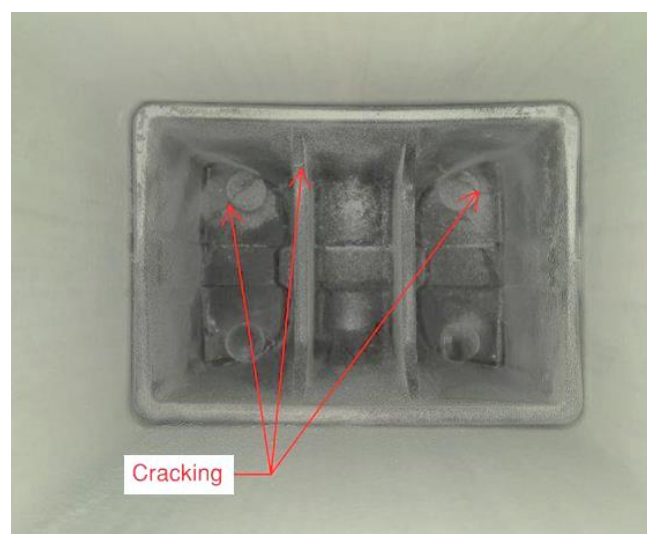


Figure 4-9: Cracking and slight gapping of the right-hand hold-down insert, for panel FSE

Minor compression crushing of the base of the right-hand side vertical stud against the supporting steel beam occurred, see Figure 4-10. This damage was localised and there was no indication of other cracking in this area or buckling of the stud.



Figure 4-10: Minor crushing of right-hand vertical stud, for panel FSE

No debonding of the sheathing from the frame or cracking of the sheathing was noted. Apart from the damage at the hold-down and minor crushing of the compression stud as outlined above, the panel appeared to generally be in the same condition as prior to testing.

4.2.2.3 Load-Strain Behaviour

The load and strain behaviour is shown in Figure 4-11. It can be seen that the strain gauge at the midpoint of the outside of the left-hand side stud (SG1) exhibited linear load-strain behaviour until approximately 118 microstrain and the yield load of 6.5 kN, correlating to audible cracking of the bottom plate or the hold-down insert and a change in gradient of the load-deflection graph. The gradient of the load-strain curve then increases to 183 microstrain and an 8.1 kN load, at which point further cracking was heard. This increase in the steepness of the curve indicates that some load was released from the left-hand stud after the occurrence of the initial cracking at the hold-down. This is supported by comparison with the load-deflection curve which showed a reduction in global stiffness of the panel itself, suggesting deflection was occurring due to deformation at the bottom plate and hold-down and not through deformation of the panel as a whole. A final linear portion occurs until a maximum of 193 microstrain at the ultimate load of 11.6 kN, at which point the panel failed. The slope of the final section prior to ultimate load appears similar to that of the initial section prior to yielding.

In contrast, strain gauge SG2, at the midpoint of the right-hand stud, exhibits near constant linear behaviour, reaching -124 microstrain at the yield load of 6.5 kN and increasing to a peak strain of -213 microstrain at the ultimate load of 11.6 kN. After ultimate load, the strain values reduce to 134 and -136 microstrain in the tension and compression studs respectively. The positive and negative sign strain values for the left and right-hand side studs respectively is to be expected and is typical of a panel undergoing in-plane bending and shear loading.

Strain gauges on the sheathing are characterised by an initial high stiffness up until a load of approximately 700 N where minimal strain is recorded. After this period, both the +45° and -45° gauges,

SG3 and SG4 respectively, exhibit linear behaviour, reaching 88 and -34 microstrain at the yield load of 6.5 kN, and increasing to a load of approximately 8 kN and microstrains of 110 and -40 respectively. After this point the strain behaviour is less linear, particularly in SG4 where strain drops to approximately -29 microstrain. This lack of linearity correlates with loud cracking that was heard during the testing, indicating that load on the sheathing was reduced when cracking at the hold-down occurred. Finally, after peak microstrains of 157 and -80 respectively at the ultimate load of 11.6 kN, the strain reduces until the end of loading to values of 8 kN and 115 and -44 microstrains. The positive and negative sign microstrains occurring in SG3 and SG4 respectively are expected and are typical of a sheathed panel undergoing bending and in-plane shear.

It is highlighted that after peak load the hydraulic jack continued to extend, even as the strain values reduced. This indicates that load on the studs and sheathing was reduced upon failure of the hold-down, and the subsequent horizontal deflection was due to rocking rather than bending and in-plane shear deflection.

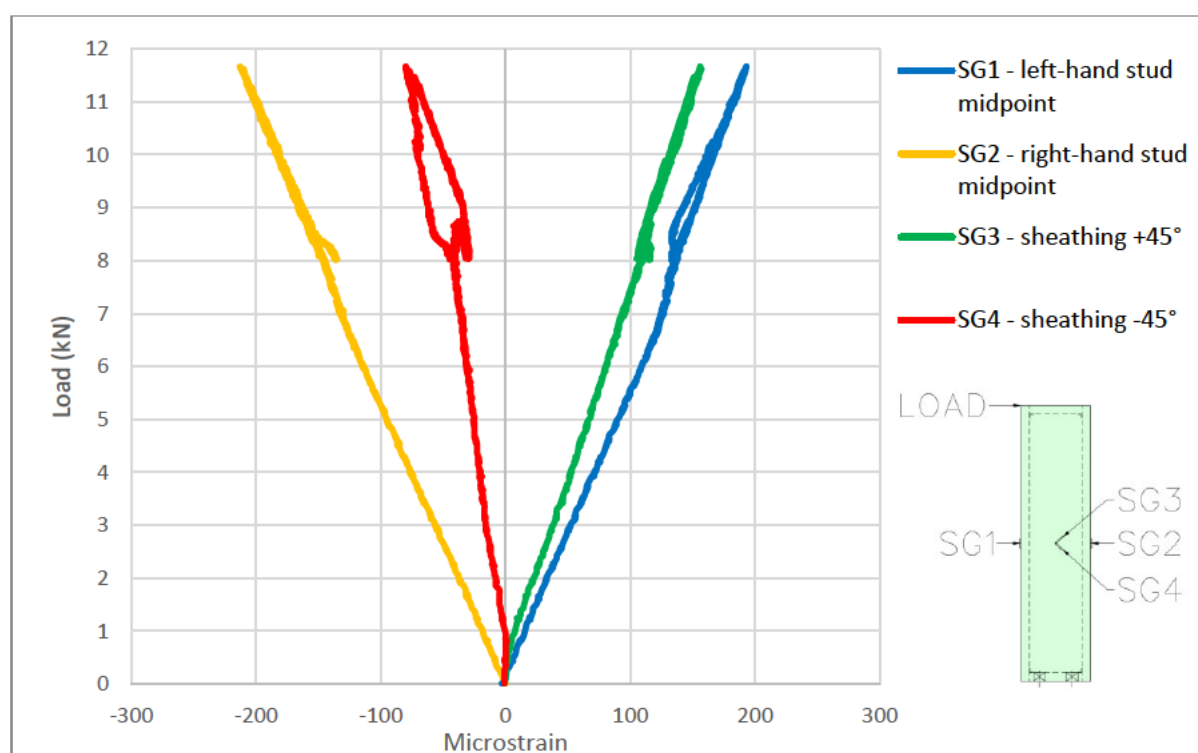


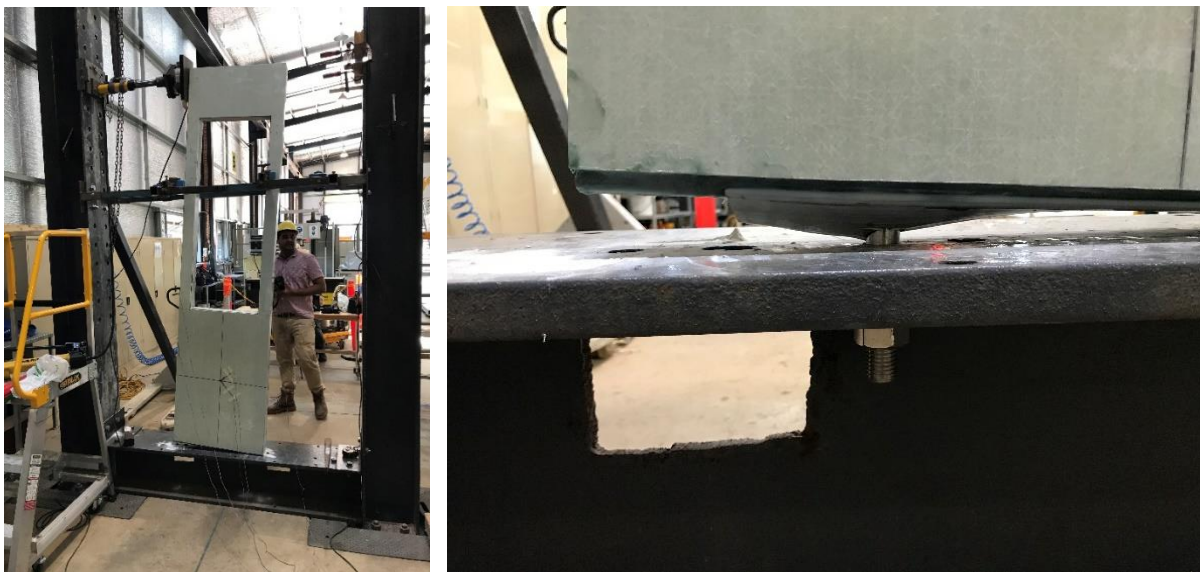
Figure 4-11: Load and strain behaviour of panel FSE

4.2.3 Panel FSO_{37.5E} – Sheathed with Window Opening

4.2.3.1 Load-Deflection Behaviour of Whole Panel

It is noted that for panel FSO_{37.5E}, horizontal deflection was measured at the top right-hand corner as well as both vertical and horizontal deflection at the four corners of the opening. This section addresses load-deflection behaviour of the whole panel.

Under in-plane shear loading panel FSO_{37.5E} rotated around a point at the base of the right-hand vertical stud, see Figure 4-12(a), and there was no significant sliding of the bottom plate. The panel also appeared to bend at the base of the opening, with the two vertical studs acting as cantilevers fixed at the base of the opening. Uplift of the bottom plate occurred, highest at the left-hand end of the bottom plate on the same side as the load application, see Figure 4-12(b). The bottom plate remained relatively straight and exhibited no visible signs of bending, with the amount of uplift appearing to linearly increase from the point of rotation to the left-hand corner. The wall continued to deflect until ultimate failure.



(a) Global deflection and rotation of panel

(b) Uplift of bottom plate at left-hand side

Figure 4-12: (a) Global deflection and (b) uplift of panel FSO_{37.5E}

The load-horizontal deflection at the top of panel FSO_{37.5E} is shown in Figure 4-13. When loaded, the panel exhibited relatively linear behaviour and stiffness up to a load of approximately 5.5 kN and a deflection of 36 mm, at which point load cracking occurred. This load crack is considered to have been due to initial cracking and splitting of the wall of the RHS bottom plate or cracking of the bolt insert at the hold-down, both of which occurred in this panel and are shown in Figure 4-17 and Figure 4-19. A reduction in stiffness followed, shown by a decrease in the load-deflection slope gradient. This is considered the yield point of the panel. The panel then showed non-linear behaviour between 5.5 kN and 6.5 kN and a deflection of about 61 mm, followed by an increase in stiffness to a load of about 9.3 kN and a deflection 91 mm. A number of load cracks occurred at approximately 8 kN and 9 kN, the latter of which is reflected in the graph by a change in the curve slope. These load cracks are considered to have been due to propagation of cracks in wall of the RHS bottom plate or the hold-down insert. After this point, the panel continued to resist load until failure at an ultimate load of approximately 9.8 kN and deflection of 108 mm. After ultimate load, the panel lost load carrying capacity, shown by the downward slope on the graph, with a significant drop in load occurring at a deflection of 115 mm. The

panel continued to deflect until the end of the hydraulic jack's stroke, at which point the panel deflection was 145mm.

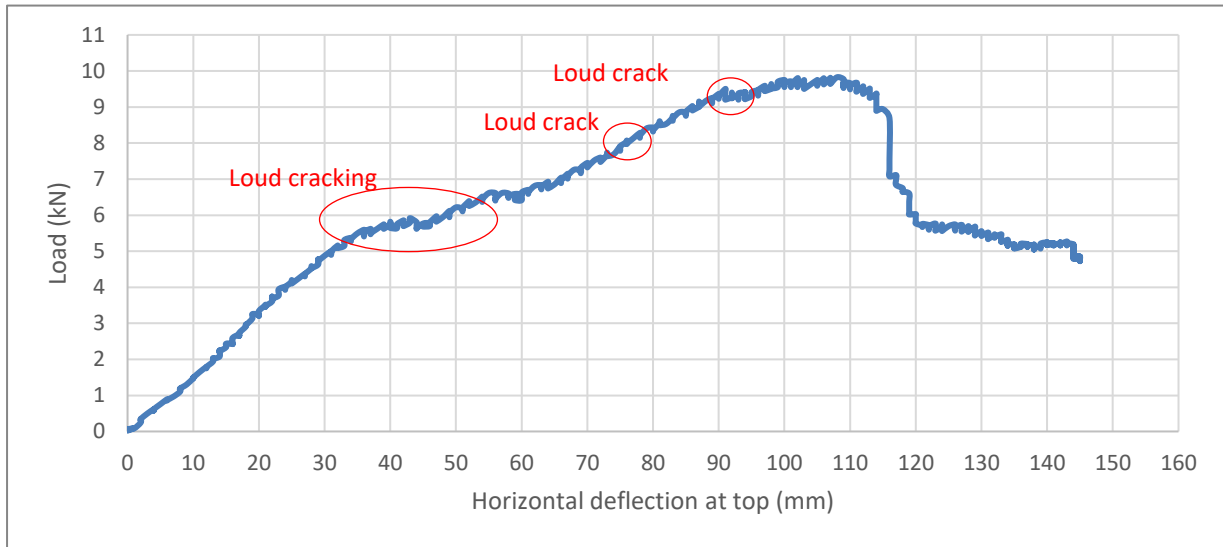


Figure 4-13: Load and horizontal deflection behaviour at top of panel FSO_{37.5E}

4.2.3.2 Load-Deflection Behaviour of Opening Corners

Load-deflection behaviour at the corners of the window opening was recorded by the DIC camera in both the vertical and horizontal direction, as shown in Figure 4-15 and Figure 4-16. With reference to Figure 4-14, note that ‘TL’ stands for ‘top left’, ‘BL’ stands for ‘bottom left, and so on. Positive vertical deflection is taken as upward, and negative is taken as downward.

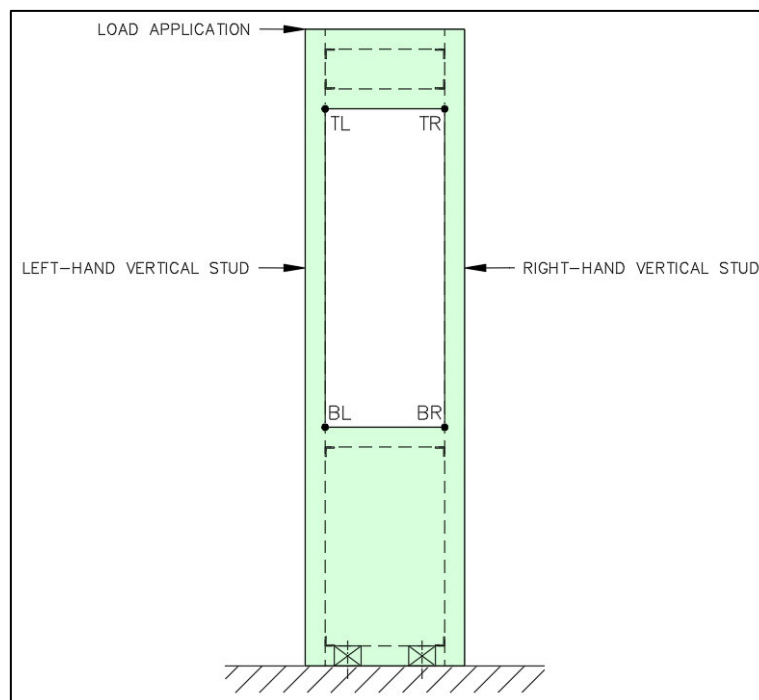


Figure 4-14: Points of measurement by DIC camera of deflection of opening corners

4.2.3.2.1 Horizontal Deflection at Opening Corners

Load-horizontal deflection of the opening corners is shown in Figure 4-15, along with the deflection at the top of the panel. It can be seen that the TL and TR corners exhibited near identical behaviour, with an initial linear behaviour shown to a yield load of 5.5 kN and deflections of 31 mm. At this point audible cracking was heard, and non-linear behaviour occurred through to a load of about 6.5 kN and deflections of approximately 55 mm. Linear behaviour was shown until a load of about 9.3 kN and deflections of 80mm, at which point cracking was heard. Deflection continued through to 96 mm at the ultimate load of 9.8 kN at which point the panel failed. Maximum deflection was 131 mm after panel failure. The shape of the curves are similar to that of the top of panel deflection.

The BR and BL corners also behaved similarly to each other, with the BL generally exhibiting slightly more deflection than the right. Deflection at a yield load of 5.5 kN was 9 mm, at 6.5 kN was 16-17 mm, and at the ultimate load of 9.8 kN was 33-34 mm. After panel failure, maximum deflection was 51-52 mm. Throughout the duration of the test similar linear and non-linear behaviour to that of the other points occurred.

Due to their larger radial distance from the point of rotation at the toe of the right-hand side vertical stud, it is expected that the top corners will generally deflect more horizontally than the bottom corners, whether rotation, bending, or shear deformation occurs. As such, the fact that the top points deflected more does not inherently provide understanding of whether the panel underwent bending or if it remained as a perfectly rigid body. To determine this, further geometric analysis is required, taking into account both horizontal and vertical deflections.

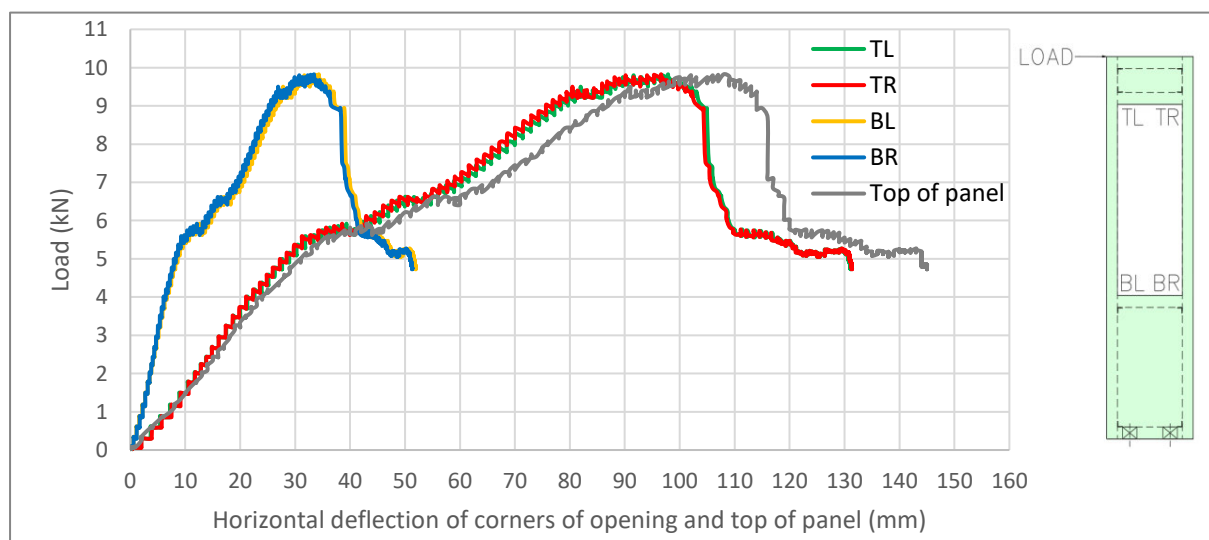


Figure 4-15: Load and horizontal deflection behaviour at the corners of the opening and top of panel
FSO_{37.5E}

4.2.3.2.2 Vertical Deflection at Opening Corners

The vertical deflection of the opening corners is shown in Figure 4-16. Upon loading, both the TL and BL corners underwent upward deflection. Initial deflection was characterised by linear but relatively stiff behaviour, with only 2.6 mm at the top and 3.7 mm at the bottom at a yield load 5.5 kN. After this, a non-linear period occurred, corresponding to audible cracking, to a load of about 6.5 kN and a deflection of 6.4 mm at the TL and 7.8 mm at the BL. A linear portion was again observed to a load of 9.3 kN and a deflection of 9.2 mm at the TL and 12.3 mm at the BL. The ultimate load of 9.8 kN occurred with deflections of 12.9 mm at the TL and 15.4 mm at the BL, after which the panel failed and vertical deflection continued to maximums of 25.8 mm at the TL and 24.5mm at the BL.

It is noted that the BL deflected vertically more than the TL for the majority of the test. There are three main possibilities of why this occurred. Firstly, as both points are rotating about the same centre of rotation, their relative position will affect the amount of vertical movement that occurs. Points at a lower angle to the centre of rotation, measured to the horizontal, will deflect more vertically than points at higher angles. For example, if a point is at the same level as the centre of rotation and is at 0° to the horizontal, rotation will primarily cause it to move vertically, with very little initial horizontal movement. On the other hand, a point directly above the centre of rotation and with an angle of 90° to the horizontal will move primarily horizontally upon rotation, with very little initial vertical movement. The BL has a lower angle and therefore may be expected to have more vertical displacement. Additionally, for a given change in angle, points with longer radial distances will deflect more than those with smaller radial distances but at the same angle from the horizontal. In this case, the TL has a longer radial distance. Finally, if shear deformation occurs and the opening itself is no longer rectangular, the top corners of the opening would move downward whilst the bottom corners would remain in place, apart from any rotation that was also occurring. This may have contributed to the TL generally showing less vertical deflection than the BL.

The TR and BR corners both underwent slight negative, downward vertical deflection. Deflection was relatively linear for both TR and BR corners, reaching -3.1 mm and -0.88 mm at a yield load of 5.5 kN for the TR and BR respectively, up until ultimate load of 9.8 kN and deflections of -6 mm and -1.4 mm for the TR and BR respectively. After peak load the wall lost load resistance, and the TR vertical deflection reduced to about -2 mm whilst the BR increased to -2.1mm.

The fact that the TR and BR both underwent downward vertical deflection is not unexpected for a number of reasons. Firstly, as the right-hand side stud is under compression, some slight downward deflection would be expected due to this side of the panel pressing into the support, noting that the panels did not sit perfectly flush against the supporting steel beam. Additionally, as these two points are offset only 75mm inward from the centre of rotation, downward vertical deflection is possible once the points pass over the centre of rotation, particularly for the TR which passed this point at a load of

approximately 8.7 kN. Finally, any shear deformation of the opening would have resulted in downward deflection.

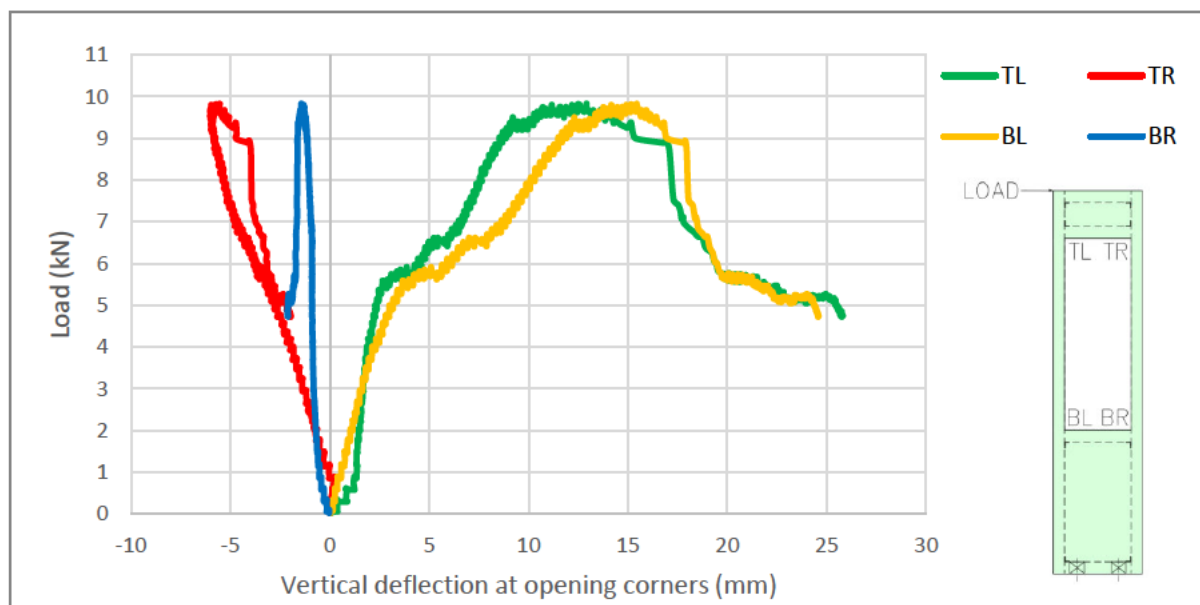


Figure 4-16: Load and vertical deflection behaviour of opening corners of panel FSO_{37.5E}

4.2.3.3 Failure Behaviour

As noted previously, primary failure occurred at a load of 5.5 kN when audible cracking was heard. It is considered that this primary failure is associated with longitudinal cracks that developed in the bottom wall of the RHS bottom plate on both sides of the left-hand hold-down, as shown in Figure 4-17(a) and (b). This is a transverse failure of the bottom plate wall, indicating the development of high transverse tensile stresses in the section. At this location, the bottom wall of the bottom plate RHS section was subject to local outward bending, creating an apex in the centre of the wall in-line with the hold-down, shown in Figure 4-17(c) and (d). This bending caused tensile stress development on the outer surface of wall of the RHS, contributing to the transverse crack formation. At the wall-shank interface minor crushing of the RHS wall against the hold-down also occurred, indicating horizontal load transfer from the wall to the bolt shank. The friction that resulted at this interface would have created a resisting, downward force when combined with the observed vertical uplift of the bottom plate. The deformation of the bottom of the RHS bottom plate was also noted to be higher on the left-hand side of the bolt, where the RHS is pressing against the shank, than on the right-hand side, as shown in Figure 4-18(a) and (b). This frictional force is therefore considered to have contributed to the bending of the wall of the RHS and subsequently toward the primary failure of the wall. It is likely that if the RHS could slide freely along the length of shank of the bolt, lower deformation would have occurred.

It is noted that longer and wider cracks appeared on panel FSO_{37.5E} as compared panel FSE, however this may be partially due to the fact that a longer jack stroke and therefore higher deflection was achieved with the panel FSO_{37.5E} than panel FSE.



Figure 4-17: Failure of the RHS bottom plate at left-hand hold down, with (a)-(b) longitudinal splitting, (c) bending deformation, and (d) gapping between bottom plate and vertical stud, for panel FSO37.5E

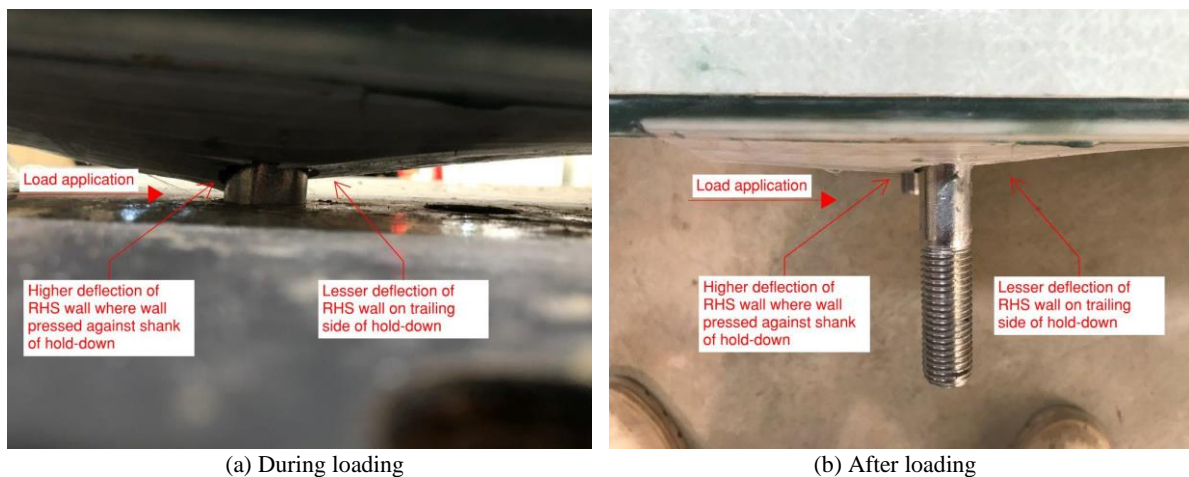
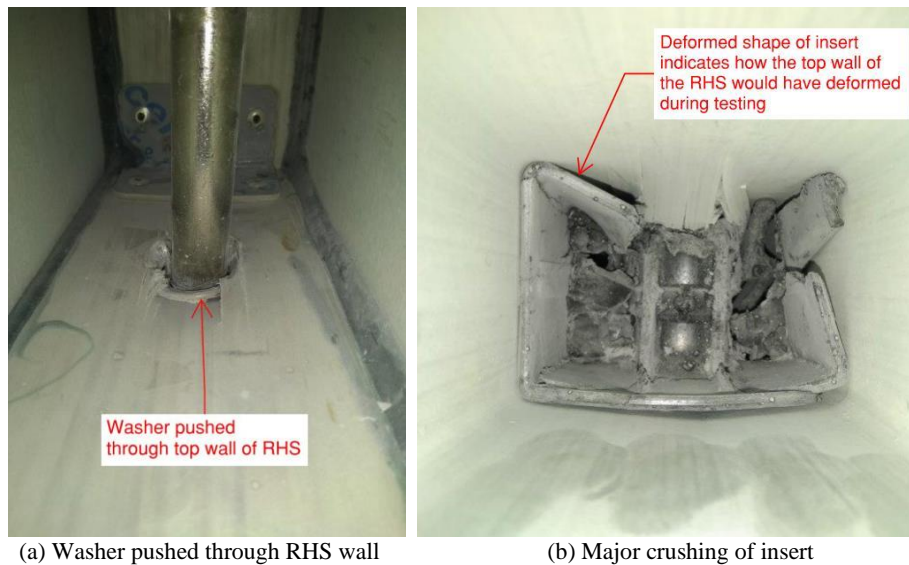


Figure 4-18: Deformation of the bottom wall of bottom plate was higher on side of loading, visible both (a) during and (b) after loading, for panel FSO37.5E

Additional failure mechanisms at the left-hand hold-down include failure of the washer, which had been pushed completely through the top wall of the RHS section, see Figure 4-19(a). Longitudinal splitting of the RHS section had also begun to occur. The hold-down insert had also failed significantly and was considerably cracked and crushed, see Figure 4-19(b). The shape of the crushed insert gives strong indication of the degree of deformation of the top wall of the RHS that occurred during testing, with the top of the insert being deformed at a sharp angle compared to its original shape. There was also residual

deformation of the RHS section, with the top wall deflection inwards and the bottom wall deflection outwards. The cracking of the insert is considered to have contributed toward the audible cracking heard during the testing.



(a) Washer pushed through RHS wall (b) Major crushing of insert
Figure 4-19: Failure mechanisms at left-hand side hold-down included (a) washer failure and (b) insert failure, for panel FSO_{37.5E}

The right-hand side hold-down washer showed minimal signs of deformation or damage; this would be expected as this hold-down was under considerably less load than the left-hand side. However, the insert at the right-hand hold-down had begun to crack, see Figure 4-20(a), and had begun to deform, leaving gapping at its edges in some locations. Minor compression crushing of the base of the right-hand side vertical stud against the supporting steel beam occurred, see Figure 4-20(b). This damage was localised and there was no indication of other cracking or buckling of the stud in this area.



(a) Slight cracking of right-hand insert (b) Minor crushing of right-hand vertical stud
Figure 4-20: (a) Minor cracking of the right-hand hold-down insert and (b) minor crushing at base of right-hand vertical stud, for panel FSO_{37.5E}

No debonding of the sheathing from the frame or cracking of the sheathing was noted. Apart from the damage at the hold-down and minor crushing of the compression stud as outlined above, the panel appeared to generally be in the same condition as prior to testing.

4.2.3.4 Load-Strain Behaviour

The load and strain behaviour is shown in Figure 4-21 below. It can be seen that the strain gauge at the midpoint of the outside of the tension, left-hand side stud (SG1) exhibits linear load-strain behaviour throughout the test, reaching a microstrain of 536 at a yield load of 5.5 kN - the limit of the linear deflection behaviour. Relatively linear behaviour continued until the ultimate load of 9.8 kN and 961 microstrain. After failure of the panel, strain reduced in a relatively linear manner to 462 microstrain and a load of 4.737 kN. It is noted that during the initial loading phase, at a load of 4.737 kN the microstrain was 451, negligibly lower than at the end of testing.

The strain gauge located on the tension stud adjacent to the base of the opening (SG1.b) exhibited very similar linear behaviour but at higher strains, with a microstrain of 779 at the yield load 5.5 kN, and 1458 microstrain at the ultimate load of 9.8 kN. Final strain after panel failure was 692 microstrain at a load of 4.737 kN. Strain during the loading phase at this load was 653 microstrain, a very small difference. It is noted that the strain at the base of the opening was considerably higher than that at the midpoint of the stud. This is expected for a structure acting as cantilevered beam, where higher stress and strain would be experienced closer to the restraint, which is at the base of the panel. It is also expected due to the lower stiffness and load carrying area of the section of panel with the opening, which will have resulted in higher load and strain concentrations at the corners of the base of the opening

Strain gauge SG2 at the midpoint of the compression stud, exhibited similar near constant linear behaviour, with a strain of -464 microstrain at a yield load of 5.5 kN, and a peak strain of -820 microstrain at an ultimate load of 9.8 kN. After peak load, the strain values reduced linearly to -381 microstrain. Corresponding strain at this load during the loading phase was -395 microstrain.

Strain gauges on the sheathing are characterised by an initial linear phase, with strains of 58 and -34 microstrain at an applied load of 5.5 kN for the +45° gauge (SG3) and -45° gauge (SG4) respectively. Linear behaviour continued up until a load of approximately 6.5 kN and microstrains of 71 and -38 respectively. This corresponds with a loud crack heard during testing, and after which a slight reduction in strain occurred. Linear strain was then exhibited to the ultimate load of 9.8 kN, with microstrains of 100 and -97 respectively. After peak load, strains reduced and at peak horizontal deflection strains had in fact reversed. Strain in SG3, typically in tension, reversed to -46 microstrain. Strain in SG4, typically in compression, reversed to 28 microstrain. For clarity, the strain on the sheathing alone is shown in Figure 4-22. This is of note, indicating that upon failure of the hold-down, load on the sheathing reduced significantly and then entered opposite sign loading. This indicates that after peak load the sheathed

section at the base of the panel was undergoing shear in the opposite manner to what typically occurs. This is likely due to the major failure of the left-hand hold-down and possible load transfer from this hold-down to the other, right-hand hold-down which was relatively intact in comparison. Once this occurred, it could be expected that the left-hand stud would have been pulled upward relative to the right-hand stud, causing the reverse shear deformation.

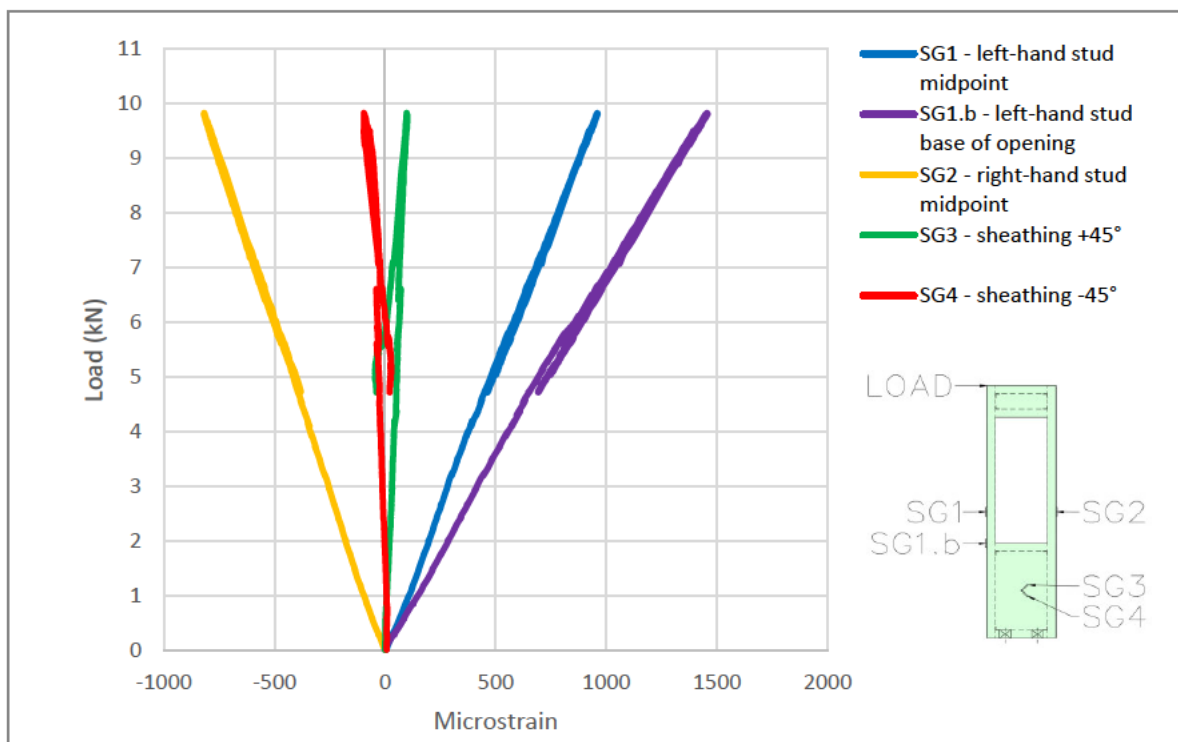


Figure 4-21: Load and strain behaviour of panel FSO_{37.5E}

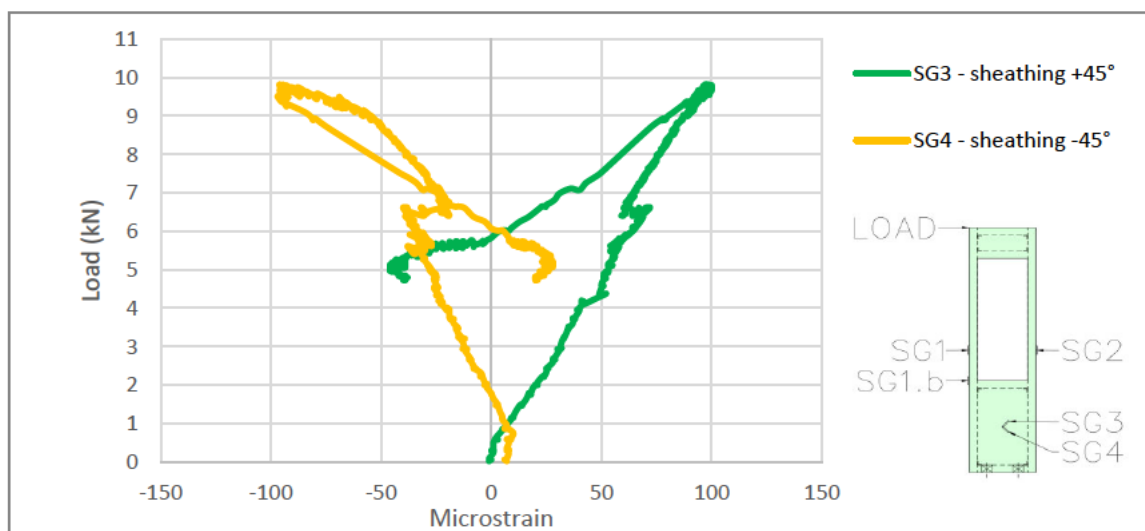


Figure 4-22: Load and strain behaviour of sheathing of panel FSO_{37.5E}

4.3 Analysis and Discussion

4.3.1 Introduction

The following section includes analysis and discussion of the results of the experimental investigation, comparing the results of the three experimental panels in terms of load-deflection and failure behaviour, as well as discussing other critical observations.

4.3.2 Effect of Sheathing and Openings on In-Plane Shear Stiffness

Comparison between the experimental panels was made to understand how sheathing and openings affect the in-plane shear behaviour of the wall system. Compared to both sheathed panels, panel FE exhibited starkly different behaviour and had a very low stiffness. This indicates that the sheathing contributed significantly toward the panel stiffness. There were no distinct changes in load-deflection behaviour throughout the loading for panel FE, which is expected as no distinct failure mechanisms were observed.

Panels FSE and FSO_{37.5}E showed similar load-behaviour, with initial relatively linear-elastic behaviour prior to yielding. Yielding was evident by a decrease in stiffness and audible cracking of the bottom plate and bolt insert at the hold-downs. Panel FSE showed noticeably higher stiffness through this initial elastic behaviour, and the primary failure occurred at a load of 6.5 kN, higher than the 5.5 kN of panel FSO_{37.5}E. After primary failure, both panels continued to resist loads until ultimate failure at 11.6 kN and 9.8 kN respectively, approximately 180% of their respective primary failure loads. During this loading period, both panels showed non-linear behaviour and exhibited propagation of the cracks in the bottom plate. After ultimate failure, both panels lost load carrying capacity. Whilst maximum final deflection for panel FSO_{37.5}E was considerably higher than panel FSE, this was due to the hydraulic jack shaft failing to continue to extend when testing FSE, whilst for panel FSO_{37.5}E a longer stroke was achieved. Based on the above, it is considered that the presence of an opening had minimal influence on the in-plane deflection behaviour, however the stiffness was affected.

To quantify the influence that the presence of sheathing and openings have on in-plane shear stiffness, the global shear stiffness of the panel can be calculated using Equation 4.1, as outlined in ASTM E564-06 (ASTM International 2006). The global stiffness includes rotational, translational, and shear deformational deflection of the wall.

$$G' = \frac{P}{\Delta} \times \frac{a}{b}$$

Equation 4.1

where: P = applied load (kN)
 Δ = horizontal deflection or displacement of the top of the wall (m)
 a = height of the panel (m)
 b = width of the panel (m)

As noted in ASTM E564-06, the values of P and Δ are taken from the linear portion of the wall’s deflection. Similar to both Manalo (2013) and Branco, Matos and Lourenço (2017), a value of $0.4P_u$ will be used to calculate the stiffness of the walls, along with its respective displacement $\Delta_{0.4P_u}$. The global stiffnesses of the experimental panels are shown in Table 4-1 and Figure 4-23, noting that for panel FE the peak load was used as no failure occurred and the panel behaved in a linear manner throughout its loading.

As can be seen, the presence of sheathing on panel FSE increased the stiffness to approximately 68 times that of panel FE. This result suggests that the sheathing provides most of the in-plane stiffness in the wall panel. As noted by Manalo (2013), this result is consistent with the expected behaviour of framed walls with thin sheathing, whereby the shear strength and stiffness is provided by the sheathing and the sheathing-to-frame connection is critical for the transfer of loads between the two.

The presence of an opening in panel FSO_{37.5}E resulted in a reduction in stiffness of about 40% to that of panel FSE, indicating that the percentage change in stiffness is closely related to the size of the opening. The impact of opening size on stiffness is discussed in more detail later with reference to FEA of the wall system, however it is apparent that openings result in a reduction in in-plane stiffness. This is consistent with the findings of previous research (Dujic, Klobcar & Zarnic 2009; Grossi, Sartori & Tomasi 2015b, 2015a; Anil et al. 2016; Abdullah et al. 2017; Shahnewaz et al. 2017; Husain, Eisa & Hegazy 2019).

Table 4-1: Global stiffnesses of experimental panels

PANEL	P_u (kN)	$0.4 P_u$ (kN)	$\Delta_{0.4P_u}$ (mm)	G' (kN/m)
FE	0.47	N/A	117	16.03
FSE	11.6	4.666	17	1097.88
FSO _{37.5} E	9.8	3.930	24	655

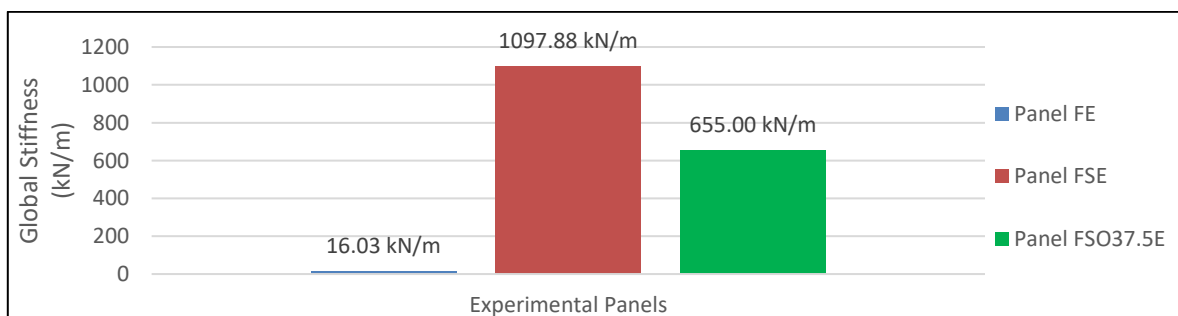
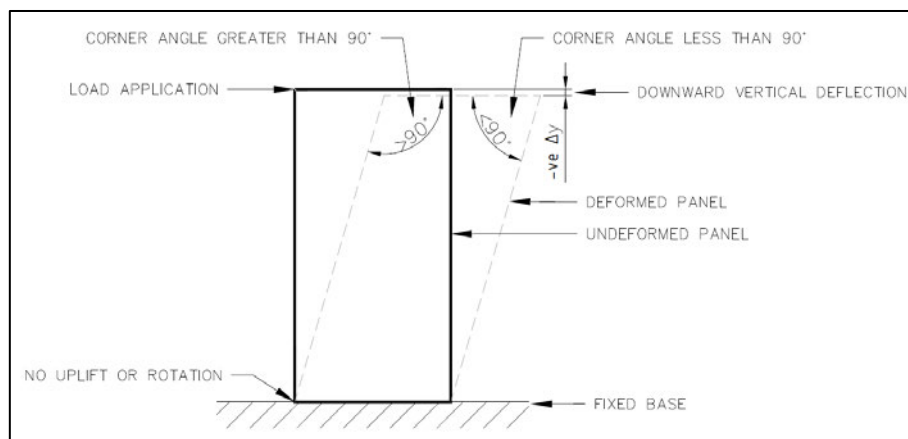


Figure 4-23: Global stiffnesses of experimental panels

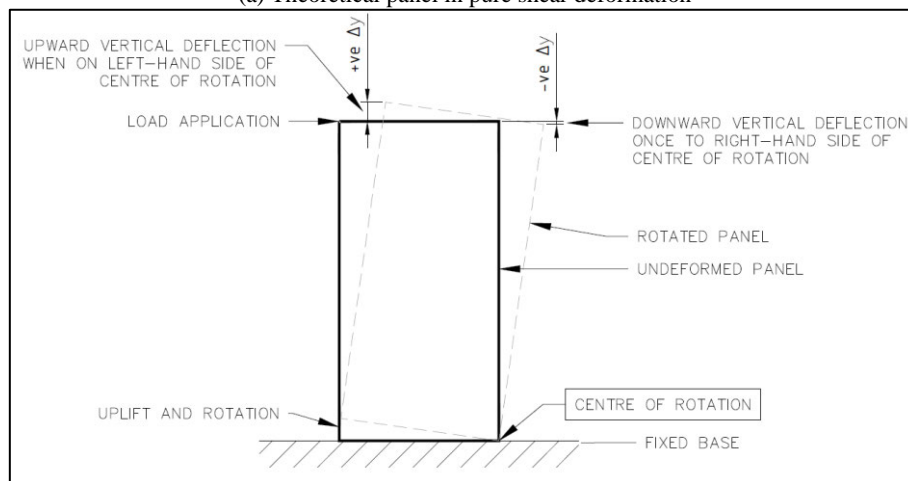
4.3.3 Effect of Openings on In-Plane Shear Deflection Behaviour

Analysis of the opening corner deflection data can show how much rotation occurred, how rigid the panel remained during loading, whether bending occurred along the length of the panel, and if the panel underwent shear deformation.

Referring to Figure 4-24(a), if the theoretical rectangular panel is in pure shear deformation, with no rotation or uplift, the top of the panel would deflect downward as the rectangular panel changes to a rhomboid with corner angles other than 90° . Conversely, as shown in Figure 4-24(b), in pure rotational behaviour, the panel would remain perfectly rectangular and the vertical deflections would be upward for any points that are to the left of a vertical line through the centre of rotation. Once the points pass to the right of the centre of rotation, vertical deflections would begin to reduce.



(a) Theoretical panel in pure shear deformation



(b) Theoretical panel in pure clockwise rotation

Figure 4-24: Behaviour of a theoretical panel in (a) pure in-plane shear deformation and (b) pure clockwise rotation

The opening in panel FSO_{37.5E} can be analysed in the same way as these theoretical panels by plotting the deflection of the corners of the opening. Comparison of the deformed shape of the opening with a perfectly rectangular shape will show if the panel underwent bending and shear deformation, or a combination of both.

Figure 4-25 shows the deformed shapes at three different loads; at the yield load of 5.5 kN, at the ultimate load of 9.8 kN, and at the highest horizontal deflection at the end of the test and after failure. A perfectly rectangular, undeformed opening is also plotted, and has been aligned with the BL and BR corners of the deformed opening. As can be seen, the opening underwent shear deformation, with an angle between the theoretical, perfectly rectangular opening and the experimental, deformed opening of 0.475° at a load of 5.5 kN, 0.876° at 9.8 kN, and 0.413° at the end of the test, with the higher angle indicating larger shear deformations. More shear deformation occurred at the peak load as compared with the other points. This is expected as shear deformation requires strain and bending of the frame members and hence would require higher loads. After failure, applied loads reduced whilst deformation continued by the rotation mechanism, and less shear deformation occurred. Shear deformation of the opening will have also resulted in bending of the vertical frame members due to the relatively strong and stiff adhesion between the sheathing and frame which creates a fixed, moment type connection at the base of the opening.

Comparing these observations and results with the deformation of panel FSE, it is apparent that openings result in a combined rotation, shear deformation, and frame bending behaviour. In contrast, when fully sheathed, rotation and possibly some minor shear deformation of the sheathing occurred, although the latter was observed but not measured. The addition of frame bending will change the stress distribution within frame members as compared to a fully sheathed panel. This will be explored further later with reference to the FEA undertaken.

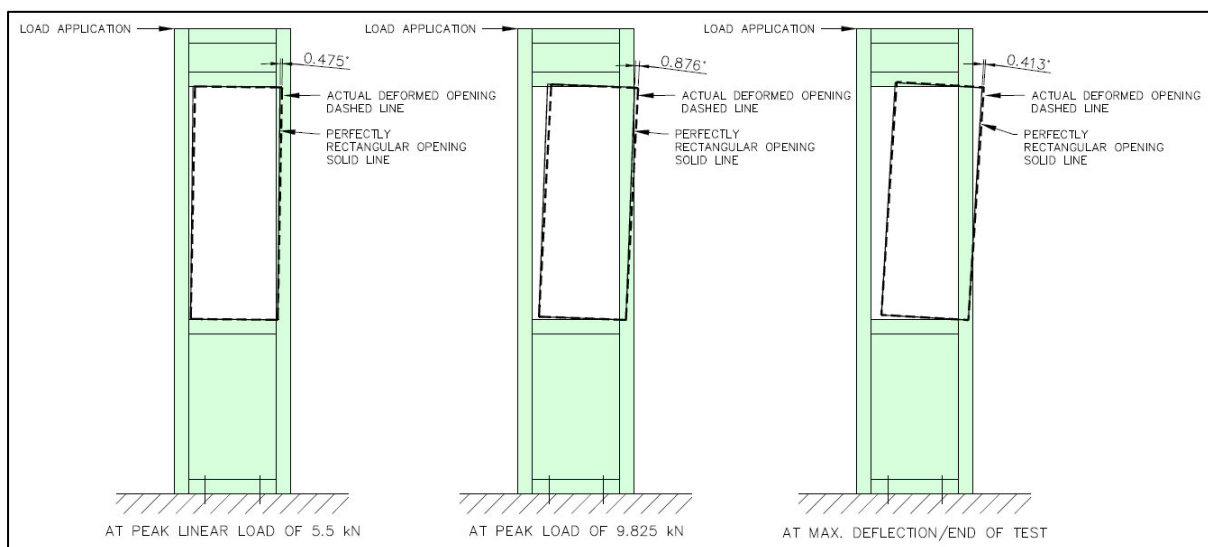


Figure 4-25: Deformed shape of panel FSO_{37.5E} opening at various loads

4.3.4 Effect of Sheathing and Openings on Failure Behaviour and Strength

4.3.4.1 Failure Modes

Panel FE did not fail during testing; however, plastic deformation of the angle brackets occurred due to the relative rotation between horizontal and vertical frame members. In contrast, the sheathed panels

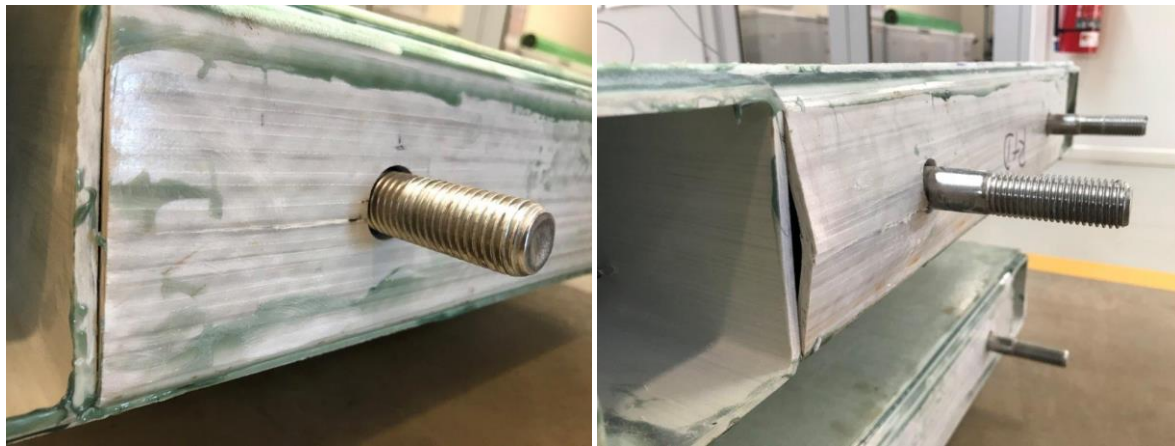
remained fairly rectangular in comparison. This shows that the presence of the sheathing results in a more rigid structure that acts as a cantilever beam, whilst the unsheathed panel behaved like a frame with a combination of fixed and pinned connections, which places strain on the angle brackets.

Failure of both panels FSE and FSO_{37.5}E was governed by longitudinal splitting of the GFRP bottom plate adjacent to the left-hand hold-down, shown in Figure 4-26, and cracking of the bolt insert. The cracking of the bottom plate is considered to be due to the development of transverse tensile stresses, which were largely created by local bending of the wall of the RHS bottom plate. This bending occurred through the combined action of friction between the bolt and the RHS and uplift of the bottom plate. Such tension failure in the weaker transverse direction is recognised as a common failure mode for thin walled GFRP profiles (Hizam et al. 2018). In comparison with testing undertaken by Hizam et al. (2018, 2019) on similar GFRP structures with bolted connections, in this case other failure modes such as shear out or bearing failure did not occur. This is not unexpected given the comparatively low applied loads and that edge distances were relatively high. However, in contrast with Hizam et al. (2018, 2019), the tension failure was exacerbated by local bending of the RHS. It is considered that had this local bending not occurred, higher strengths may have been achieved. The initial cracking of the bottom plate caused yielding and a subsequent reduction in stiffness in both panels, although they continued to carry load. Ultimate failure was brought on by propagation of this longitudinal cracking and further degradation of the insert to a point at which the bottom plate was no longer able to carry the load placed on it by the hold-down.

Whilst a high degree of bolt insert crushing and washer bending was observed for panel FSO_{37.5}E when compared to panel FSE, this is likely due to the longer extension of the hydraulic jack shaft. As the shaft extended further, higher final deflection was able to be achieved for panel FSO_{37.5}E compared to panel FSE. It is considered that if a higher jack extension was achieved for panel FSE, similar damage and washer pull-through would have occurred. As such, the high degree of damage is not considered to be due to the presence of an opening.

Based on the consistent failure behaviour between the panels, it is considered that the failure mode observed was not influenced by the presence of an opening with an area of 37.5% of the panel area. It is noted that in previous research, the presence of openings often results in a change in failure behaviour, with cracking at the corners of openings a common occurrence (Richard et al. 2002; Kozem Šilih & Premrov 2012; Grossi, Sartori & Tomasi 2015b, 2015a; Anil et al. 2016). However, in this case the weakest component remained the hold-down arrangement. It is also noted that standalone walls with no vertical restraint or compressive load will likely have higher reaction loads on the hold-downs and are more likely to fail at the hold-down. In reality, shear walls will have vertical loads and restraint through attachment to upper floor or roof structures and adjacent walls, which will reduce loads on the hold-downs and therefore the hold-downs may not be the critical point in terms of failure (Liew, Duffield &

Gad 2002). Testing of the GFRP wall system with vertical applied loads would be useful to explore this further, but is beyond the scope of this project. However, the potential impacts that improving the hold-down arrangement and increasing the opening size may have on the failure mode of the wall system is explored later with reference to the FEA undertaken.



(a) Panel FSE

(b) Panel FSO_{37.5E}

Figure 4-26: Consistent failure mode of splitting of bottom plate for panels (a) FSE and (b) FSO_{37.5E}

No apparent failures of the sheathing-to-frame adhesive were noted during the testing for either panel FSE or FSO_{37.5E}. This is similar to the results obtained by Manalo (2013), and indicates that the structural adhesive was effective in transferring the in-plane loads carried by the sheathing to the frame members. This ensures the capacity of the sheathing itself is more fully utilised, but can result in brittle and undesirable failure modes (Liew, Duffield & Gad 2002; Grossi, Sartori & Tomasi 2015b, 2015a). Gradual, ductile failure of sheathing-to-frame connection is a preferred failure mode but was not observed in this testing. It is noted that this result is also in contrast to the findings of Manalo (2013), who experienced brittle tensile failure of the sheathing and buckling of the compression stud due to the high strength of the adhesive and ability of the panel to withstand high loads without earlier failure. This is likely due to the relatively higher strength of GFRP sheathing used in this study compared to that of brittle and low strength MgO boards used by Manalo (2013). The failure experienced at the hold-down is considered preferable in terms of ductility to sheathing or buckling failure, however overall strength may not be as high.

4.3.4.2 Failure Strength

The applied loads on panels FSE and FSO_{37.5E} were 6.5 kN and 5.5 kN at primary failure and 11.6 kN and 9.8 kN at ultimate failure respectively, a difference of about 16%. Whilst this may indicate that the presence of an opening reduces the strength of the panel, such a conclusion is not considered to be accurate, as is outlined below.

The bottom plates remained relatively straight and rigid during the loading. Similarly, the panels themselves remained relatively rigid, and behaved much like cantilever walls. On the principle that the loads on each hold-down are directly proportional to the deflection of the bottom plate at each hold-

down, the loads applied to the left and right hold-downs would be approximately linearly related to their distance from the point of rotation of the bottom plate, as illustrated in Figure 4-27. This would result in the right-hand hold-down can be estimated to carry carrying a load with a magnitude of 36.36% of the load carried by the left-hand hold-down, based on the ratio of its distance from the point of rotation (160 mm) to that of the left-hand hold-down (440 mm). To maintain static equilibrium, the resultant reactions in each hold-down must oppose the moment created by the applied horizontal load, with a smaller applied load resulting in smaller hold-down reaction loads. In other words, if the same load were applied to each panel, it is considered that the hold-down reactions would also be roughly equal between panels. As panel FSO_{37.5E} had a lower applied load than FSE, the force in the left-hand hold-down would have also been lower. For this not to have been the case, the left-hand hold-down would have had to carry a higher portion of the moment resisting load; however, based on statics and experimental observations, there is limited evidence to support such an occurrence. As such, on the assumption that transverse stresses that caused failure of the bottom plate were proportional to the load on the hold-down, the lower strength of FSO_{37.5E} is not considered to be due to the presence of the opening and was likely the result of another influence. This theory will be explored further with FEA in Chapter 5, where an accurate FEM will provide a more reliable indication of the loads on the hold-downs.

In consideration of possible causes of the difference in failure strengths between the panels, the brittle nature of GFRP as a material and its relatively low strength in the transverse direction may have had an effect. Alternatively, a manufacturing error or anomaly in the quality of the bottom plate RHS between the two panels may account for the difference. Finally, the local bending of the wall of the RHS caused by friction at the bearing point on the bolt shank may not be conducive to linear, predictable behaviour, and any catching of the RHS against the bolt due to slight anomalies in the touching surfaces may have resulted in higher bending stresses. To further explore this and reduce the uncertainty around the failure strength of the panels, testing of additional specimens would be required.

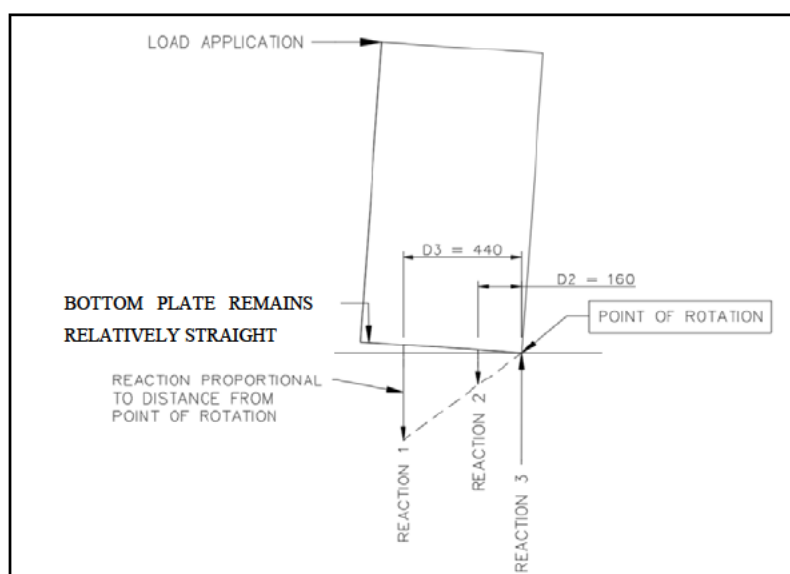


Figure 4-27: Rigid bottom plate hold-down reaction theory, indicating linearly proportional loads on left and right-hand hold-downs

4.3.5 Effect of Sheathing and Openings on In-Plane Shear Ductility

Ductility of structural components is a desirable characteristic, and a reduction in brittle failure improves the safety of a structure. Achieving a progressive, ductile failure with FRP structures is an area of ongoing research and interest (Bank 2013). Analysis of the ductility of this system is therefore of interest.

As per Husain, Eisa and Hegazy (2019), a displacement ductility ratio Δ_u/Δ_y can be used to evaluate the ductility of a structure, where Δ_u is the displacement at 85% of the ultimate load and Δ_y is the displacement at yielding. The ductility ratio for panels FSE and FSO_{37.5}E are shown in Table 4-2. As can be seen, there is a reduction in ductility between panel FSE and FSO_{37.5}E of about 10%. It is noted that Anil et al. (2016) found that openings actually increased the ductility of panels, in contrast with this result. The results are therefore considered to be inconclusive, noting that there is a relatively small difference in ductility and only three panels were tested. More testing would be required to be more conclusive with respect to the effect of openings on the panel ductility.

Whilst these ductility ratios are lower than that achieved by some other wall types, which are typically in excess of 3 for sheathed panels (Branston, Boudreault, et al. 2006; Branco, Matos & Lourenço 2017), it still represents moderately ductile and progressive failure behaviour. This is a good result, as a major industry concern is the brittle nature of FRP structures (Bank 2013). In contrast, PUF framed walls with MgO sheathing tested by Manalo (2013) showed poor ductility and brittle failure of the sheathing in tension. This indicates that failure of the hold-down represents a somewhat ductile failure mode and is preferred to failure of the sheathing itself. On the other hand, progressive failure exhibited by nailed type sheathing-to-frame fixation is more desirable still. It is considered that if improvement to the

strength of the hold-down system were undertaken, consideration of the potential reduction in ductility or transfer to a more brittle failure mode would be required.

Table 4-2: Ductility ratio of experimental panels

PANEL	YIELD DISPLACEMENT, Δ_y (mm)	DISPLACEMENT AT 85% OF ULTIMATE LOAD, Δ_u (mm)	DUCTILITY RATIO Δ_u/Δ_y
FSE	26.5	80	2.45
FSO _{37.5E}	36	80	2.22

4.3.6 Effect of Sheathing and Openings on Load-Strain Behaviour

4.3.6.1 Frame Strain Behaviour of Sheathed Panels

Figure 4-28 shows the load-strain behaviour for the mid-point, outer face of the vertical frame members for panels FSE and FSO_{37.5E}. Both panels exhibited relatively linear-elastic strain in the vertical studs, and there are no notable, sudden changes in strain that would correlate with initial or ongoing splitting of the bottom plate. This indicates that the splitting of the bottom plate did not cause changes in the loads placed on the frame members. In the left stud, panel FSO_{37.5E} exhibited tensile strain approximately 4.5 times higher than panel FSE, and in the right stud, panel FSO_{37.5E} exhibited compressive strain approximately 6 times higher than panel FSE. This indicates that the presence of an opening results in higher tensile and compressive strain at the midpoint, outer faces of the left and right studs respectively. This correlates well with the deflected shapes of the panels, with the presence of an opening resulting in bending of the studs above the opening, with the studs behaving as beams. This bending would result in additional tension and compression being placed at these locations. There is no evidence of any plastic deformation of the frame members, with the strain returning through the same data points upon load reduction.

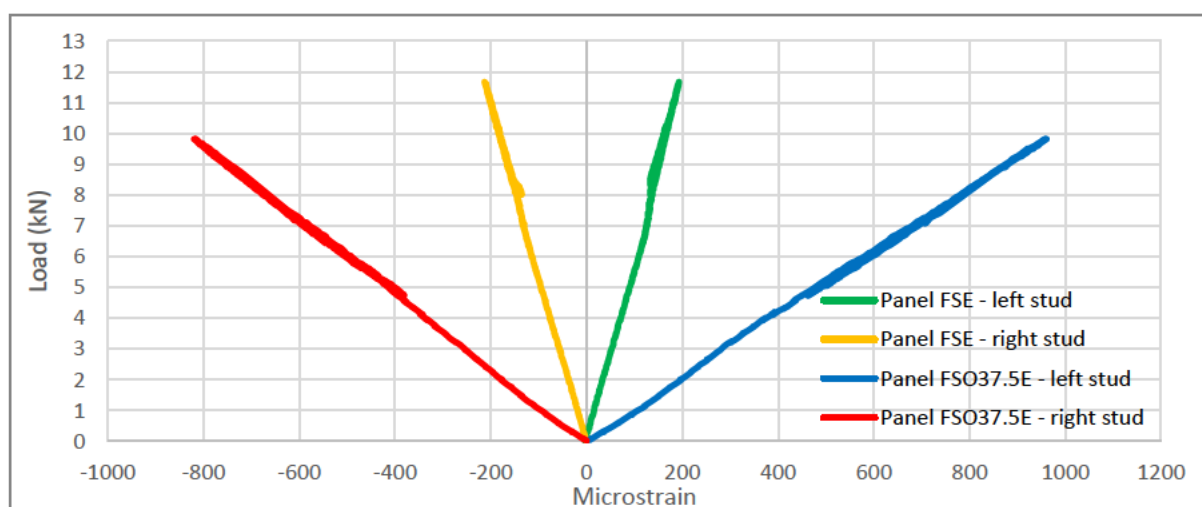


Figure 4-28: Combined frame load-strain behaviour for sheathed panels

4.3.6.2 Sheathing Strain Behaviour

The load-strain behaviour for the sheathing for panels FSE and FSO_{37.5E} is shown in Figure 4-29, as measured at the midpoint of the sheathed sections. In the +45° direction, panel FSE exhibited higher overall tensile strain than panel FSO_{37.5E}, whilst in the -45° direction panel FSE exhibited lower overall compressive strain than panel FSO_{37.5E}. Whilst these differences are considered to be due to the presence of an opening, on this evidence alone it cannot be concluded that openings necessarily cause an increase in the compressive strain and a decrease in the tensile strain. Rather, it is considered that the opening changes the aspect ratio of the sheathing, which results in a different stress distribution through the sheathing, and also creates a discontinuity for shear strain around the opening. It is also noted that the sheathing strain readings in panel FSO_{37.5E} showed greater sensitivity to the progressive cracking and failure of the bottom plate. This is indicated by the non-linear behaviour exhibited for much of the loading, which is in contrast to the predominantly linear behaviour exhibited by panel FSE. Again, this is likely due to the different stress distribution and noting that the strain readings for panel FSO_{37.5E} are taken closer to the bottom plate and any localised stress development that is associated with the hold-downs. More testing and data analysis would be required to investigate this further.

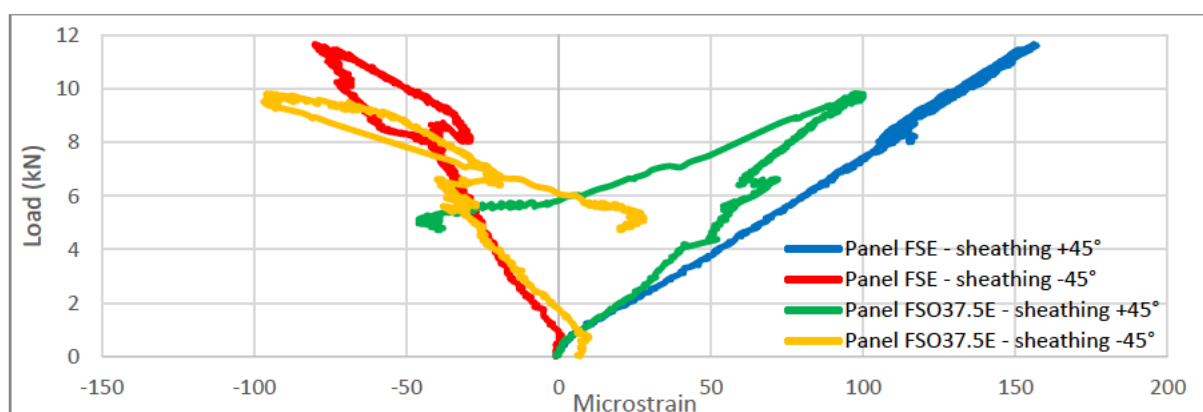


Figure 4-29: Combined sheathing load-strain behaviour for sheathed panels

4.4 Summary

The experimental testing has provided data and observations on the in-plane shear behaviour of the GFRP wall system with and without sheathing and openings. Using this data, comparison between panels has been undertaken, indicating how sheathing and the presence of openings affect the in-plane shear stiffness, load-deflection behaviour, failure behaviour, ductility, and frame and sheathing strain.

The panel with no sheathing exhibited minimal stiffness and behaved almost as a pin-jointed frame. In contrast, both sheathed panels showed elastic-linear deflection and stiffness to an initial yield point, and then continued to carry increasing loads to ultimate failure. Sheathing was found to increase the in-plane global shear stiffness by approximately 68 times when compared to a panel with no sheathing. When fully sheathed, the wall system behaved like a stiff, cantilevered beam, with limited shear

deformation. The panel with an opening behaved similarly but with added bending deformation above the opening, with the vertical frame members acting as cantilevered beams fixed at the base of the opening. With an opening size of 37.5% of the total panel area, the global stiffness was reduced by about 40% to that of a fully sheathed panel.

Both sheathed panels failed in a consistent manner, with the development of transverse stresses in the underside of the RHS bottom plate adjacent to the hold-down resulting in longitudinal splitting of the base plate and subsequent loss of in-plane load carrying capacity. These stresses were exacerbated by the local bending of the wall of the bottom plate bending due to the combined action of friction between the bolt shank and the bottom plate and the vertical uplift of the bottom plate. Cracking and crushing of the bolt insert was also noted in both panels. The sheathing-to-frame adhesive exhibited good load transfer and strength with no failures or cracking observed. The observed failure mode was found to be moderately ductile in comparison with failure modes of other panels with adhesive sheathing-to-frame connection, with load carrying capacity at ultimate failure of about 180% of the initial yield load. Ductility ratios for the sheathed panels were moderate, at about 2.2-2.4, and it is inconclusive as to whether the opening affected the ductility ratio. It is noted that these walls are not considered as ductile as other traditional construction wall systems with nail or screw type sheathing-to-frame fixation.

The frame strain behaviour for the frame only panel indicated a combination of pinned and fixed, moment connections at the joints, resulting in bending of the vertical frame members. However, overall loads and strain were very low. In contrast, both sheathed panels showed tensile strain on the outside of the left stud and compressive strain on the outside of the right stud. Linear elastic behaviour was observed for both panels. The presence of an opening resulted in an increase in strain of 4.5 to 6 times at the midpoint, outside face of the vertical frame members. This is explained by the bending of the frame members due to the opening, which increases the strain in the frame at the locations measured.

The overall sheathing strain behaviour between the fully sheathed and panel with an opening was similar, with tensile strain in the $+45^\circ$ direction and compressive strain in the -45° direction. It is noted that after ultimate failure, the panel with an opening exhibited opposite strain behaviour, indicating that the shear stress on the sheathing reversed. This is considered to be due to the longer hydraulic jack stroke and subsequent larger overall deflection that was achieved for the panel with an opening, and is not necessarily related to the presence of an opening.

The experimental results and observations will be used to develop and validate finite element models of the GFRP wall system, which will enable more extensive investigation of the in-plane shear behaviour to be undertaken, as is outlined in the following chapter.

Chapter 5 Finite Element Analysis and Parametric Investigation

5.1 Introduction

The experimental testing and results presented in Chapter 4 provide an understanding of how the GFRP wall system behaves when subject to in-plane shear loads. However, physical testings were limited to a small number of samples and configurations, and the limited number of measurements that could be made during the testing. Computer based finite element analysis enables a more extensive investigation to be undertaken to provide a deeper understanding of the GFRP wall system's behaviour. In this chapter, the methodology utilised to undertake this FEA in Strand7 will be outlined. Development and validation of the models will also be explained, followed by presentation of results and analysis of the parametric investigation whereby window opening sizes on sheathed panels will be varied and the impacts analysed.

5.1.1 Strand7 Software

Strand7 is a commercially available finite element modelling software in which models can be built, analyses run, and results reviewed. It has the ability to run both linear and non-linear analyses on elastic, orthotropic and isotropic materials. It also has an unlimited entity creation, allowing large and complex models to be constructed (Strand7 n.d.-a). For these reasons, Strand7 is considered suitable for this study.

5.1.2 Linear Elastic Analysis

The FEA undertaken in this project consists of linear elastic analysis. As such, any plastic and failure behaviour is not investigated. This is considered appropriate to further understand how the GFRP wall system behaves prior to failure when subject to in-plane shear. As such, material properties relating to elastic behaviour are required, whilst no plastic or post-failure behaviour information is used. The loads selected will also correspond to experimental loads prior to failure of the panels and within the elastic portion of the panels load-deflection behaviour. These are outlined in the relevant sections of Chapter 4 and are 0.47 kN for panel FE, 6.5 kN for panel FSE, and 5.5 kN for panel FSO_{37.5E}.

5.2 FEA and Parametric Investigation Methodology

In order for the results obtained from FEA to be considered reliable, care must be taken in developing the models. Appropriate analysis of the results provided by the FEA in the parametric study is then

required, ensuring the impacts parameter variation has on critical components of the wall system are considered. The basic methodology to undertake the FEA used in this study is as follows:

1. **Model Development:** Develop models of experimentally tested panels in Strand7, establishing how each physical component of the system will be modelled, including the frame, sheathing, adhesive, angle brackets, rivets, inserts, hold-down bolts, connections, contact points, applied loads, and boundary conditions and supports.
2. **Model Refinement:** Refinement of the model includes reducing mesh size to increase accuracy whilst managing computational time.
3. **Model Validation and Results:** Validation of the model against experimental results is then required to ensure the model is accurately reflecting the physical panel's behaviour. This validation will include use of load-deflection and load-strain data, as well as comparison of deflected shapes of the whole panel, joints, and connections. Often this is an iterative process and occurs somewhat concurrently with the model development, as validation often requires adjustments to the model.
4. **Develop and Undertake Parametric Study:** define the range of window opening sizes to be assessed and develop models of the panels with these variations
5. **Obtain and Analyse Results:** Obtain results for all window opening sizes, including deflection and stiffness of the whole panel, loads on hold-down bolts, as well analysis of stress concentrations and potential failure points. Analyse the results to ascertain how variation in the opening size changes the panel's behaviour

5.3 Panel Naming Convention

A naming convention as outlined in Chapter 3 will be used and is shown in Table 5-1 below.

Table 5-1: FEM panel naming convention

NAME	SHEATHING	OPENING (% of total panel area)
FFE	No sheathing	N/A
FSFE	Sheathed	No opening
FSO _{37.5} FE	Sheathed	37.5%

5.4 Model Development

5.4.1 General

FEMs of the three experimental frames were developed for validation, including creating all components, contact points, and boundary conditions to ensure the model behaves in a stable and realistic manner. Depending on the analysis to be undertaken, the type of element within Strand7 that most suitably represents the actual material and component must be determined. Based on a review of previous literature and modelling, an understanding of the wall system components and known behaviour from testing, and an understanding of the types of analyses Strand7 undertakes for various element types, the components have been chosen to be modelled as outlined in the following sections.

5.4.2 Frame Members

The GFRP rectangular hollow section frame members are to be modelled using Plate/Shell elements, as recommended for thin plates (Strand7 n.d.-b) and consistent with approaches taken by previous researchers (Richard et al. 2002; Abdullah et al. 2017; Szczepański & Migda 2020; Sharda et al. 2021). This is a three-dimensional surface element type that allows for out-of-plane displacements and bending, as well as in-plane membrane behaviour (Strand7 n.d.-b). Due to the observed behaviour of bending of the wall of the bottom plate at the hold-downs, this is considered a critical requirement to accurately represent the whole panel behaviour. An alternative element type considered was the Beam element; however, this element does not allow for orthotropic materials and Strand7 analyses these using conventional beam bending theories which would not allow for the detailed assessment of plate stresses required for this project. Hence, the plate element was chosen. The RHS profile will be constructed of four plates on orthogonal planes. The majority of plate elements are Quad4 quadrilateral, with some Tri3 triangular elements where mesh refinement was required. Both Quad4 and Tri3 have nodes at each corner of the element, with nodes having six degrees of freedom, including translations along and rotations about the X, Y and Z axis.

For analysis of orthotropic plates, Strand7 requires three elastic moduli, one in each orthogonal direction, and one shear modulus in the XY-plane, along with corresponding Poisson's ratios. Densities and membrane thicknesses are also required. The material property values were provided in Chapter 3 and the Property Sheet in Strand7 is shown in Figure 5-1 below. For the RHS, a plate thickness of 5 mm was used. In Strand7, the elastic modulus E1 and shear modulus G12 relate to the local x-axis, and E2 relates to the local y-axis. The axis of all plate members were set to ensure the local x-axis is correctly aligned. For example, E1 and the local x-axis for the RHS sections were aligned longitudinally with the member.

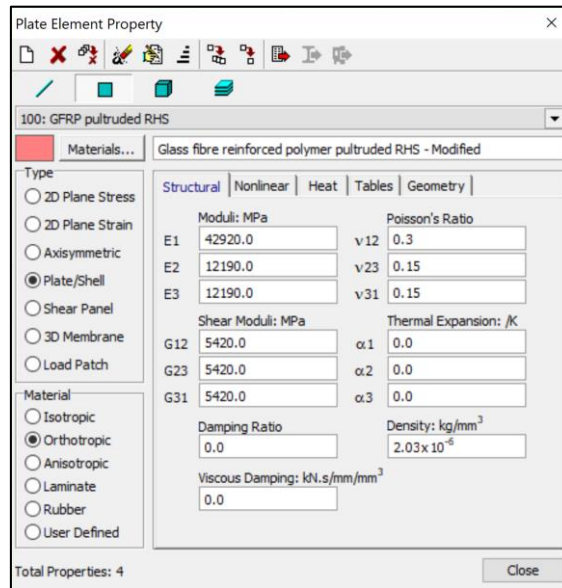
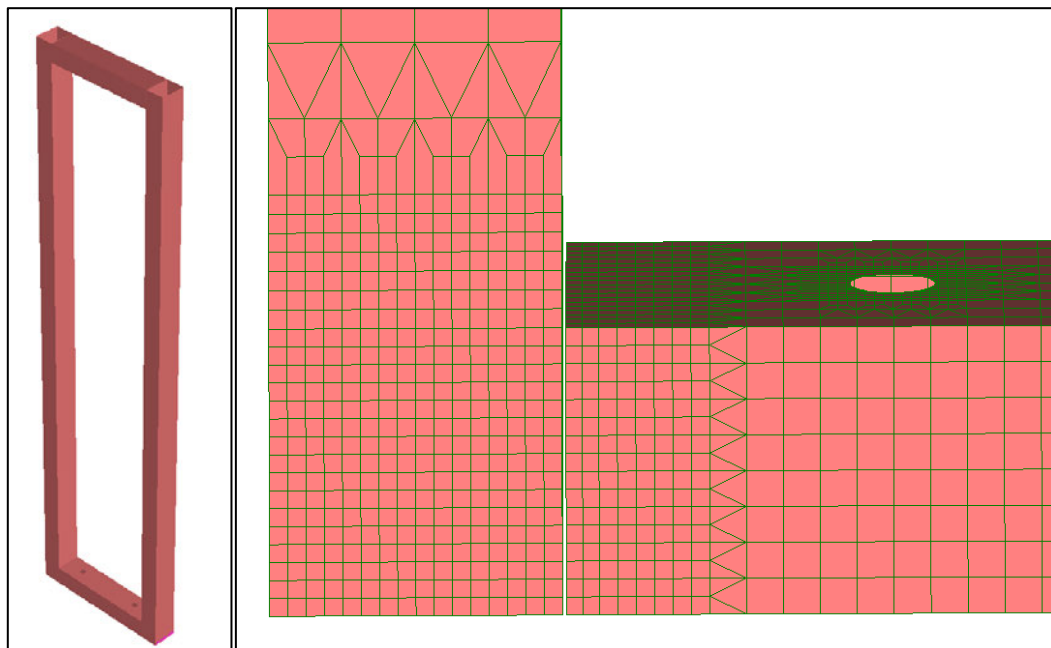


Figure 5-1: Frame material properties in Strand7

The vertical studs were modelled to their full length of 2.4 m. In Strand7, coincident nodes between elements will result in no relative motion between these elements. As such, the top and bottom plates were shortened by 1 mm at each end to provide a small gap between the nodes of the vertical stud and those of the top and bottom plate, allowing independent movement of these frame members. Figure 5-2(a) shows the full frame, whilst Figure 5-2(b) shows the gap provided between the horizontal and vertical members. The plates have been subdivided to provide a finer mesh, which will be discussed in more detail in a later section. It is noted that in Figure 5-2 the plate thickness is turned off in the entity display settings.



(a) Full frame

(b) Gap between horizontal and vertical frame members

Figure 5-2: Image of (a) full frame and (b) gap between vertical and horizontal members in Strand7

5.4.2.1 Frame-to-Frame Contact

In the experimental setup, frame members were only attached to each other by the angel brackets and sheathing. However, once the frame began to deform, vertical and horizontal members would bear against each other at joints. In particular, at joints that were being opened up due to deformation, the inside face of the vertical member would bear against the outer most wall of the horizontal member. To model this affect, Point Contact beam elements were used, which allow load transfer from one surface to another. These elements require a stiffness, selected as 10 kN/mm, and two friction factors, set at 0.1. This is given the name ‘Point Contact Type 1’, and the property sheet is shown in Figure 5-3. Images of these Point Contacts on the frame are shown in Figure 5-4.

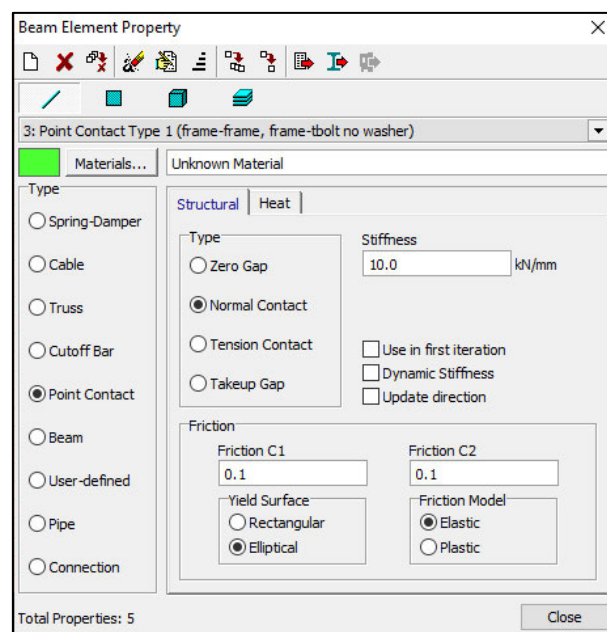


Figure 5-3: Point Contact Type 1 property sheet

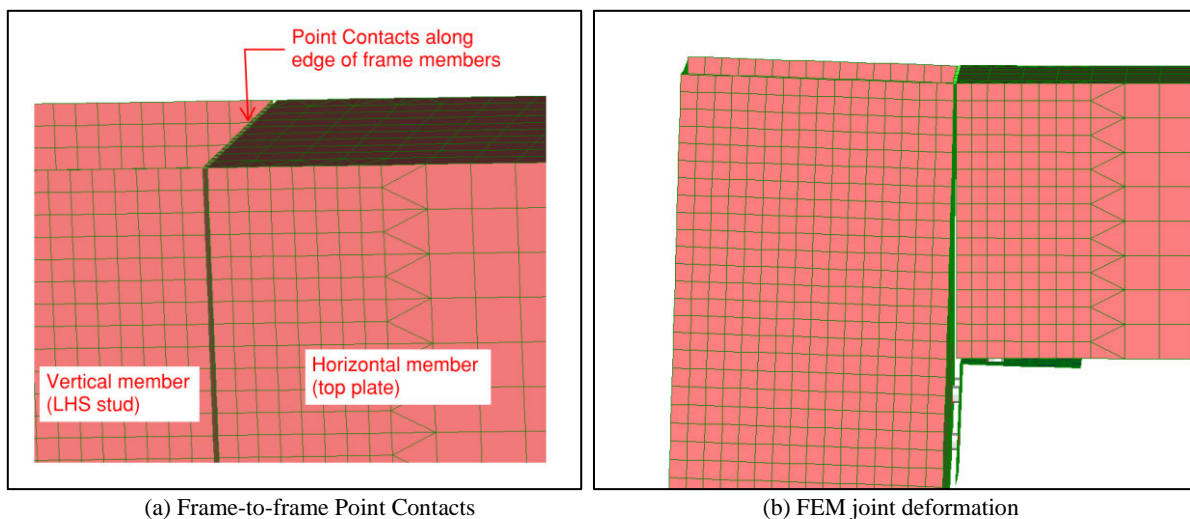


Figure 5-4: Images showing (a) the location of frame-to-frame Point Contacts and (b) joint deformation at this location

5.4.3 Hold-Down Bolts and Inserts

The SS hold-down bolts were modelled using the two-node Beam element, similar to the approach taken in previous research for screws, nails, and bolts (Oktavianus et al. 2018; Sharda et al. 2021). A diameter of 20 mm was given to define the element geometry. The properties are shown in Figure 5-5.

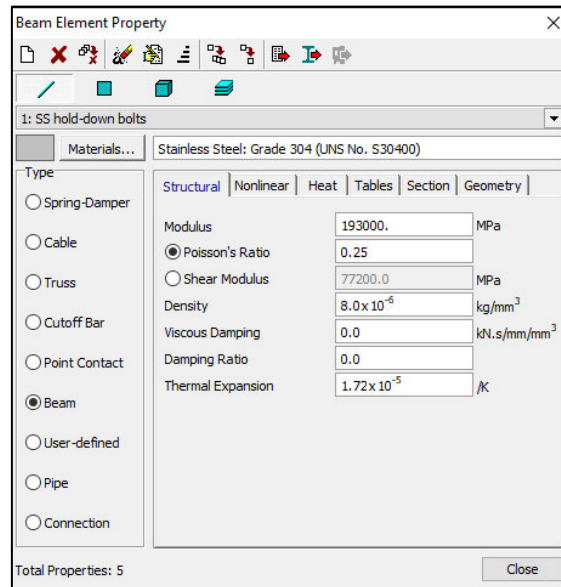


Figure 5-5: Hold-down bolt properties in Strand7

5.4.3.1 Bolt-to-Frame Contact

During experimental testing it was observed that the bottom walls of the RHS bottom plate pressed horizontally against the shank of the hold-downs, and friction between the two surfaces caused the RHS wall to deform. To model this affect, Point Contact Type 1 was used. To model the contact patch, approximately one quarter of the hole circumference is attached to the bolt, as shown in Figure 5-7(a).

At the bolt head and washer location, the RHS is pressing against the bolt shank and is also restrained by the washer in the vertical direction. To model this, a Point Contact was used, however in this case it was applied around the perimeter of the bolt hole and was given a friction factor of 1.0. This is called Point Contact Type 2, with the property sheet shown in Figure 5-6 and the Point Contacts between the frame and bolts shown in Figure 5-7(b).

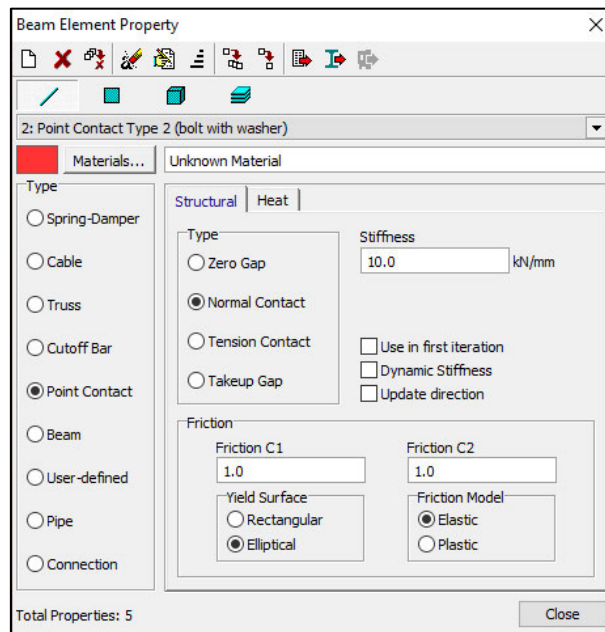
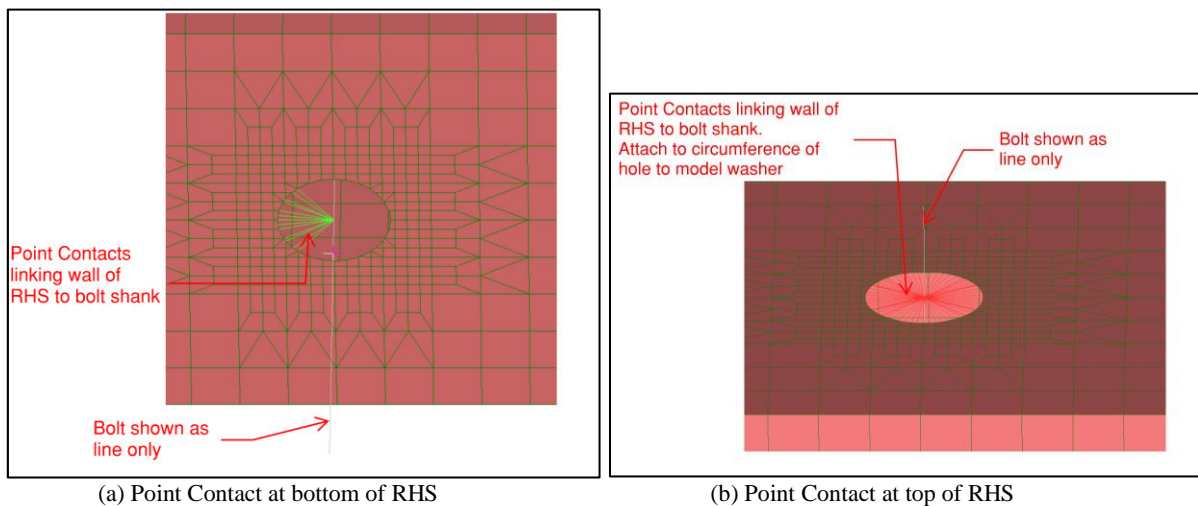


Figure 5-6: Point Contact Type 2 property sheet



(a) Point Contact at bottom of RHS

(b) Point Contact at top of RHS

Figure 5-7: Images of (a) the bottom wall of RHS to bolt shank Point Contact and (b) top wall and washer Point Contacts in Strand7

5.4.3.2 Bolt Inserts

The bolt inserts were modelled as a solid, 3D Brick elements, similar to the approach used by Hizam et al. (2019). The actual insert shape is complex, and it was not possible to accurately model this shape. Instead, a solid, rectangular prism shape with a central hole was adopted. Consequently, the elastic modulus of these inserts therefore required adjustment to compensate for this. The process of determining this modulus will be discussed further in a later section, however a final modulus of 100 MPa was chosen. The properties entered in Strand7 are shown in Figure 5-8.

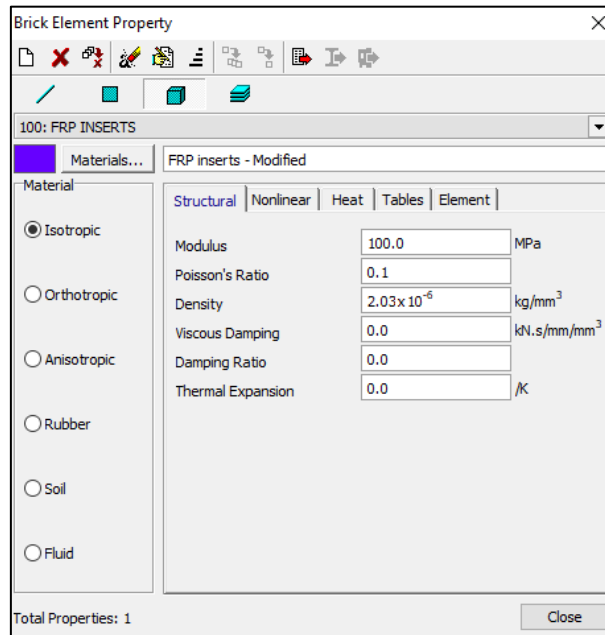
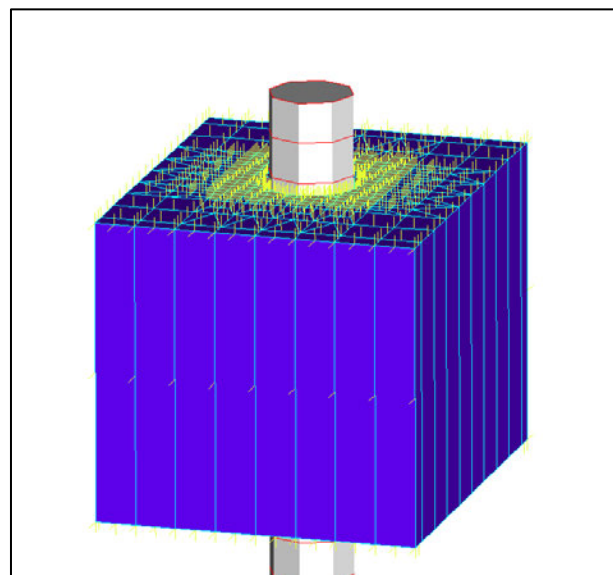
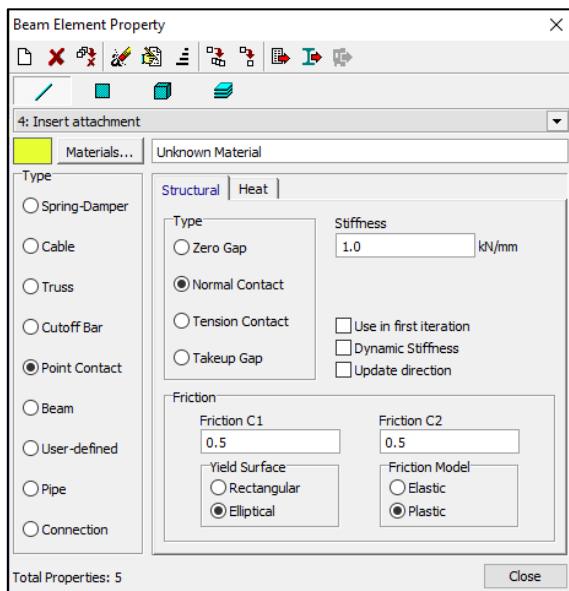


Figure 5-8: Mechanical bolt insert material properties in Strand7

As the inserts were not attached to the inside of the frame with an adhesive, only compressive and friction load transfer are required to be modelled. Face attachments using a Point Contacts were utilised to allow load transfer between the RHS and the inserts. Within Strand7, Face Attachments enable linking of incompatibly meshed surfaces to each other. The material properties are shown in Figure 5-9(a) below, along with an image of the Point Contact links on the insert in Figure 5-9(b).



(a) Insert Point Contact properties

(b) Point Contacts on insert

Figure 5-9: Bolt insert Point Contact (a) property sheet and (b) image of Point Contacts on insert

5.4.4 Angle Brackets and Rivets

The SS angle brackets were modelled as an isotropic Plate element with a membrane thickness of 4 mm, with the properties sheet shown in Figure 5-10(a). The rivets were modelled as Beam elements as flexible Face Attachments between the frame and the bracket. The rivet diameters were 4.8 mm, with

the properties shown in Figure 5-10(b). In addition, for angle brackets being closed by deformation of the frame and therefore pressed against the frame, Point Contacts were used along two edges of the bracket. The rivets and Point Contacts are shown in Figure 5-11 below.

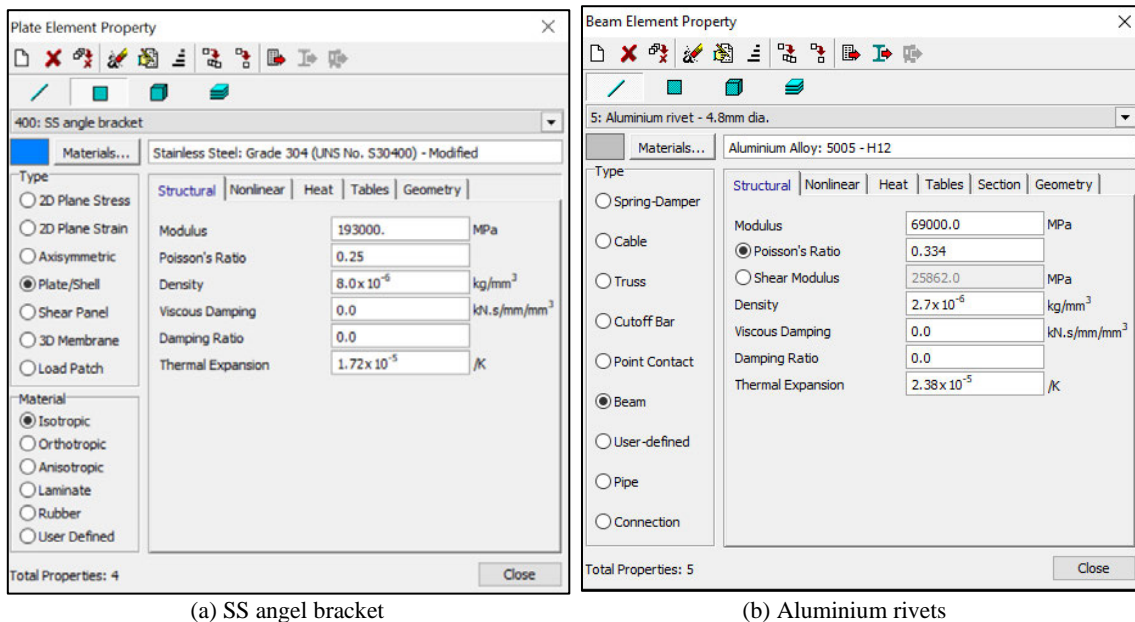


Figure 5-10: Property sheets for (a) SS angle bracket and (b) aluminium rivets in Strand7

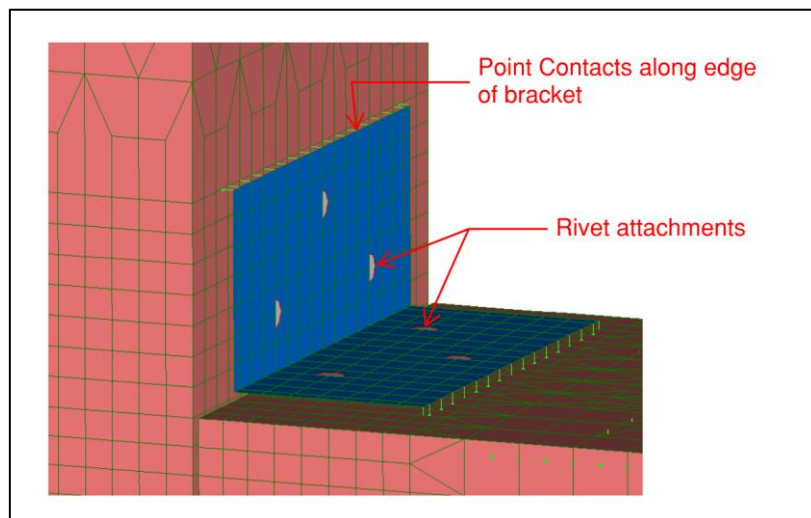


Figure 5-11: Angle bracket attachment and Point Contacts

5.4.5 Sheathing

The sheathing was also modelled as an orthotropic Plate/Shell element, with properties shown in Figure 5-1. A membrane thickness of 6 mm was used. The sheathing extended the full width and height of the panel, except that a 10 mm vertical offset from the base off the wall was provided, as per the experimental panels. The local x-axis, corresponding to the E1 modulus, was aligned vertically.

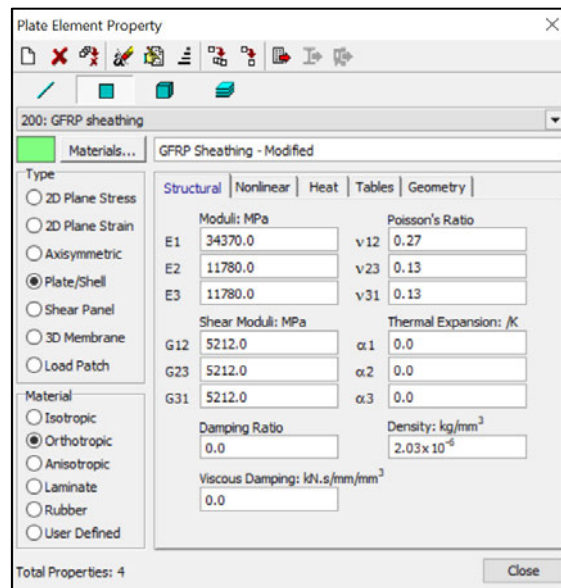


Figure 5-12: Sheathing material properties in Strand7

5.4.5.1 Sheathing-to-Frame Attachment

During testing, no observable deformation or failure of the adhesive between the sheathing and frame was noted. It is therefore considered reasonable to model this interaction as a perfect connection, whereby there is no relative movement between nodes of the sheathing and nodes of the frame. To achieve this, the sheathing and frame are modelled with compatible meshes and will share nodes at points of contact. Within Strand7 this allows both the sheathing and frame materials to contribute to stiffness and stress distribution at these points and prevents relative motion between the two. Using rigid attachment links is an alternative, however this greatly increases computational time due to the high number of links that would be required. An offset property of 3 mm is applied to the sheathing which ensures stress distribution through the thickness of the sheathing is more realistically represented, whilst maintaining the coincident nodes. Figure 5-13 shows the coincident nodes between the sheathing and frame, and the sheathing offset is also apparent.

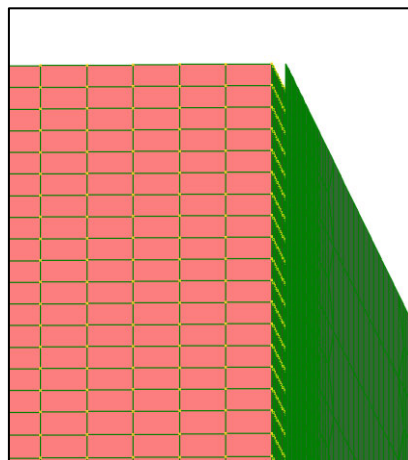
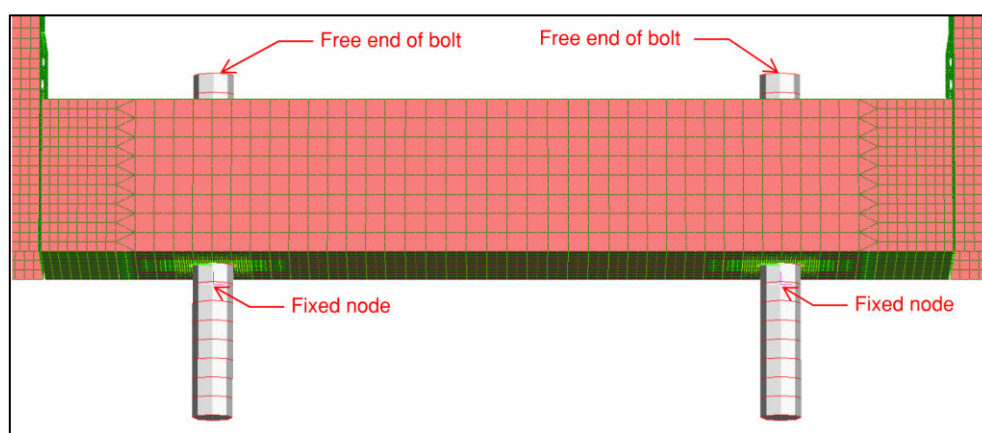


Figure 5-13: Sheathing-to-frame connection and sheathing offset in Strand7

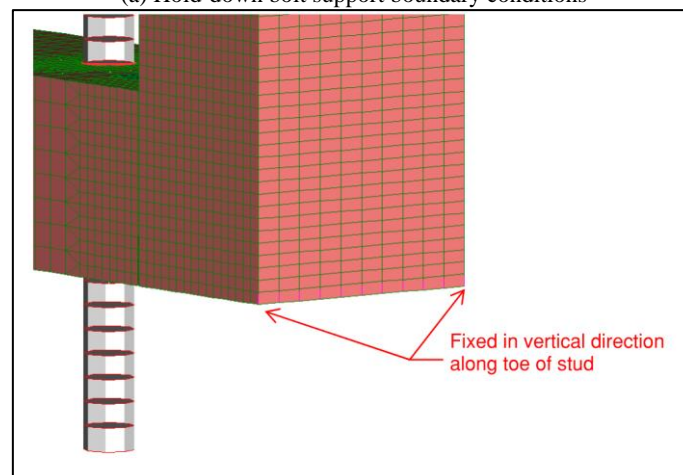
5.4.6 Supports and Boundary Conditions

During experimental resting of the frame, three reaction points were present; one at each hold-down where the panel is pulling up on the bolts, and a third at the base of the right-hand stud where the panel is pushing down into the base support. As such, within the FEM, three support points are required.

The portions of each hold-down bolt extending above the top of the supporting beam were able to deflect and rotate, whilst where the bolt is within the supporting beam it is effectively unable to move; therefore, a node on each bolt is given fixed boundary conditions at a location just below the bottom of the frame, as shown in Figure 5-14(a). The third support at the base of the right-hand stud was fixed in the vertical direction only, as shown in Figure 5-14(b).



(a) Hold-down bolt support boundary conditions



(b) Base of right-hand stud support boundary conditions

Figure 5-14: FEM support conditions in Strand7

5.4.7 Applied Loads

To model the distribution of the applied load on the surface of the frame, the applied load is divided by an assumed area of $7,500 \text{ mm}^2$, equal to the end area of a 100×75 RHS member. The applied loads and pressures for each panel type are shown in Table 5-2. These loads are based on the peak linear load for each panel obtained during the experimental testing, as outlined in Chapter 4. The pressure was applied as a Global Face Pressure to selected elements at the top of the left-hand vertical stud. In addition, as at

the bolt locations, an insert was placed inside the stud at the point of load application during the experimental testing; therefore, one has been included within the FEM. An example of the load application is shown in Figure 5-15.

Table 5-2: Applied load pressures for FEM

PANEL	APPLIED LOAD	EQUIVALENT PRESSURE
FFE	0.469 kN	0.06253 MPa
FSFE	6.5 kN	0.86667 MPa
FSO _{37.5} FE	5.5 kN	0.73333 MPa

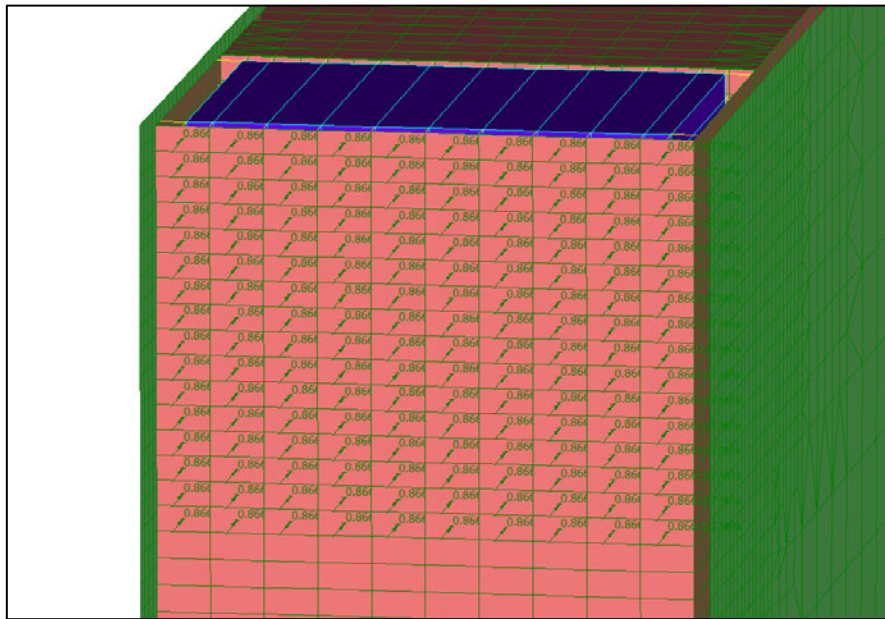


Figure 5-15: Applied load and insert

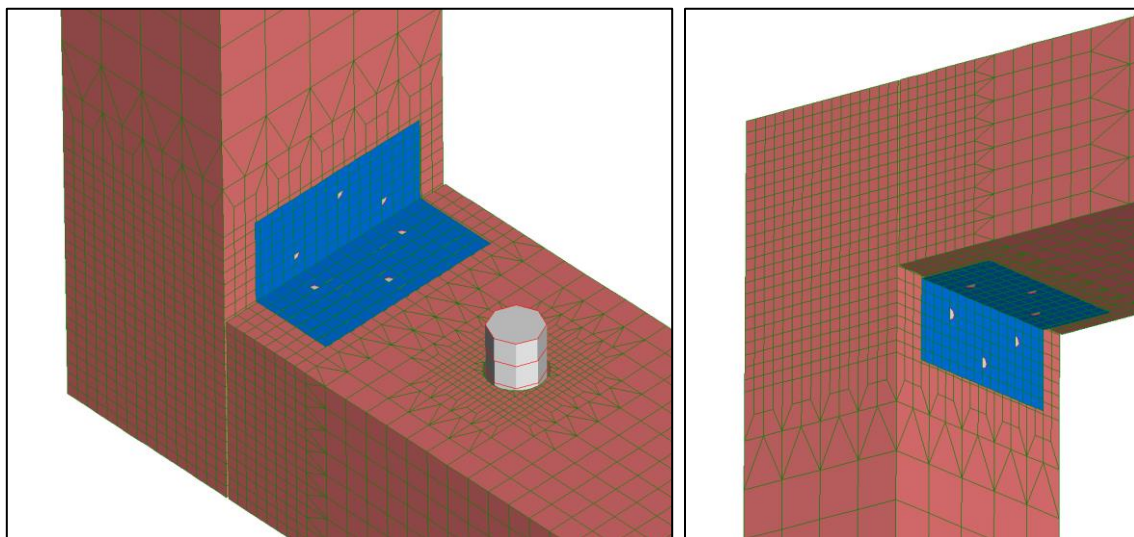
5.5 Model Refinement

To ensure the FEM produces an accurate result and is sensitive to stress created due to applied loads, the elements sizes are to be reduced and refined. This is consistent with approaches taken by previous researches and is standard procedure when undertaking any sort of FEA. This mesh refinement improves the stress distribution through the elements and allows for more accurate deformation of elements. However, it also increases modelling and computational time. It is therefore common to refine the mesh to a point at which further decreases in mesh size will result in minimal change in results. Typically, finer mesh elements are required around joints and points of high stress or deformation, and larger mesh elements are acceptable in other areas. For these panels, key areas are:

- Around the hold-down bolts.
- Around the angle brackets.
- At the ends of the frame members where they connect to angle brackets.

- Near the corners of openings in the sheathing.

During development of the models, finer meshes were created around the hold-down bolts, angle brackets, and opening corners, with elements side lengths of approximately 2.5-5 mm, as shown in Figure 5-16. This included refinement of the mesh on the bottom plate, top plate, and vertical studs within the vicinity of the angle bracket joints. Due to its higher imposed stresses, the mesh size on the bottom plate was kept to a maximum of approximately 10 mm square. In contrast, as the vertical studs and top plate are not exposed to as high stresses and deformations, a larger maximum mesh size of approximately 20 mm square was used for much of the area, similar to sizes utilised by Lei et al. (2019). Mesh refinement of the sheathing was similar to that for the frame members, noting that identical, compatible meshes were used for overlapping sections of sheathing and frame. A mesh size of approximately 5 mm square was used in the vicinity of the centre of the main sheathed sections, to ensure accurate strain values could be obtained for comparison with the experimental measurements. Maximum mesh size for the sheathing was approximately 20 mm. Further refinement of the mesh was found to provide negligible change in result but increased computational time.



(a) Mesh refinement at hold-down and angle bracket

(b) Mesh refinement at top plate and angle bracket

Figure 5-16: Refined mesh locations for frame members at (a) the hold-downs and (b) joint between top plate and stud

Overall images of the frame and sheathing for a panel with an opening are provided in Figure 5-17, showing the locations of mesh refinement.

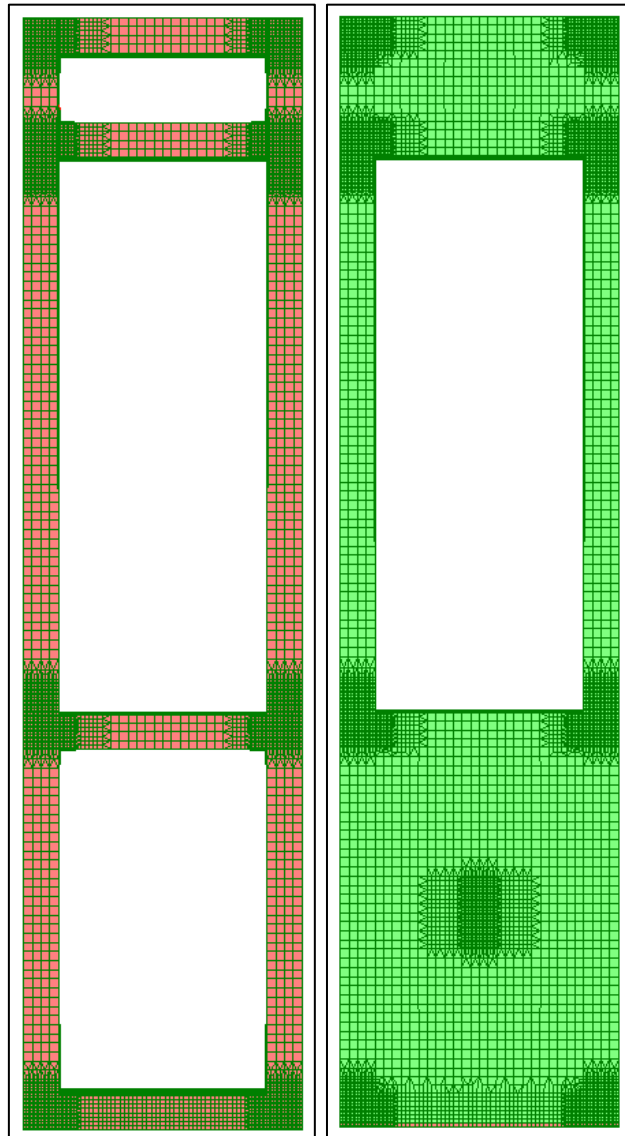


Figure 5-17: Refined mesh locations for frame and sheathing

5.6 Model Validation and Results

5.6.1 General

Validation of the model by comparison of the FEM deflection and strain values with the experimental values was undertaken to ensure the FEM could be considered reliable. In addition, observations of visible aspects such as the shape of the deformed panel, and investigation of high stress concentrations that may indicate failure locations were also used for comparison. This section outlines these results, and provides some discussion on notable discrepancies.

5.6.2 Panels FE and FFE

5.6.2.1 Overview

For the frame only panels FE and FFE, the deflection at the top of the panel and strains on the outside faces of the studs and top of the top plate were used to validate the FEM, with values of each shown in Table 5-3. A large discrepancy between deflections is noted, whilst reasonable correlation of strain values was achieved, particularly on the vertical studs.

Table 5-3: Comparison of FEA results and experimental data for panels FE and FFE

LOCATION	EXPERIMENTAL	FEA	% DIFFERENCE
Deflection at top of panel (mm)	117	49.3	58%
Left stud midpoint strain (microstrain)	-112.7	-106	6%
Right stud midpoint strain (microstrain)	-172.9	-149	14%
Top plate midpoint strain (microstrain)	-107.3	-81	25%

5.6.2.2 Discussion

The negative strain obtained on the left-hand stud on both panel FE and FFE is noted, which indicates that the midpoint of the left-hand stud is subject to bending, with the compression side on the outside face. This is corroborated by comparison of the overall deformed shape and mechanical behaviour of the panels, which was observed to be relatively similar between the FEA and experiment, with both showing this slight stud curvature. Based on both FEA and experimental observations, it is considered that the joints at the top left, adjacent to the load, and bottom right effectively acted as moment connections due to the combined action of the angle bracket rivets intension and the vertical and horizontal members bearing against each other in compression. This created resistance to rotation between the vertical and horizontal frame members. In contrast, the top right and bottom left joints exhibited pinned connection behaviour, with limited resistance to rotation. Figure 5-18 shows the deformed shape of the top of panel FFE where this behaviour can be observed.

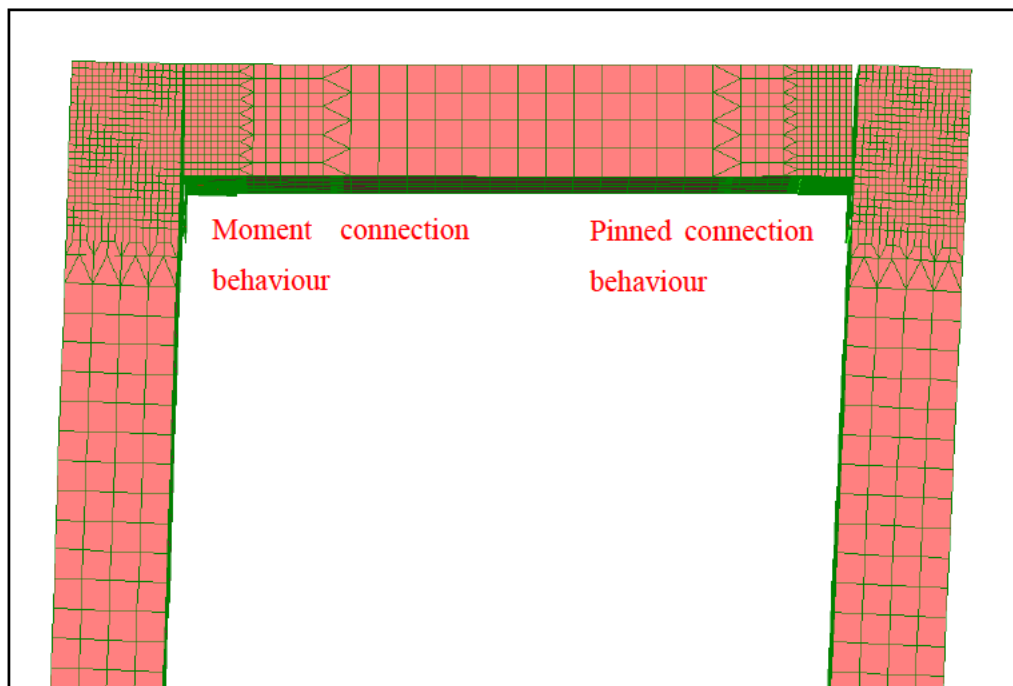


Figure 5-18: Joint deformation of panel FFE, noting moment connection behaviour of top left and pinned connection behaviour at top right

As no failure of the experimental panel was observed, correlation of a failure mechanism is not possible. However, stress analysis of the angle brackets indicates high tensile and compressive stresses occurring, as shown in Figure 5-19. As peak stresses are in the order of 200 MPa, the yield stress of the material, it is considered that slight yielding and plastic deformation of the angle brackets likely occurred. This possibility is supported by the fact that in the experimental testing, upon release of the load the panel did not return to its original shape and remained slightly deformed, indicating plastic deformation of the brackets.

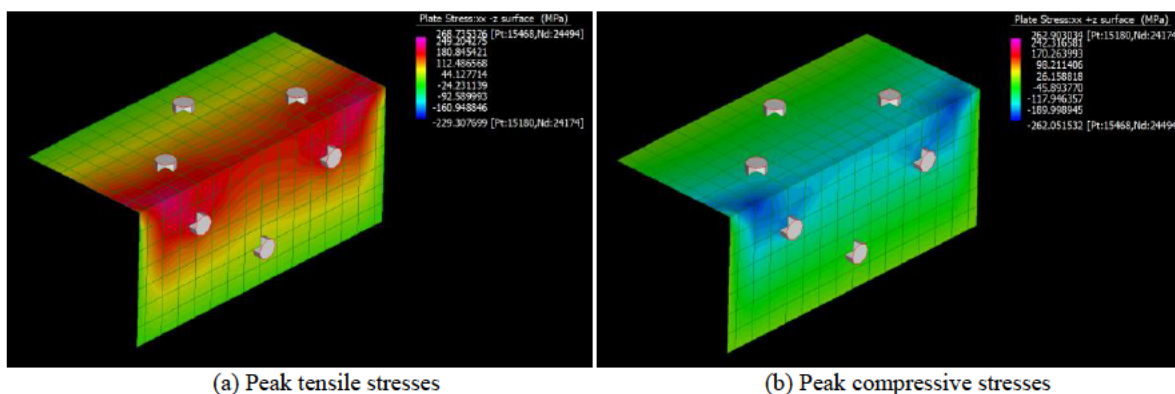


Figure 5-19: Stress concentrations at angle bracket in both (a) tension and (b) compression indicating possible yielding of the bracket

5.6.2.3 Discrepancies Between Panels FE and FFE

The discrepancy in overall deflection between panels FE and FFE can possibly be explained by a number of effects that are not accounted for in the FEM. Firstly, closing of small gaps such as between the bottom plate and hold-down bolts or between the horizontal and vertical members may have occurred in the experiment. Similarly, the panel may have not sat perfectly flat on the supporting frame

and loading will have resulted in the panel being pressed into the support near the bottom of the right-hand stud, closing any small gaps. Further, due to high stress concentrations in the vicinity of the angle brackets and rivets, some yielding and plastic deformation may have occurred. Finally, due to limitations in availability of specimens for this project, only one such experimental panel was tested. Without further experimental testing it is difficult to make further conclusions. Additional research beyond the scope of this project may be required to fully understand the frame only panel behaviour.

It is noted that the parametric study utilises sheathed panels with openings, for which the deformation of the frame joints is much smaller. As such, the discrepancies noted for panel FFE are not considered critical and should not prevent the additional investigation from proceeding.

5.6.3 Panels FSE and FSFE

5.6.3.1 Overview

For the fully sheathed panels FSE and FSFE, the deflection at the top of the panel, strains on the outside faces of the studs, and strain at the middle of the sheathing were used to validate the FEMs, with values of each shown in Table 5-4. Good correlation between deflection and strains on the studs was found, however strains on the sheathing are considerably different between FEA and experimental results. Visually, the panel deflection shape and movement was observed to be similar between the FEA and experiment, with uplift and rotation occurring whilst the panel itself remained rectangular with no noticeable shear deformation. Deformation of the bottom plate at the hold-down was also observed, as shown in Figure 5-20, consistent with the experimental observations.

Table 5-4: Comparison of FEA results and experimental data for panels FSE and FSFE

LOCATION	EXPERIMENTAL	FEA	% DIFFERENCE
Deflection at top of panel (mm)	26	26.5	2%
Left stud midpoint strain (microstrain)	118	126	7%
Right stud midpoint strain (microstrain)	-124	-129	4%
Sheathing +45° strain (microstrain)	88	111	26%
Sheathing -45° strain (microstrain)	-33	-113	242%

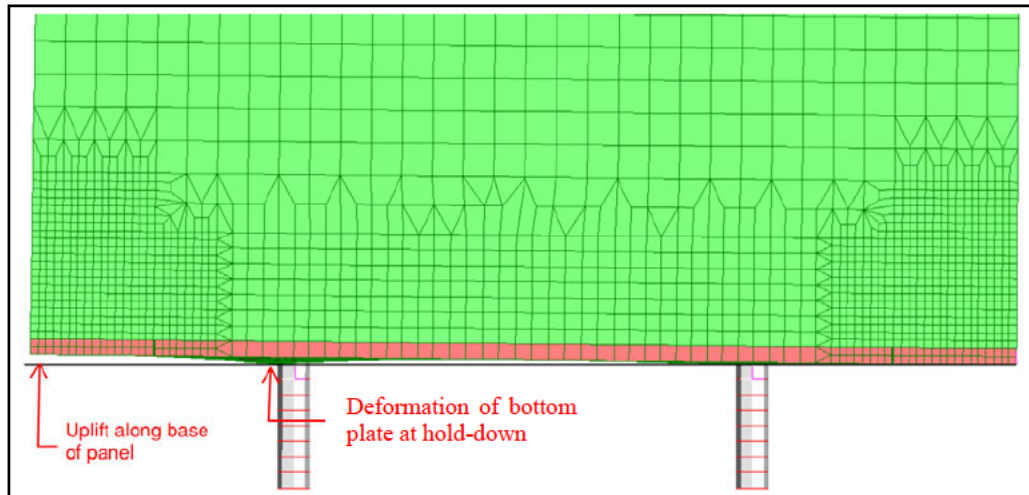
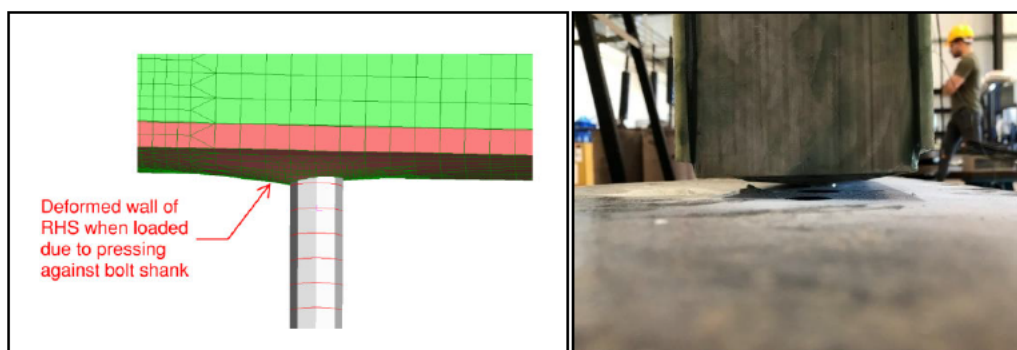


Figure 5-20: Uplift along base and deformation of bottom plate at hold-down of panel FSFE

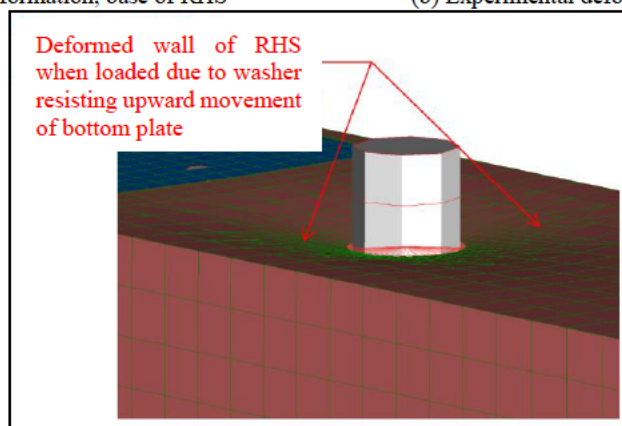
5.6.3.2 Discussion

Failure of the experimental panels occurred at the hold-down, with longitudinal splitting of the RHS bottom plate due to deformation of the bottom plate and high transverse tensile stresses. A comparison of the FEM deformation of the bottom wall of the RHS with the experimental deformation is shown in Figure 5-21(a) and (b), showing good correlation between the two. Figure 5-21(c) shows the deformation at the washer location in the FEM, also showing good correlation.



(a) FEM deformation, base of RHS

(b) Experimental deformation, base of RHS



(c) FEM deformation, top of RHS at hold down

Figure 5-21: RHS wall deflection at the hold-down in Strand7

The FEM shows high transverse stresses in the bottom plate either side of the hold-down, with Figure 5-22(a) indicating transverse tensile stresses on the outer face in the order of 500 MPa, noting that the transverse tensile strength of the GFRP RHS is approximately 46.8 MPa. Similarly, Figure 5-22(b) shows transverse compressive stresses on the inner face in the order of 500 MPa, noting that the transverse compressive strength of the GFRP RHS is approximately 147.7 MPa. This indicates that failure initiation at this point is likely, as seen in the experimental testing. It is possible that minor inter-lamina delamination and pin bearing crushing of the GFRP may have occurred prior to the main failure occurring. This may have helped relieve the stresses at the hold-down prior to the major failure that occurred at an applied load of 6.5 kN. Noting that the FEM does not account for progressive inter-lamina delamination, this might explain the large stress magnitude seen in the FEM. Regardless, this stress concentration correlates well with the experimental observations.

It is also shown in Figure 5-22(b) that high tensile transverse stresses near the corners of the inner surface of the bottom plate were developed. Whilst no observed failure at this location was noted in the experiment, such high stress development indicates a possible area of failure of the RHS.

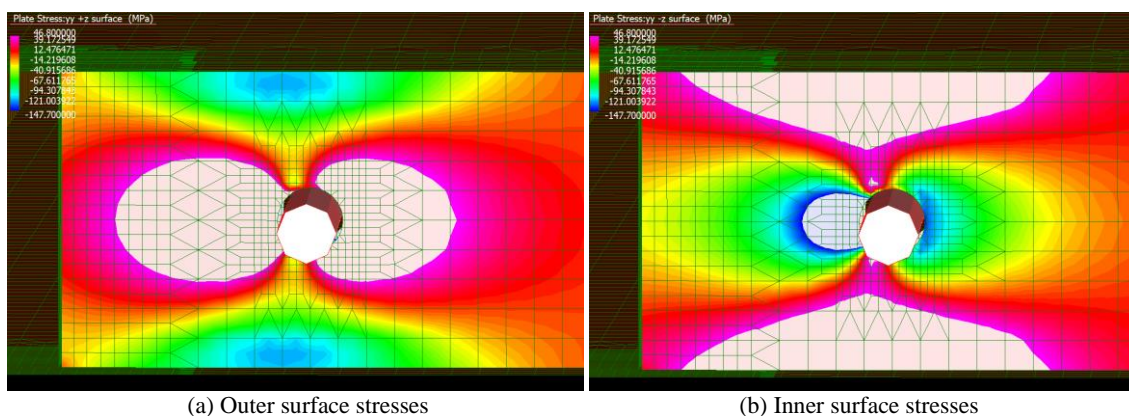


Figure 5-22: Transverse stress concentrations on the underside of the bottom plate at the left-hand hold-down on both the (a) outer surface and (b) inner surface, indicating likely failure of RHS bottom plate, for Panel FSFE

5.6.3.3 Discrepancies Between FSE and FSFE

The large discrepancy between sheathing strains requires further investigation to be fully understood. Such investigation may include additional material characterisation of the sheathing, particularly with respect to its shear modulus. In addition, FEA using a ply and laminate element could also be worthwhile, as well as investigation into the interaction of the sheathing and frame with the adhesive and the load transfer that occurs at this connection. The discrepancy may also be due to the strain gauges in the experiment not being properly bonded to the sheathing, resulting in lower measured strain than the FEA results. Further, it is noted that shear distribution of a thin sheet such as the sheathing is complex and it may be that the experimental data was influenced by other subtle effects which are not apparent in the model or visually observable, such as slight out-of-plane deflection of the sheathing. Such aspects are beyond the scope of this project, and the poor correlation in this regard will limit the

investigation of the sheathing stress, particularly in the middle of the panel. Stress distribution where the sheathing overlaps frame members is considered to be more reliable as it is directly linked to the deflection of the frame itself. Finally, due to limitations in availability of samples for this project, only one such experimental panel was tested. Additional testing may provide further clarity in these areas.

As there is good correlation between failure mechanism and deflection and frame strain results from the FEA and experiments, it is considered that the model represents the overall panel behaviour acceptably well and can be used for further analysis of the wall system. Care should be taken in using sheathing strain results from the FEA, particularly where the sheathing is not directly connected to the frame members.

5.6.4 Panels FSO_{37.5E} and FSO_{37.5FE}

5.6.4.1 Overview

For the panels with openings, FSO_{37.5E} and FSO_{37.5FE}, the deflection at the top of the panel, strains on the outside faces of the studs, strain at the middle of the sheathing, and deflection of the corners of the opening were used to validate the FEM. These values are shown in Table 5-5. Good correlation between deflection and strains on the studs was found. In contrast, strains in the sheathing are again considerably different between FEA and experimental data, similar to the results for panel FSFE. Horizontal deflection of the opening corners showed good correlation, whilst vertical deflection did not. Visually, the panel deflected shape was observed to be similar between the FEA and experiment, with uplift and rotation occurring, and bending of the frame above the base of the opening evident, as shown in Figure 5-23. Deformation of the bottom plate at the hold-down was again exhibited, consistent with the experimental observations.

Table 5-5: Comparison of FEA results and experimental data for panels FSO_{37.5E} and FSO_{37.5FE}

LOCATION	EXPERIMENTAL	FEA	% DIFFERENCE
Deflection at top of panel (mm)	36	32.7	9%
Left stud midpoint strain (microstrain)	536	476	11%
Left stud base opening strain (microstrain)	779	697	11%
Right stud midpoint strain (microstrain)	-464	-474	2%
Sheathing +45° strain (microstrain)	58	127	119%
Sheathing -45° strain (microstrain)	-34	-154	353%
TL horizontal deflection (mm)	31	29	6%
TR horizontal deflection (mm)	31	29	6%
BL horizontal deflection (mm)	9	8.8	2%
BR horizontal deflection (mm)	9	8.8	2%
TL vertical deflection (mm)	2.6	4.83	86%
TR vertical deflection (mm)	-3.1	0.41	113%
BL vertical deflection (mm)	3.7	4.74	28%
BR vertical deflection (mm)	-0.88	0.5	157%

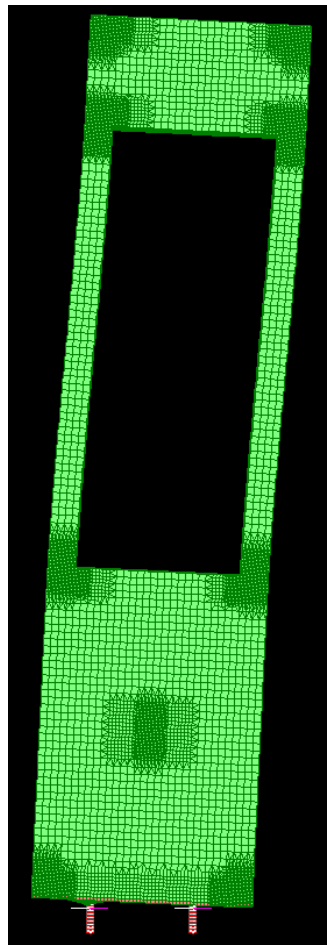
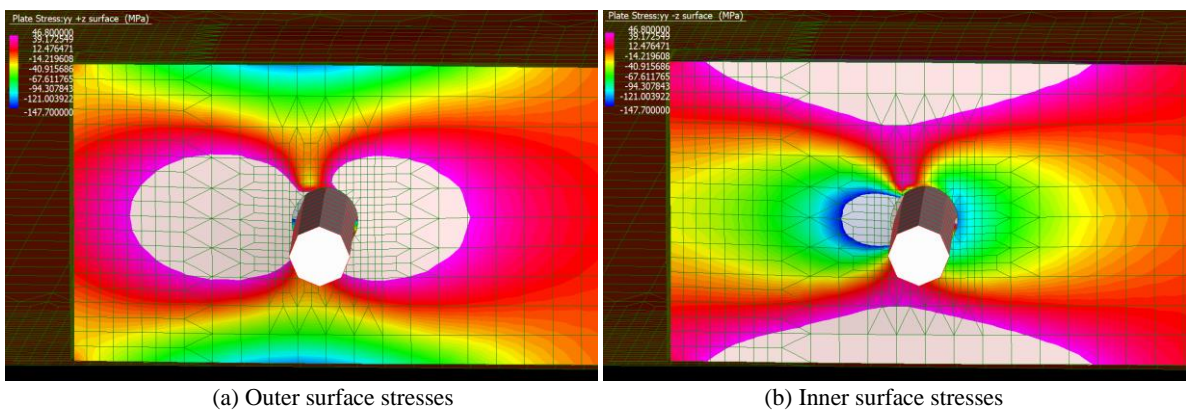


Figure 5-23: Deformed shape of panel FSO₃₇.FE (with five times exaggeration)

5.6.4.2 Discussion

Similar to the model for panel FSFE, high transverse stresses in the bottom plate at the hold-down were developed, as shown in Figure 5-24. This indicates likely failure by longitudinal splitting of the bottom plate, as occurred in the experiment.



(a) Outer surface stresses

(b) Inner surface stresses

Figure 5-24: Transverse stress concentrations on the underside of the bottom plate at the left-hand hold-down on both the (a) outer surface and (b) inner surface, indicating likely failure of RHS bottom plate, for Panel FSO₃₇.5FE

5.6.4.3 Discrepancies Between FSO_{37.5}E and FSO_{37.5}FE

Similarly to the fully sheathed panels, further investigation is required to fully understand the stress distribution and behaviour of the sheathing. In terms of the poor correlation of vertical deflections of the opening between the FEA and experimental data, it is noted that the overall magnitude of these deflections are small. There is also potential that small gaps may have been closed upon loading, such as between the bottom plate and hold-down bolts and between the right-hand toe of the panel and the supporting frame, effects that are not fully accounted for within the FEM and may have contributed to some of this deflection. Finally, due to limitations in availability of samples for this project, only one such experimental panel was tested. These factors combined may help to account for the poor correlation of sheathing strain.

As good correlation between the overall panel and opening corner horizontal deflection and the frame strain was observed, it is considered reasonable to utilise this FEM as the base for further parametric investigation, with caution to be used with respect to those aspects of the FEA that are not well correlated.

5.7 Parametric Investigation

5.7.1 General

The FEA has shown satisfactory correlation with the experimental testing, in particular with respect to panel deflection, frame strain, and stress concentrations at the known failure point at the hold-down. As such, a parametric study was undertaken, investigating how the presence and size of openings affects the panel behaviour, stiffness, hold-down reactions, and development of stress concentrations that may lead to failure of the panel. The results of this parametric investigation are outlined and discussed in the following sections.

5.7.2 Panel Configurations

To undertake the parametric investigation, a range of panels with various opening sizes were developed. These were based on the original panel with an opening, with a 300 mm high sheathed section of panel above the opening, a full width opening between vertical studs, and a sheathed section below the opening. For this study, the dimension varied is the height of the lower sheathed section. The opening sizes investigated range from 12.5% to 56.25% of the total panel area, generally increasing in 12.5% increments. A panel with 56.25% opening has a 300 mm high sheathed section below the opening, which is considered a reasonable minimum height for a window opening. The five panels with openings, including panel FSO_{37.5}FE, are shown in Figure 5-25.

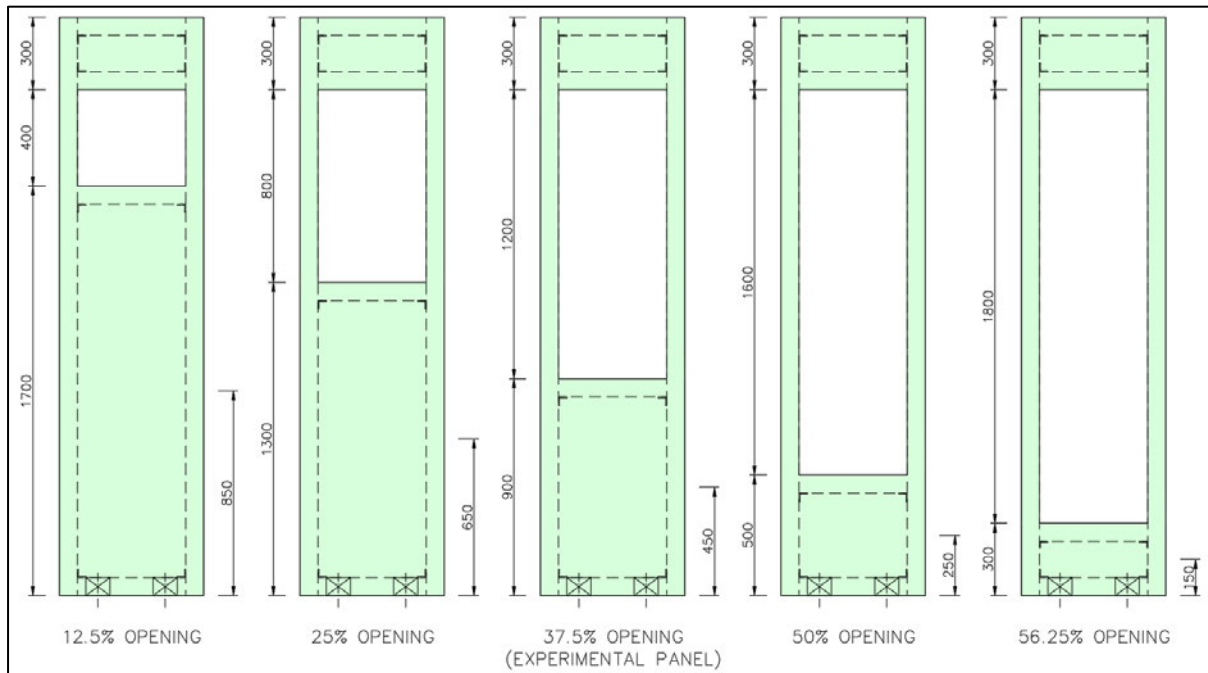


Figure 5-25: Drawings of panels used in parametric investigation

The naming convention as outlined in Chapter 3 will be used and is shown in Table 5-6 below. An FEM of a fully sheathed panel was developed with an applied load of 5.5 kN to allow for direct comparison between the panels with and without openings. This panel is named FSFE-5.5.

Table 5-6: FEM panel naming convention for parametric study

NAME	OPENING (% of total panel area)
FSFE-5.5	No opening
FSO _{12.5} FE	12.5%
FSO ₂₅ FE	25%
FSO _{37.5} FE	37.5%
FSO ₅₀ FE	50%
FSO _{56.25} FE	56.25%

5.7.3 Effect of Opening Size on In-Plane Shear Stiffness

To assess the influence opening size has on in-plane shear stiffness, a load of 5.5 kN was applied to all panels. The peak deflections and stiffnesses from the FEA for all panels, including FSFE-5.5, are shown in Table 5-7. As can be seen, an increase in opening size results in an increase in horizontal deflection and decrease in panel stiffness, indicating that the panel stiffness is primarily due to the sheathing. The additional deflection is due to bending of the frame above the base of the opening, and not due to uplift and rotation. An opening area of 56.25% resulted in an increase in deflection of 111% to that of a fully sheathed panel, giving a reduction in stiffness of 53%. Such a result is consistent with the findings of Dujic, Klobcar and Zarnic (2009), Kozem Šilih and Premrov (2012), Grossi, Sartori and Tomasi (2015b, 2015a), Anil et al. (2016), Abdullah et al. (2017), Shahnewaz et al. (2017), and Husain, Eisa and Hegazy

(2019) who all found that the larger the opening size the greater the reduction in in-plane stiffness. The relationship between normalised global stiffness and opening size is shown in Figure 5-26, with the stiffness expressed as the ratio of the stiffnesses of the panels with openings to the stiffness of the fully sheathed panel. A relatively linear relationship is observed, indicating that the stiffness reduction is proportional to the opening size. This linear relationship is somewhat in contrast to the findings of Shahnewaz et al. (2017), who tested CLT panels with and without openings and found an 86% reduction in stiffness with about a 50% opening size and a non-linear relationship between stiffness and opening size. This further indicates that the sheathing is the primary cause of in-plane stiffness for this GFRP wall system, and that the frame itself provides relatively minimal resistance to in-plane loads.

Table 5-7: Deflection and calculated global stiffness of all panels with an applied load of 5.5 kN

MEASUREMENT With an applied load of 5.5 kN	PANEL					
	FSFE-5.5	FSO _{12.5} FE	FSO ₂₃ FE	FSO _{37.5} FE	FSO ₅₀ FE	FSO _{56.25} FE
Deflection at top of panel (mm)	22.45	25.33	27.66	32.72	41.33	47.35
Difference from fully sheathed panel	0%	13%	23%	46%	84%	111%
Global stiffness (kN/m) *	979.96	868.54	795.37	672.37	532.30	464.63
Difference from fully sheathed panel	0%	-11%	-19%	-31%	-46%	-53%

**It is noted that the global stiffness was calculated using Equation 4.1, however a load of 5.5 kN was used rather than 0.4P_u. As the global stiffness is based on the slope P/Δ of the elastic-linear portion of the load-deflection behaviour, for a linear material moving within its elastic range this will give the same result.*

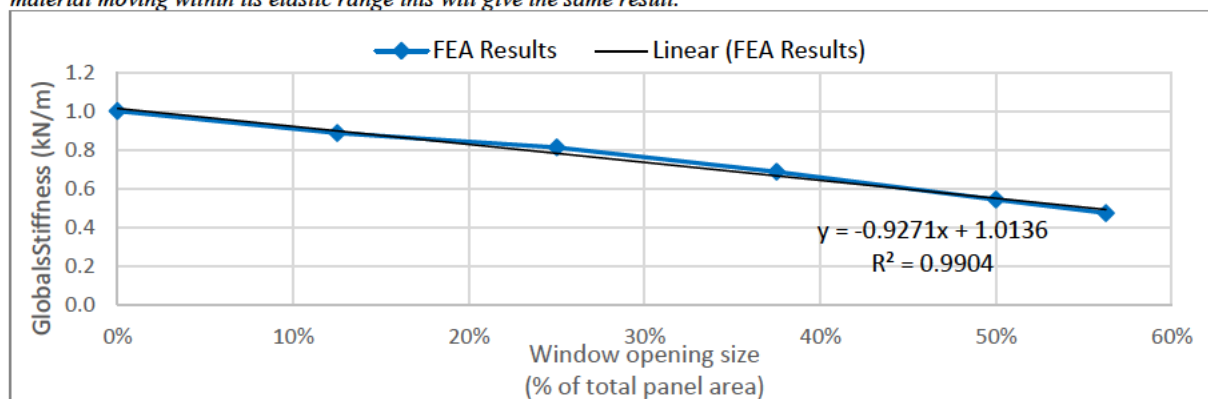


Figure 5-26: Relationship between opening size and normalised global stiffness

5.7.4 Effect of Openings on Hold-Down Reactions and Stress

Concentrations

Analysis of how the reactions in the hold-down bolts change with varying opening sizes is of importance as the failure of the experimental panels occurred at the hold-downs. If the reactions change due to opening size, this may indicate that the failure strength of the panels is also affected by the opening size. This was discussed previously in Chapter 4 in relation to the experimental panels, and will be explored in more detail below.

The reaction loads at the hold-downs for all FEM panels are shown in Table 5-8, indicating a very minor transfer of load from the left-hand to the right-hand hold-down as the opening size increases. The magnitude of this change is very small, indicating that the size of the opening has minimal influence on the load at the hold-downs.

The loads in the right-hand hold-downs are approximately 30-32% of those in the left-hand hold-downs. This supports the theory developed in Chapter 4, that the hold-down load is proportional to its distance from the point of rotation of the bottom plate. As noted previously, based on this theory, this would give a load in the right-hand hold-down of approximately 36.36% of the left-hand hold-down, which is similar to the results of the FEA. This indicates that the FEA is producing reasonable and expected results, with both experimental observations and the FEA indicating the loads on the hold-down are not significantly affected by the presence of an opening. It therefore follows that if the magnitude of the stresses developed in the GFRP bottom plate at and around the hold-downs are directly related to the load placed on the hold-downs, then the failure of this wall system is not significantly influenced by the presence and size of an opening, based on this particular failure mode. This is somewhat consistent with the findings of Dujic, Klobcar and Zarnic (2009) for CLT panels with openings, who noted that compared to the reduction in stiffness, load-bearing capacity was not as affected by openings due to failures mainly being concentrated at anchors. Whilst the presence and size of openings may not result in decreased failure strength at the hold-downs, as the opening size increases other failure mechanisms may be initiated. This is explored further in the following section.

Table 5-8: Hold-down reactions for all panels with an applied load of 5.5 kN

MEASUREMENT With an applied load of 5.5 kN	PANEL					
	FSFE-5.5	FSO _{12.5} FE	FSO ₂₅ FE	FSO _{37.5} FE	FSO ₅₀ FE	FSO _{56.25} FE
Reaction at left hold-down (kN)	24.97	24.85	24.85	24.85	24.82	24.74
Difference from fully sheathed panel	0%	0%	0%	0%	-1%	-1%
Reaction at right hold-down (kN)	7.59	7.75	7.75	7.75	7.83	8.03
Difference from fully sheathed panel	0%	2%	2%	2%	3%	6%

5.7.5 Effect of Opening Size on the Development of Stress Concentrations and Possible Alternate Failure Modes

As noted above, the loads on the hold-downs and resultant stresses in the bottom plate are not significantly affected by the opening size. Noting that the transverse failure of the bottom plate was the primary failure mode in the experimental panels, if improvements to the hold-down arrangement are made, the strength of the wall system may increase. Such improvements may include use of adhesive between the insert and the RHS (Hizam, Karunasena & Manalo 2013; Hizam et al. 2019), the use of larger, stronger washers, or other improvements. Regardless of the exact details of the improvements

made, strengthening of the hold-down to prevent transverse failure may result in the development of stresses in other areas and could lead to new failure modes. This is explored in more detail below.

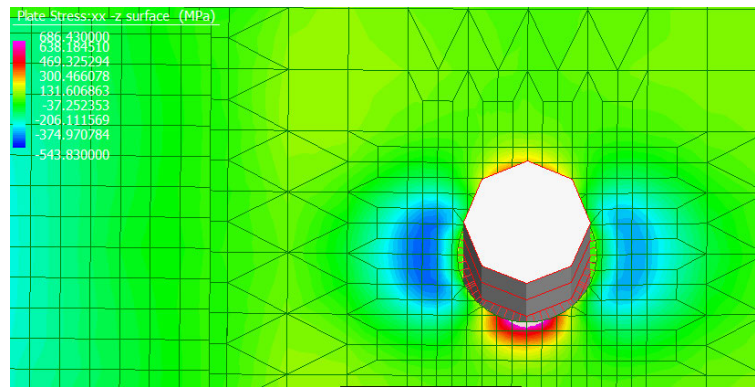
To account for possible improvements in the hold-down strength, the elastic modulus of the insert brick element was arbitrarily increased to a very high value of 5 GPa. In addition, attachment links between the underside of the left-hand insert and inside of the RHS were added. These two changes combine to make the hold-down arrangement significantly stiffer and prevent large deformations of the bottom plate. This is considered a reasonable approach to mimic possible improvements that could be made to the hold-down and enable a broader study of other failure modes to be undertaken. It is noted that even with the modifications, transverse stresses larger than the material strengths are shown in the FEM. This reinforces the conclusion that transverse failure at the hold-down is a critical aspect and represents a weak component of this wall system. However, for the purposes of this investigation into possible alternate failure modes it is assumed that the transverse stresses at the hold-down are no longer the critical failure mode.

Utilising the FEMs developed, applied loads were incrementally increased for each panel, and subsequent stress concentrations were analysed for exceedance of the material strengths, as outlined in Chapter 3. Strength exceedance may indicate local failures of the component, which may subsequently lead to global failure of the panel. The loads at which possible material failures occurred can then be compared to assess how the opening size effects possible failure modes. Based on stress concentrations, three main potential failure modes were found, which are outlined below. Other failures may occur, but it is considered that the ones outlined below are likely to occur at the lowest loads.

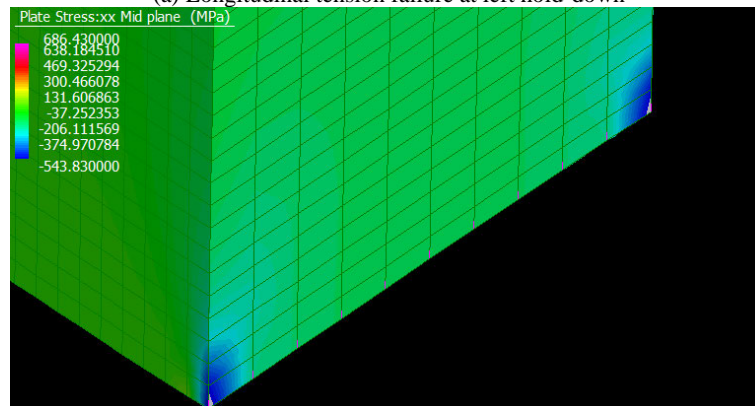
1. **Longitudinal tension failure of the bottom plate at the left-hold down, see Figure 5-27(a).**
This stress is a result of both horizontal load transfer between the hold-down and the bottom plate, as well as local bending stresses due to the uplift of the bottom plate, similar to the transverse stresses found in the experiments. A crack forming at this location may be expected to propagate away from the hold-down and perpendicular to the main fibres in the bottom plate, consistent with failure modes of GFRP bolted connections noted by (Hizam et al. 2018). This would likely result in loss of load transfer ability between the bottom plate and hold-down. Whilst improvements to the hold-down arrangement may reduce this potential outcome; however, it is still noted as being a possible failure mode.
2. **Longitudinal compression failure at the base of the right vertical stud, see Figure 5-27(b).**
This failure may result in local splitting, buckling, or crushing of the base of the stud, as was found for similar GFRP pultruded sections loaded in compression by Guades, Aravinthan and Islam (2014) and Sharda et al. (2021). If this failure propagates it could lead to high stresses between the sheathing and frame, or cause the sheathing to bear against the ground if the vertical

stud is sufficiently crushed. Both occurrences may result in debonding of the sheathing from the frame, similar to the result found by Manalo (2013), leading to failure of the panel.

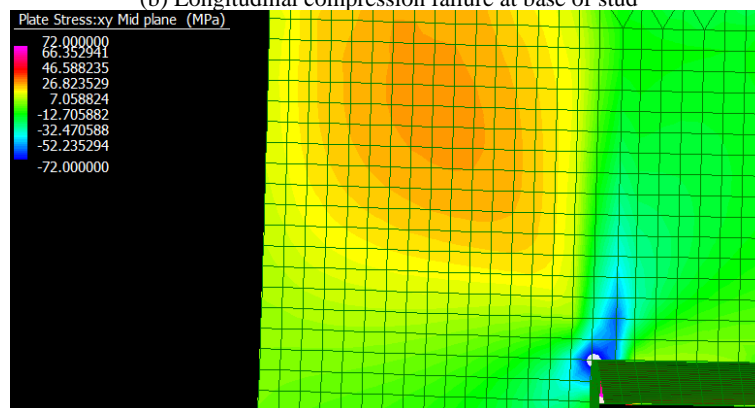
3. **Shear failure of the sheathing at the top corners of the opening, see Figure 5-27(c).** Failure at the corners of the opening is consistent with the findings of Richard et al. (2002), Kozem Šilih and Premrov (2012), Grossi, Sartori and Tomasi (2015b, 2015a), and Anil et al. (2016). However, it is noted that rather than an adhesive, these authors utilised nailed type sheathing-to-frame fixation which tends to allow higher relative movement between the sheathing and frame. Whilst this provides some ductility to the panel behaviour, this may contribute to the failure of the sheathing in such a manner, as the sheathing load cannot be as effectively transferred to the frame. In contrast, the panels tested in this project were attached by structural adhesive and high load transfer was able to occur. This will likely minimise the potential of cracking in the manner found with other systems.



(a) Longitudinal tension failure at left hold-down



(b) Longitudinal compression failure at base of stud



(c) Shear failure at the top corners of the opening

Figure 5-27: Possible alternate failure modes shown in FEM, including (a) longitudinal tension failure at the left hold down, (b) longitudinal compression failure at the base of the right stud, and (c) shear failure at the top corners of the opening

The loads at the onset of these failure modes for each panel are shown in Table 5-9 and are graphed in Figure 5-28. As is evident, the load to produce failure due to longitudinal tension at the hold-down was consistent between panels of all opening size, at approximately 18 kN. This is consistent with previous findings in that the load and subsequent stresses at the hold-down are not significantly affected by the presence and size of the opening. This failure load represents a potential increase to the failure loads found during experimental testing.

Similarly, with failure loads of about 20 kN, compression failure at the base of the studs was mostly consistent between all panels, except for a slight increase in load for panel FSO₅₆25FE which has the largest opening. Whilst not a significant change, this may be due to the interaction of frame member

bending at the base of the opening with the vertical reaction load at the base of the stud. Overall, however, it is considered that compression failure at the base of the study is not significantly affected by the size of opening.

Failure due to shear stress at the top corners of the opening was strongly related to the size of the opening, with a smaller opening providing a much higher load of 60 kN to develop failure stresses, compared to the panel with the largest opening which failed at about 20 kN. This result is expected, as larger, taller openings result in higher bending moments and subsequent stresses at the corners of the opening where the frame is restrained by the sheathing. It is noted that for each panel, similar but slightly lower stresses were found at the bottom corners of the opening and it is possible failure could also occur there.

Table 5-9: Loads at onset of possible alternate failure modes

FAILURE MODE	LOAD (kN)				
	FSO _{12.5FE}	FSO _{25FE}	FSO _{37.5FE}	FSO _{50FE}	FSO _{56.25FE}
Longitudinal tension failure of bottom plate at hold-down	18.75	18.75	18.75	18.75	18.75
Longitudinal compression failure at base of vertical stud	20.625	20.625	20.625	20.625	22.5
Shear failure of sheathing at top corners of opening	60	41.25	30	22.5	20.625

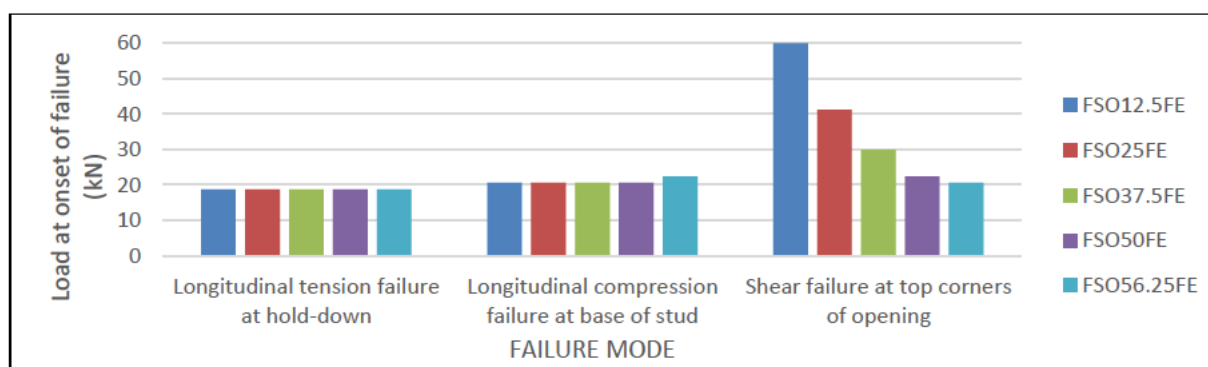


Figure 5-28: Graph of loads at onset of potential failure modes

The results of this analysis are of significance, as they indicated that if the hold-down is improved so as to prevent the transverse failure seen in the experimental testing, the overall yield strength of the wall system may be able to be increased substantially. Noting that the yield strengths observed in the experiment were between 5.5 and 6.5 kN, and ultimate strengths were between 9.8 and 11.6 kN, according to the FEA, yielding of the materials may not occur until 18 to 20 kN for alternate failure modes, and depending on the opening size could be as high as 60 kN. It can be concluded that, depending on the failure mode that becomes critical, significant strength increases may be achievable.

It is also concluded that whilst opening size did affect the strengths of the shear failure at the corners of the opening, strengths of 20 kN or higher were still achieved. Additionally, as noted previously, whilst openings reduce the stiffness of the panel, a panel with an opening of 50% still provided about half the stiffness of a fully sheathed panel. As was also concluded by Kozem Šilih and Premrov (2012), wall

panels with openings may therefore be able to be considered to contribute to the load carrying capacity of a structure, which is often not considered in the design of structures. It should be noted that the advantage of higher strength would need to be balanced against the benefit of a ductile failure mode. Additional testing with an improved hold-down arrangement would be required to explore this further.

To briefly consider a potential real-world, industry benefit of these findings, comparison of the above results with traditional wall systems can be made. AS 1684.2 – *Residential timber-framed construction, Part 2: Non-Cyclonic Areas* (Standards Australia 2013) outlines accepted wall bracing capacities in clause 8.3.6. Under this clause, the highest bracing capacity is 9 kN/m, using 4.8 mm hardboard sheathing. Factoring this by 1.5 to obtain an ultimate capacity gives 13.5 kN/m. In comparison, based on the FEA outlined above, a 20 kN capacity for a 0.6 m wide wall may be possible with this GFRP wall system. This gives a bracing capacity of 33.3 kN/m, significantly higher than the capacity achieved under AS 1648.2. Based on these values, a 60% reduction in the length of shear wall required could potentially be achieved using this GFRP system, rather than a system under AS 1648.2. Some potential benefits of this are listed below:

- Potential reductions in cost, depending on the cost of the GFRP wall system
- Flexibility with sizes, location, and number of openings.
- Flexibility with floor plans, allowing more open floor plans be achieved
- Opportunities for use in the renovation sector, where removal of a large length of existing shear wall could be compensated by a small section of this wall system
- Opportunities for use in areas subject to high lateral loads such as earthquake or cyclone prone areas, where high capacities may be achievable

Whilst this a very high-level estimate and significant further research is required to understand and develop this GFRP wall system, it provides a good illustration of what benefits may be achievable.

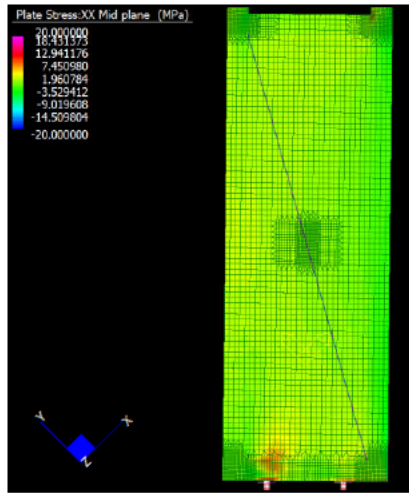
5.7.6 Effect of Opening Size on Sheathing Tensile Stresses

Development of high tensile stresses within the sheathing can result in failure of the panel, as was found by Manalo (2013). As opening sizes increase, the sheathed sections experience higher stresses, and the potential for such failure to occur is more likely. The following section outlines how openings affect the stresses within the sheathing.

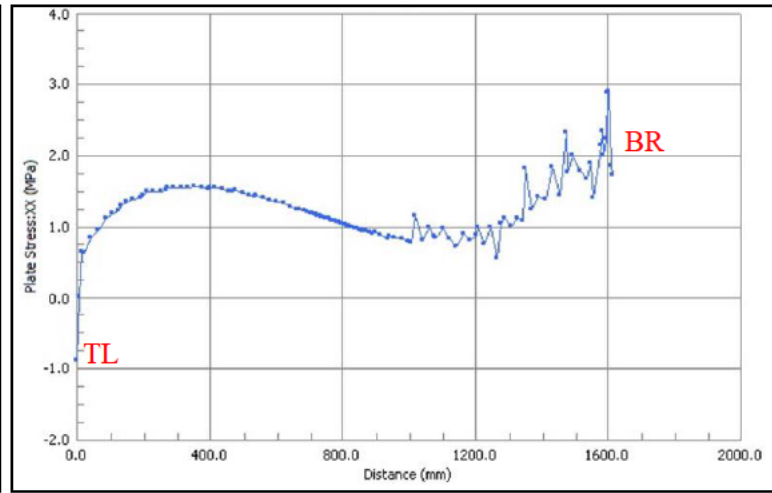
Figure 5-29 shows the sheathing stress in the direction of +45° angle along a diagonal from top left (TL) to bottom right (BR) of the sheathing for panels. The panels are under tension in this direction. The general pattern is relatively consistent between panels, with stress generally increasing to a peak

value in the mid to upper left-hand quadrant, followed by a slight decline and final sharp increases in stress at the bottom right quadrant. It is obvious from these figures that as the opening size increases the peak sheathing stresses near the middle of the sheathing also increase, varying from approximately 1.5 MPa for panel FSO_{12.5}FE to 5.5 MPa in panel FSO_{56.25}FE.

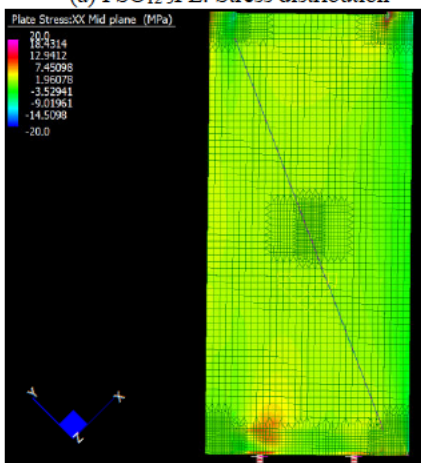
The stress values at the bottom-right are not considered reliable due to their inconsistent nature, which can be attributed to the complex stresses occurring in the vicinity of the frame members and hold-downs. However, it is noted that the increase in stress in the vicinity of the bottom right corner correlates with the findings of Manalo (2013), who found that a diagonal tensile crack in the sheathing propagated from the bottom right corner which, with the crack also associated with buckling of the compression stud. A wall system with strong sheathing-to-frame fixation, such as that investigated by Manalo (2013) and as used in this project, may be prone to such failure as the full capacity of the sheathing is able to be utilised. This type of failure may be brittle, which is in contrast with systems with deformable fixation such as nails. It is also noted that the values in Figure 5-29 do not represent the absolute maximum stress values experienced by the sheathing, which occur somewhere near the left hold-down. Rather, these values help demonstrate how increasing opening size results in increases in the sheathing stresses. It is also noted that the magnitude of the stresses exhibited in the sheathing are relatively low in comparison with the material strengths, indicating that such failure was not immanent. However, any improvements to the failure strength of the panel may result in increases in the sheathing strain that may lead to such a tensile failure, which is an undesirable brittle failure mode. As such, further research and development of this wall system should take this into consideration.



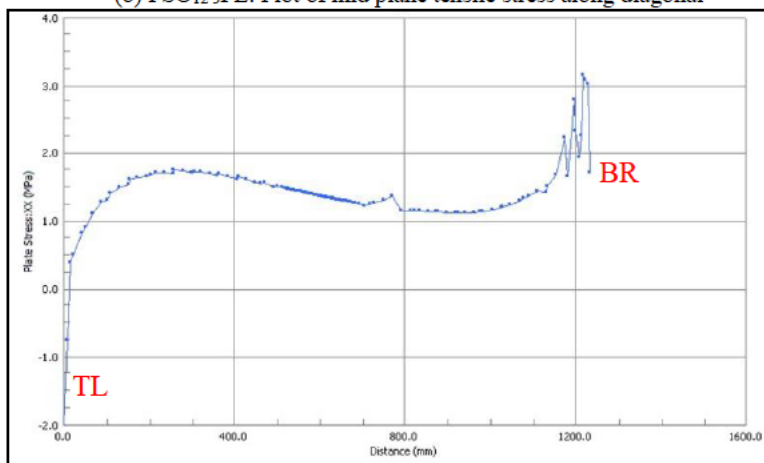
(a) FSO₁₂ 5FE: Stress distribution



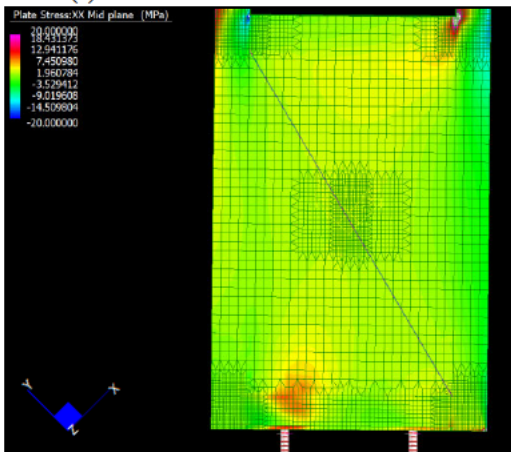
(b) FSO₁₂ 5FE: Plot of mid plane tensile stress along diagonal



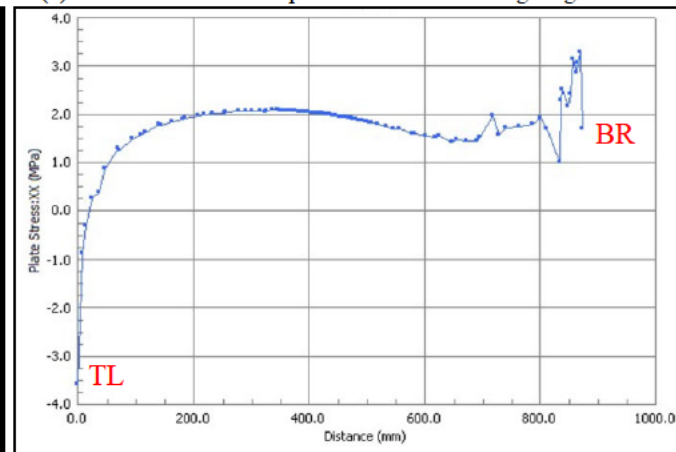
(c) FSO₂₅ 5FE: Stress distribution



(d) FSO₂₅ 5FE: Plot of mid plane tensile stress along diagonal



(e) FSO₃₇ 5FE: Stress distribution



(f) FSO₃₇ 5FE: Plot of mid plane tensile stress along diagonal

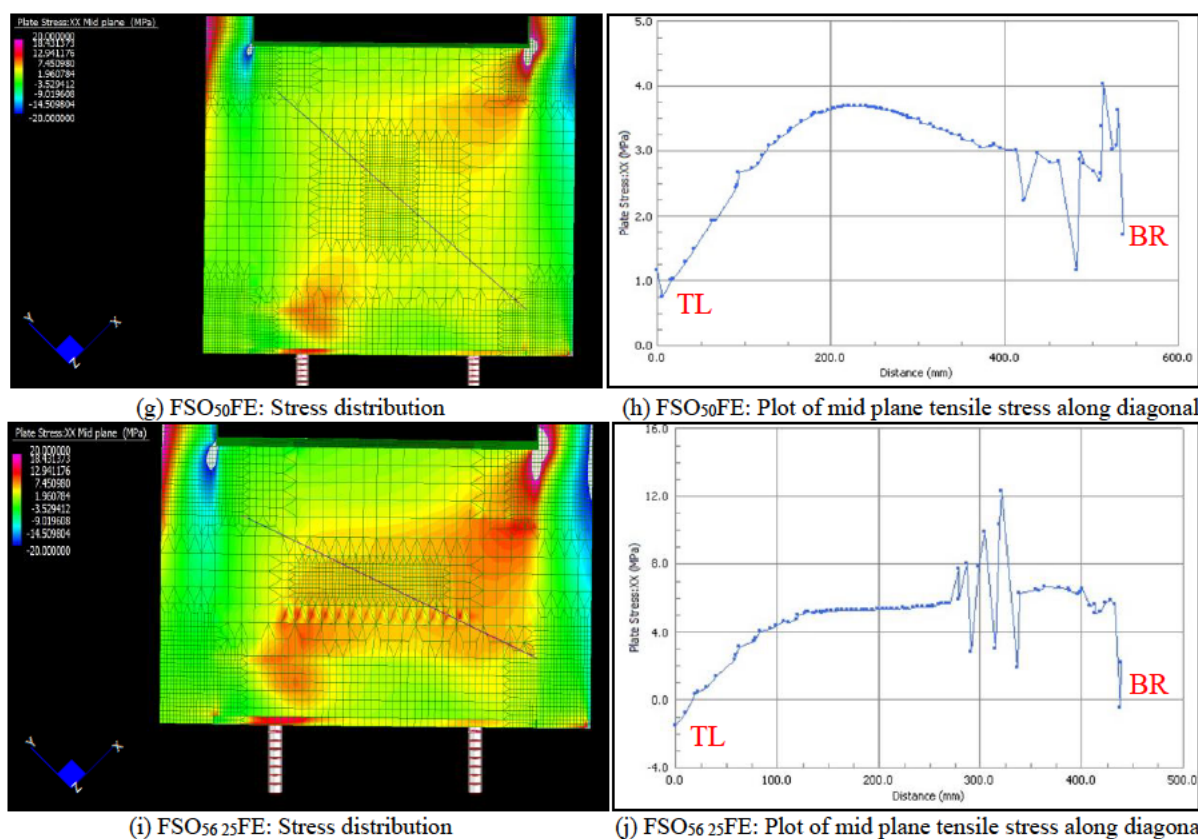


Figure 5-29: Sheathing tensile stress distribution and plot along diagonal for panels (a)-(b) FSO_{12.5}FE, (c)-(d) FSO_{2.5}FE, (e)-(f) FSO_{37.5}FE, (g)-(h) FSO₅₀FE, and (i)-(j) FSO_{56.25}FE

5.7.7 Effect of Openings on Compression Stud Stresses

Stresses within the frame, and in particular compressive and bending stresses in the right-hand compression stud, are important due to the potential for frame failures such as buckling, as was noted by Manalo (2013) and Branston, Chen, et al. (2006). Due to their relatively long and thin nature, frame members can be prone to these failure types which may be of concern when the shear wall is also carrying vertical compression loads (Branston, Boudreault, et al. 2006). The following section investigates how window openings affect frame stresses and the potential for buckling.

Figure 5-30 shows plots of mid plate stresses along the inner and outer walls of the right-hand stud members for all panels, noting that negative is compressive stress. This shows that the right-hand stud in the fully sheathed panel remained in compression across its full section, indicating that the wall as a whole behaved as a cantilever and the right-hand stud behaved somewhat like a column braced by the sheathing. In contrast, the presence of openings resulted in the right-hand stud bending, shown by the tension on the inner face and compression on the outer face at the base of the openings, and vice versa at the top of the openings where opposite bending occurred. This bending action indicates deformation of the opening shape itself. It also indicates that the vertical forces being transferred from the sheathing to the stud are applied below the opening, whilst a horizontal force causing bending is applied above the opening. Noting that in accordance with Euler's critical buckling load, which is inversely proportional to the square of the effective length of a column (Bhoi & Kalurkar 2014), this may indicate

that larger openings result in a shorter effective length of the column and therefore may reduce buckling of the right-hand stud compared to a fully sheathed panels or panels with smaller openings. This does not necessarily mean that openings increase the strength of the panel; rather, that if stud buckling were to become the critical failure mode in sheathed panels, the presence and size of the opening may reduce the likelihood of buckling and may result in a shift to a different failure mode. If this were to result in the failure mode being shifted to a more ductile failure mode, this may be of benefit to the overall behaviour of the panel. It is possible, however, that the combined bending and compressive force could result in local buckling of the thin walled RHS member, similar to what was found by Branston, Chen, et al. (2006) with light-gauge steel frame members.

It is noted that whilst frame buckling was not critical for the relatively narrow panels tested in this project, wider panels with both adjacent walls and compressive loads applied may be more prone to frame buckling due to the increased overall loads that can be generated and that would be carried by the vertical frame members. This is considered an area that warrants further research, noting that in practice shear walls will be wider and have vertical loads.

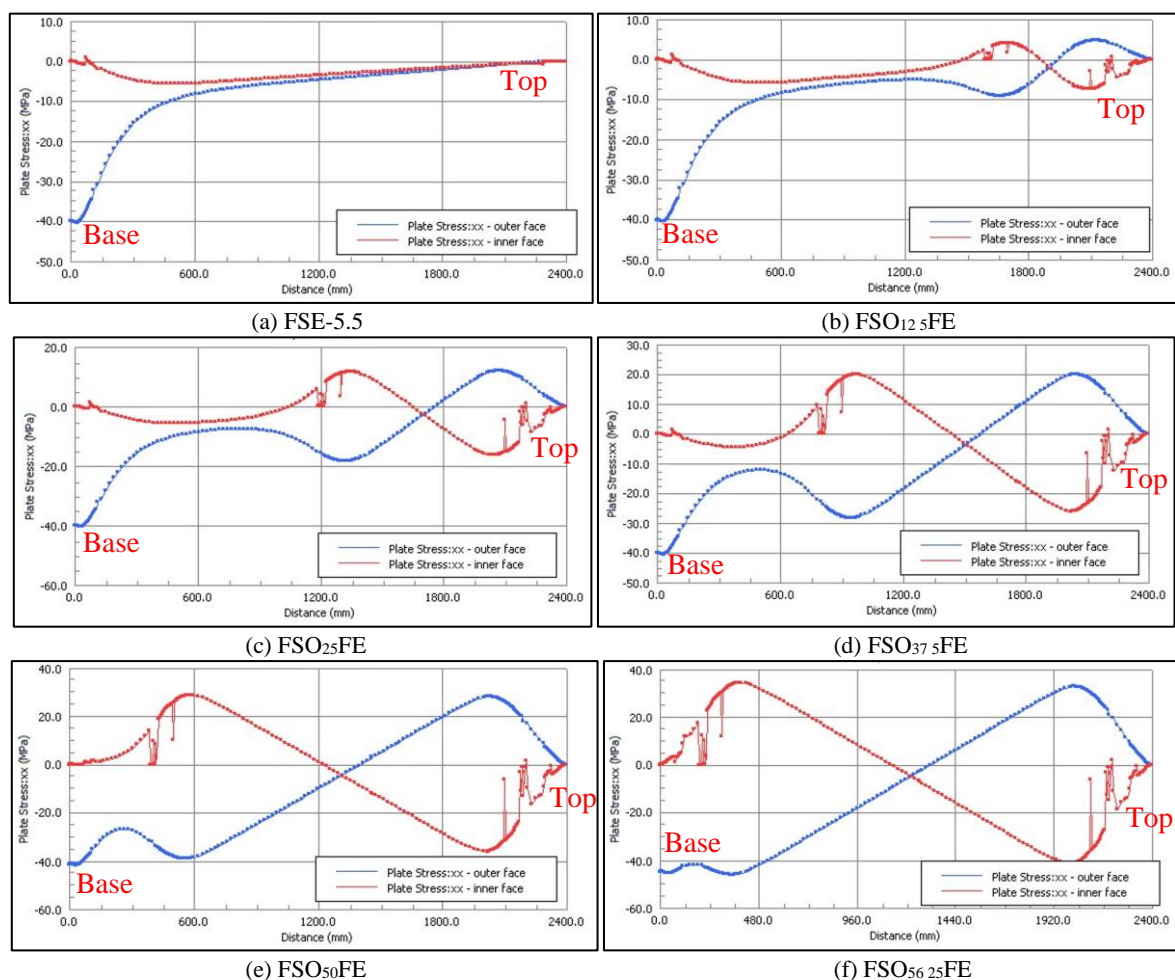


Figure 5-30: Stress distribution within right-hand compression stud on both outer and inner walls of the RHS, for panels (a) FSE-5.5, (b) FSO_{12.5}FE, (c) FSO₂₅FE, (d) FSO_{37.5}FE, (e) FSO₅₀FE, and (f) FSO_{56.25}FE

5.8 Summary

Development of finite element models of the wall system has been undertaken utilising Strand7, and comparison with the experimental results has validated the models. These validated models could then be used in the parametric investigation, with key findings outlines below.

The parametric study has shown that the in-plane global stiffness varies approximately linearly with the size of opening, with a 56.25% opening size resulting in a 53% reduction in stiffness. The additional deflection was found to be due to bending of the frame above the base of the opening, and not due to additional uplift and rotation.

It was also found that the reaction and stress development in the bottom plate at the hold-down are not significantly affected by the presence of an opening. In this way, the strength capacity of the wall based on failure at the hold-down is not affected by the opening size.

Further, if improvements to the hold-down arrangement are made so as to strengthen and stiffen the hold-down and prevent high transverse stress development, the failure capacity of the wall may be increased significantly, with capacities for this wall system potentially in the order of 20 kN. Of the potential failure modes that may occur, failure at the corners of the opening is the only mode significantly affected by the size of the opening, with an increase in size resulting in a decrease in capacity. A high-level comparison between these results and traditional wall systems covered under AS 1684.2 indicates that a 60% reduction in shear wall length may be achievable with this system.

An increase in the size of the opening was found to increase the tensile shear stress within the sheathing, however the magnitude of the stresses was found to be relatively low and below the failure strengths of the material for the applied loads tested, noting that other failure modes are considered to be more critical.

The stresses in the vertical frame members were also found to be affected by the opening size. Without an opening, the right-hand stud was found to be in compression across its section, much like a column. This loading condition may leave the stud prone to global buckling, as has been seen in previous experimental testing of wall systems with thin frame members. In contrast, with an opening the stud exhibited compression stresses below the opening, and bending stresses at and above the base of the opening, due to the cantilever action of the frames above the base of the opening. The net effect was to lower overall compression stress in the lower portion of the stud. The opening may also reduce the effective length of the stud in terms of compression loading and buckling, potentially reducing the likelihood of global buckling. Local buckling due to the combined compression and bending stresses may however still result, and further testing and investigation is recommended to explore this further.

Overall, this parametric study has provided deeper understanding of how sheathing and opening size affects the in-plane shear behaviour the GFRP wall system, and has highlighted potential areas of improvement and areas that would benefit from additional experimental testing and FEA investigation. Based on these findings and the experimental testing, final conclusions and recommendations for areas of further research can be made.

Chapter 6 Conclusions and Recommendations

6.1 Conclusions

6.1.1 Overview

As traditional materials continue to exhibit limitations in solving the challenges facing the construction industry, exploration of new construction methods and materials is required. In addition, new opportunities may be possible by utilising methods and materials that have not been previously considered. This project therefore aimed to investigate the in-plane shear behaviour of a load bearing wall system constructed of GFRP frame members and sheathing, with a focus on how openings affect the wall system's behaviour. Experimental testing and finite element analysis of the wall system was undertaken to establish how openings affect the in-plane shear stiffness, strength, and failure behaviour of the wall system. Then, finite element models were developed and validated using the experimental results, and a parametric investigation was undertaken. Key findings and conclusions of the project are outlined in the following sections.

6.1.2 Experimental Investigation of In-Plane Shear Behaviour

The in-plane shear behaviour of large-scale GFRP composite wall panels was investigated experimentally, with panels including a frame only panel, and panels with sheathing and with a window opening (37.5%). Based on the results of this work, the following conclusions are derived:

- The presence of sheathing significantly affected the in-plane behaviour, with the frame only panel behaving similarly to a pinned frame and exhibiting no rotation or uplift, whilst the fully sheathed panel exhibited both rotation and uplift
- The frame only panel exhibited minimal in-plane stiffness, and no distinct failure was observed; however, slight plastic deformation of the angle brackets at the frame joints occurred
- The presence of sheathing increased the in-plane stiffness to approximately 68 times that of the frame itself with no sheathing, indicating that sheathing is the primary provider of in-plane stiffness for this wall system
- The presence of sheathing significantly affected the failure behaviour, with the fully sheathed panel failing due to the development of transverse tensile stresses in the bottom plate which led to splitting of the bottom plate adjacent to the hold-down bolt and crushing of the bolt insert.

- The presence of an opening had a minor effect on the panel behaviour. Primary deflection was due to rotation and uplift of the panel, however additional deflection due to bending of the frame above the base of the opening contributed to the lower stiffness observed.
- The presence of an opening had no effect on the failure behaviour when compared to the fully sheathed panel, with failure due to splitting of the bottom plate at the hold-down bolt and crushing of the bolt insert.
- The hold-down arrangement is considered the weakest component of this wall system, due to the occurrence localised bending of the bottom plate and development of high stresses in the transverse direction
- Based on maintaining static equilibrium, it is considered that the presence of an opening did not affect the failure strength based on the failure mode observed, as was confirmed using FEA (see below for more detail)
- The failure behaviour of both sheathed panels was moderately ductile, with the panels continuing to carry loads after initial yielding caused by splitting of the bottom plate. Ductility ratios of approximately 2.2-2.4 were achieved, which are reasonable but still lower than typical wall systems with nail or screw type sheathing-to-frame fixation
- The sheathing-to-frame adhesive exhibited adequate load transfer, and no cracking or failure of the adhesive was observed

6.1.3 FEA Investigation of In-Plane Shear Behaviour

Based on the experimental testing, finite element analysis was undertaken to further investigate the wall system and to assess how window opening size affects the in-plane shear behaviour. Based on this FEA, the following conclusions can be made:

- The reaction loads in the hold-downs are unaffected by the presence or size of openings; therefore, based on failure at the hold-down, the panel strength was not influenced by the presence or size of openings.
- There is an approximately directly proportional relationship between opening size and percentage reduction in panel stiffness. For example, a 46% reduction in stiffness was observed with an opening of 50% of the panel area.
- Additional deflection of panels with increasing opening sizes was due to bending of the frame above the base of the opening, and was not due to additional uplift or rotation of the panel

- Possible alternate failure modes include longitudinal tension failure of the bottom plate adjacent to the hold-down, compressive failure at the base of the compression stud, and shear failure at the corners of the openings
- Failure at the corners of the opening was strongly affected by the size of openings, with larger openings resulting in a lower strength. Failure strengths of other potential failure modes were unaffected by the size of openings

6.1.4 General Conclusions

Apart from the key outcomes listed above, some other conclusions can also be made, as provide below:

- The wall panels with significant opening sizes provided reasonable in-plane stiffness and strength, indicating that they may be able to be considered to contribute to the shear stiffness and strength of a structure in design
- Stresses within the main sheathed section of the panels generally increases with an increase in opening size. Whilst the stresses exhibited in the FEA are relatively low and well below the materials strength, changes in stress can occur upon failure of other components that may result in sudden increases in stress in the sheathing. This is of note as tensile failure of the sheathing is considered a brittle and undesirable failure mode
- The presence and size of openings may reduce the potential for buckling of the compression stud due to a reduction in the effective length of the right-hand stud acting as a column. However, combined bending and compression could result in localised buckling failure of the RHS profile
- Comparison of the bracing capacities achieved using the FEA results and those under AS 1684.2 indicate significantly higher strengths may be achievable with the GFRP wall system compared to traditional timber construction.

6.2 Recommendations for Further Research

Further research is recommended to not only addresses aspects that were not able to be investigated in this project, but to implement improvements and study key aspects that have been revealed through this project. Some key recommendations are as follows:

- Investigate improvements and adjustments to the hold-down arrangement, such as:
 - Use of adhesive between the insert and RHS, to improve the distribution of stresses and in particular to reduce the development of transverse and bending stresses. This

was found to significantly increase strength of the connection by Hizam, Karunasena and Manalo (2013), and may have helped reduce the local bending of the wall of the RHS profile and increase the capacity of the system

- Use of a stiffer hold-down insert
 - Use of larger and thicker washers
 - Investigate the effect of different locations and edge distances of the hold down from the end of the bottom plate, to ascertain if this is a critical factor with respect to failure of the hold-down
- Investigate the effect of openings in different locations and of varying aspect ratios in wider wall panels, where the opening does not extend the full width between studs, noting that wider panels are typically used in practice (Standards Australia 2013)
 - Undertake further study to characterise material properties of the RHS, sheathing, and mechanical inserts. In particular, this may help to improve the ability to understand and model the in-plane stresses of the sheathing which were not well correlated between FEA and experimental results in this study
 - Investigate load transfer between frame and sheathing through the adhesive and undertake material characterisation of the adhesive. This may also help to improve understanding of the stresses within the sheathing, as noted above
 - Investigate the in-plane shear behaviour of this GFRP wall system with vertical applied loads to simulate roof or upper floor loads. This will likely reduce the reaction loads at the hold-downs and may result in different failure modes becoming critical to what was found in this project (Liew, Duffield & Gad 2002).
 - Investigate the behaviour of wider and double wall panels, with vertical loads, noting that these may be prone to failure modes not found in this project such as sheathing and frame buckling
 - Investigate potential out-of-plane buckling of sheathing, which may occur if the sheathing is able to bear against the ground or adjacent walls (Richard et al. 2002; Sadeghi Marzaleh et al. 2018). This may result in a different failure mode to the ones considered in this paper, and is important to consider in the context of multi-panel walls
 - Investigate behaviour of the GFRP wall system with sheathing applied to one side only. Whilst this investigation revealed a number of potential failure modes, singly sheathed walls are

common in practice, and may result in changes to stress distribution and subsequently may result in difference failure modes.

Based on the findings of this project, there appears definite potential for this system to be of benefit to the industry and undertaking the additional research outlined above will provide invaluable in the ongoing development of this GFRP wall system.

References

Abdullah, T, Anil, Ö, Karagöz İşleyen, Ü, Ediz, İ & Durucan, C 2017, 'Finite-element analyses of light timber-framed walls with and without openings', *Proceedings of the Institution of Civil Engineers - Structures and Buildings*, vol. 170, no. 8, pp. 1-15, viewed 30 November 2020,

<https://www.researchgate.net/publication/316564840_Finite-element_analyses_of_light_timber-framed_walls_with_and_without_openings>.

Ahmed, A, Guo, S, Zhang, Z, Shi, C & Zhu, D 2020, 'A review on durability of fiber reinforced polymer (FRP) bars reinforced seawater sea sand concrete', *Construction and Building Materials*, vol. 256, p. 119484, viewed 8 May 2021,

<<https://www.sciencedirect.com/science/article/pii/S0950061820314896>>.

Ajayi, SO, Oyedele, LO, Bilal, M, Akinade, OO, Alaka, HA, Owolabi, HA & Kadiri, KO 2015, 'Waste effectiveness of the construction industry: Understanding the impediments and requisites for improvements', *Resources, Conservation and Recycling*, vol. 102, pp. 101-12, viewed 13 May 2021,

<<https://www.sciencedirect.com/science/article/pii/S0921344915300203>>.

Al-Rubaye, M 2018, 'Flexural Behaviour of Concrete Slabs Reinforced with GFRP Bars and Hollow Composite Reinforcing Systems', masters thesis, University of Southern Queensland, Australia, viewed 8 May 2021, <<https://eprints.usq.edu.au/34755/>>.

Al-saadi, AU, Aravinthan, T & Lokuge, W 2019, 'Effects of fibre orientation and layup on the mechanical properties of the pultruded glass fibre reinforced polymer tubes', *Engineering structures*, vol. 198, p. 109448, viewed 27 March 2021,

<<https://www.sciencedirect.com/science/article/pii/S014102961834118X>>.

Al-Sabagh, A, Taha, E, Kandil, U, Awadallah, A, Nasr, G-AM & Reda Taha, M 2017, 'Monitoring Moisture Damage Propagation in GFRP Composites Using Carbon Nanoparticles', *Polymers*, vol. 9, no. 3, p. 94, viewed 20 February 2021, <<https://www.mdpi.com/2073-4360/9/3/94>>.

Alajarmeh, OSA 2020, 'Compressive behavior of hollow concrete columns reinforced with GFRP bars', PhD thesis, University of Southern Queensland, Australia, viewed 8 May 2021,

<<https://eprints.usq.edu.au/39948/>>.

Anil, Ö, Togay, A, Karagöz İşleyen, Ü, Söğütü, C & Döngel, N 2016, 'Hysteretic behavior of timber framed shear wall with openings', *Construction and Building Materials*, vol. 116, pp. 203-15, viewed 14 September 2021, <<https://www.sciencedirect.com/science/article/pii/S0950061816306158>>.

Asamoah, RO, Ankrah, JS, Offei-Nyako, K & Tutu, EO 2016, 'Cost Analysis of Precast and Cast-in-Place Concrete Construction for Selected Public Buildings in Ghana', *Journal of Construction Engineering*, vol. 2016, p. 8785129, viewed 20 February 2021,

<<https://www.hindawi.com/journals/jcen/2016/8785129/>>.

Ascione, F, Lamberti, M & Razaqpur, G 2015, 'Modifications of standard GFRP sections shape and proportions for improved stiffness and lateral-torsional stability', *Composite structures*, vol. 132, pp. 265-89, viewed 4 March 2021,

<<https://www.sciencedirect.com/science/article/pii/S0263822315003657?via%3Dihub>>.

ASTM International 2006, *Standard Practice for Static Load Test for Shear Resistance of Framed Walls for Buildings*, E564-06, ASTM International, USA, viewed 8 March 2021,

<<https://ewb.ihs.com/#/document/OUACGGAAAAAAAAAAAA?qid=637507426281278128&sr=re-1-10&kbid=4%7C20027&docid=943713279#h0829fe04>>.

ASTM International 2015, *Standard Test Methods of Conducting Strength Tests of Panels for Building Construction*, E72-15, ASTM International, USA, viewed 8 March 2021,

<<https://ewb.ihs.com/#/document/EZINKFAAAAAAAAAAAAA?qid=637507426457985796&sr=re-1-10&kbid=4%7C20027&docid=941459369#h60b9a3e5>>.

Attari, N, Amziane, S & Chemrouk, M 2012, 'Flexural strengthening of concrete beams using CFRP, GFRP and hybrid FRP sheets', *Construction and Building Materials*, vol. 37, pp. 746-57, viewed 11 May 2021, <<https://www.sciencedirect.com/science/article/pii/S0950061812005223>>.

Austral Wright Metals 2015, *Aluminium Grades Datasheet*, Austral Wright Metals, Australia, viewed 28 July 2021, <<https://www.australwright.com.au/products/aluminium/aluminium-data-sheet/>>.

Australian Stainless Steel Development Association 2020, *304: The Place to Start*, webpage, Australian Stainless Steel Development Association, Australia, viewed 25 May 2021,

<<https://www.assda.asn.au/technical-info/grade-selection/304-the-place-to-start>>.

Bakis, CE, Bank, L, Brown, V, Cosenza, E, Davalos, J & Lesko, J 2002, 'FRP composites in construction - State of the art review', *ASCE Compos Constr J*, vol. 6, pp. 78-87, viewed 8 May 2021,

<https://www.researchgate.net/publication/284890851_FRP_composites_in_construction_-_State_of_the_art_review/citations>.

Bank, LC 2013, 'Progressive Failure and Ductility of FRP Composites for Construction: Review', *Journal of Composites for Construction*, vol. 17, no. 3, pp. 406-19, viewed 23 August 2021,

<[https://doi.org/10.1061/\(ASCE\)CC.1943-5614.0000355](https://doi.org/10.1061/(ASCE)CC.1943-5614.0000355)>.

- Bazli, M, Ashrafi, H & Oskouei, AV 2016, 'Effect of harsh environments on mechanical properties of GFRP pultruded profiles', *Composites Part B: Engineering*, vol. 99, pp. 203-15, viewed 8 March 2021, <<https://www.sciencedirect.com/science/article/pii/S1359836816309155>>.
- Bhoi, M & Kalurkar, P 2014, 'Study of Buckling Behavior of Beam and Column', *IOSR Journal of Mechanical and Civil Engineering*, vol. 11, pp. 36-40, viewed 17 August 2021, <<https://www.iosrjournals.org/iosr-jmce/papers/vol11-issue4/Version-1/G011413640.pdf>>.
- Branco, JM, Matos, FT & Lourenço, PB 2017, 'Experimental In-Plane Evaluation of Light Timber Walls Panels', *Buildings (Basel)*, vol. 7, no. 4, p. 63, viewed 1 December 2020, <<https://www.mdpi.com/2075-5309/7/3/63>>.
- Branston, AE, Chen, CY, Boudreault, FA & Rogers, CA 2006, 'Testing of light-gauge steel-frame - wood structural panel shear walls', *Canadian Journal of Civil Engineering*, vol. 33, no. 5, pp. 561-72, viewed 22 May 2021, <<https://cdnsiencepub.com/doi/abs/10.1139/106-014?journalCode=cjce>>.
- Branston, AE, Boudreault, FA, Chen, CY & Rogers, CA 2006, 'Light-gauge steel-frame - wood structural panel shear wall design method', *Canadian Journal of Civil Engineering*, vol. 33, no. 7, pp. 872-89, viewed 17 May 2021, <<https://www.semanticscholar.org/paper/Light-gauge-steel-frame-wood-structural-panel-shear-Branston-Boudreault/15696caa08ce0956bb26dd595cfa3e0772448dec>>.
- Buckley, S 2020, 'Steel Framed Homes: Timber vs Steel Frame (Pros & Cons)', *Architecture & Design*, viewed 17 May 2021, <<https://www.architectureanddesign.com.au/features/list/steel-framed-homes-timber-vs-steel-frame-pros-cons#>>.
- Cao, X, Li, X, Zhu, Y & Zhang, Z 2015, 'A comparative study of environmental performance between prefabricated and traditional residential buildings in China', *Journal of Cleaner Production*, vol. 109, pp. 131-43, viewed 1 March 2021, <<https://www.sciencedirect.com/science/article/pii/S0959652615004953>>.
- Casagrande, D, Rossi, S, Sartori, T & Tomasi, R 2016, 'Proposal of an analytical procedure and a simplified numerical model for elastic response of single-storey timber shear-walls', *Construction and Building Materials*, vol. 102, pp. 1101-12, viewed 30 January 2021, <<http://www.sciencedirect.com/science/article/pii/S0950061815000021>>.
- Dovers, S & Butler, C 2015, *Population and environment: a global challenge*, Australian Academy of Science, viewed 13 May 2021, <<https://www.science.org.au/curious/earth-environment/population-environment#:~:text=The%20impact%20of%20so%20many,toxic%20materials%20and%20greenhouse%20gases>>.

- Dujic, B, Klobcar, S & Zarnic, R 2009, 'Influence of Openings on Shear Capacity of Wooden Walls', *NZ Timber Design Journal*, vol. 16, no. 1, viewed 12 March 2021, <[El-Abidi, K & Ghazali, F 2015, 'Motivations and Limitations of Prefabricated Building: An Overview', *Applied Mechanics and Materials*, vol. 802, pp. 668-75, viewed 20 February 2021, <\[https://www.researchgate.net/publication/282503636_Motivations_and_Limitations_of_Prefabricated_Building_An_Overview\]\(https://www.researchgate.net/publication/282503636_Motivations_and_Limitations_of_Prefabricated_Building_An_Overview\)>.

Ferdous, W, Almutairi, AD, Huang, Y & Bai, Y 2018, 'Short-term flexural behaviour of concrete filled pultruded GFRP cellular and tubular sections with pin-eye connections for modular retaining wall construction', *Composite structures*, vol. 206, pp. 1-10, viewed 6 May 2021, <<https://www.sciencedirect.com/science/article/pii/S0263822318321469>>.

Ferdous, W, Manalo, A, Aravinthan, T & Fam, A 2018, 'Flexural and shear behaviour of layered sandwich beams', *Construction & building materials*, vol. 173, pp. 429-42, viewed 20 April 2021, <<https://www.sciencedirect.com/science/article/pii/S0950061818308626>>.

Ferdous, W, Bai, Y, Almutairi, AD, Satasivam, S & Jeske, J 2018, 'Modular assembly of water-retaining walls using GFRP hollow profiles: Components and connection performance', *Composite structures*, vol. 194, pp. 1-11, viewed 6 May 2021, <<https://www.sciencedirect.com/science/article/pii/S026382231734062X>>.

Ferdous, W, Manalo, A, Van Erp, G, Aravinthan, T, Kaewunruen, S & Remennikov, A 2015, 'Composite railway sleepers – Recent developments, challenges and future prospects', *Composite structures*, vol. 134, pp. 158-68, viewed 8 May 2021, <<https://www.sciencedirect.com/science/article/pii/S0263822315007412>>.

Gand, A, Chan, T-M & Mottram, J 2013, 'Civil and structural engineering applications, recent trends, research and developments on pultruded fiber reinforced polymer closed sections: A review', *Frontiers of Structural and Civil Engineering*, vol. 7, pp. 227-44, viewed 2 March 2021, <<https://link.springer.com/article/10.1007/s11709-013-0216-8>>.

Grossi, P, Sartori, T & Tomasi, R 2015a, 'Tests on timber frame walls under in-plane forces: part 2', *Proceedings of the Institution of Civil Engineers - Structures and Buildings*, vol. 168, no. SB11, pp. 840-52, viewed 5 January 2021, <<https://www.icevirtuallibrary.com/doi/pdf/10.1680/stbu.13.00108>>.](https://www.timberdesign.org.nz/journal/engineered-timber-products/influence-of-openings-on-shear-capacity-of-wooden-walls/#:~:text=The%20study%20has%20concluded%20that,cases%20is%20reduced%20about%2050%20%25.>)

Grossi, P, Sartori, T & Tomasi, R 2015b, 'Tests on timber frame walls under in-plane forces: part 1', *Proceedings of the Institution of Civil Engineers - Structures and Buildings*, vol. 168, no. SB11, pp. 826-39, viewed 5 January 2021, <<https://www.icevirtuallibrary.com/doi/pdf/10.1680/stbu.13.00107>>.

Guades, E, Aravinthan, T & Islam, MM 2014, 'Characterisation of the mechanical properties of pultruded fibre-reinforced polymer tube', *Materials & Design*, vol. 63, pp. 305-15, viewed 27 March 2021, <<https://www.sciencedirect.com/science/article/pii/S0261306914004671>>.

Gudonis, E, Timinskas, E, Gribniak, V, Kaklauskas, G, Arnautov, A & Tamulėnas, V 2013, 'FRP reinforcement for concrete structures: State-of-the-art review of application and design', *Engineering Structures and Technologies*, vol. 5, viewed 8 May 2021, <https://www.researchgate.net/publication/262580598_FRP_reinforcement_for_concrete_structures_State-of-the-art_review_of_application_and_design>.

Hamakareem, MI n.d., *Fibre Reinforced Polymer (FRP) in Construction, Types and Uses*, The Constructor, viewed 7 May 2021, <<https://theconstructor.org/concrete/fibre-reinforced-polymer/1583/>>.

Hizam, RM, Karunasena, W & Manalo, A 2013, 'Effect of mechanical insert on the behaviour of pultruded fibre reinforced polymer (FRP) bolted joint', *Fourth Asia-Pacific Conference on FRP in Structures*, International Institute for FRP in Construction, Melbourne, Australia, viewed 23 August 2021, <<https://www.semanticscholar.org/paper/Effect-of-mechanical-insert-on-the-behaviour-of-Hizam-Karunasena/97084f6291878b899450afd3ca75bf6ff354b691>>.

Hizam, RM, Manalo, AC, Karunasena, W & Bai, Y 2018, 'Effect of bolt threads on the double lap joint strength of pultruded fibre reinforced polymer composite materials', *Construction and Building Materials*, vol. 181, pp. 185-98, viewed 23 August 2021, <<https://www.sciencedirect.com/science/article/pii/S095006181831451X>>.

Hizam, RM, Manalo, AC, Karunasena, W & Bai, Y 2019, 'Behaviour of pultruded GFRP truss system connected using through-bolt with mechanical insert', *Composites Part B: Engineering*, vol. 168, pp. 44-57, viewed 1 March 2021, <<https://www.sciencedirect.com/science/article/pii/S1359836818326234>>.

Hollaway, LC 2010, 'A review of the present and future utilisation of FRP composites in the civil infrastructure with reference to their important in-service properties', *Construction and Building Materials*, vol. 24, no. 12, pp. 2419-45, viewed 8 May 2021, <<https://www.sciencedirect.com/science/article/pii/S0950061810001947>>.

- Husain, M, Eisa, AS & Hegazy, MM 2019, 'Strengthening of reinforced concrete shear walls with openings using carbon fiber-reinforced polymers', *International Journal of Advanced Structural Engineering*, vol. 11, no. 2, pp. 129-50, viewed 1 December 2020, <<https://doi.org/10.1007/s40091-019-0216-6>>.
- Khaliq, W & Moghis, A 2017, 'Shear capacity of cold-formed light-gauge steel framed shear-wall panels with fiber cement board sheathing', *International Journal of Steel Structures*, vol. 17, no. 4, pp. 1404-14, viewed 17 May 2021, <<https://doi.org/10.1007/s13296-017-1211-z>>.
- Kozem Šilih, E & Premrov, M 2012, 'Influence of openings on horizontal load-carrying capacity of timber-frame wall elements with fibre-plaster sheathing boards', *Advances in Engineering Software*, vol. 43, no. 1, pp. 19-26, viewed 10 August 2021, <<https://www.sciencedirect.com/science/article/pii/S0965997811002407>>.
- Krall, M & Polak, MA 2019, 'Concrete beams with different arrangements of GFRP flexural and shear reinforcement', *Engineering structures*, vol. 198, p. 109333, viewed 8 May 2021, <<https://www.sciencedirect.com/science/article/pii/S0141029618322867>>.
- Lafontaine, A, Chen, Z, Doudak, G & Chui, YH 2017, 'Lateral Behavior of Light Wood-Frame Shear Walls with Gypsum Wall Board', *Journal of Structural Engineering*, vol. 143, no. 8, p. 04017069, viewed 1 December 2020, <<https://ascelibrary.org/doi/full/10.1061/%28ASCE%29ST.1943-541X.0001798>>.
- Lebeda, DJ, Gupta, R, Rosowsky, DV & Dolan, JD 2005, 'Effect of Hold-Down Misplacement on Strength and Stiffness of Wood Shear Walls', *Practice periodical on structural design and construction*, vol. 10, no. 2, pp. 79-87, viewed 18 May 2021, <<https://ascelibrary.org/doi/abs/10.1061/%28ASCE%291084-0680%282005%2910%3A2%2879%29>>.
- Lei, X, Yujun, Q, Yu, B, Chengyu, Q, Hao, W, Hai, F & Xiao-Ling, Z 2019, 'Sandwich assemblies of composites square hollow sections and thin-walled panels in compression', *Thin-walled structures*, vol. 145, p. 106412, viewed 16 August 2021, <<https://www.sciencedirect.com/science/article/pii/S0263823119306597>>.
- Liew, Y, Duffield, C & Gad, E 2002, 'The influence of plasterboard clad walls on the structural behavior of low rise residential buildings', *Electronic Journal of Structural Engineering*, vol. 2, viewed 22 February 2021, <https://www.researchgate.net/publication/228542221_The_influence_of_plasterboard_clad_walls_on_the_structural_behavior_of_low_rise_residential_buildings>.

- Liu, Y, Zwingmann, B & Schlaich, M 2015, 'Carbon Fiber Reinforced Polymer for Cable Structures—A Review', *Polymers*, vol. 7, pp. 2078-99, viewed 7 May 2021, <https://www.researchgate.net/publication/283308870_Carbon_Fiber_Reinforced_Polymer_for_Cable_Structures-A_Review>.
- Manalo, A 2013, 'Structural behaviour of a prefabricated composite wall system made from rigid polyurethane foam and Magnesium Oxide board', *Construction & building materials*, vol. 41, pp. 642-53, viewed 19 November 2020, <<https://www.sciencedirect.com/science/article/pii/S0950061813000147>>.
- Manalo, A & Aravinthan, T 2012, 'Behaviour of glued fibre composite sandwich structure in flexure: Experiment and Fibre Model Analysis', *Materials & Design*, vol. 39, pp. 458-68, viewed 23 March 2021, <<https://www.sciencedirect.com/science/article/pii/S0261306912001318>>.
- Manalo, AC, Aravinthan, T & Karunasena, W 2010, 'In-plane shear behaviour of fibre composite sandwich beams using asymmetrical beam shear test', *Construction and Building Materials*, vol. 24, no. 10, pp. 1952-60, viewed 7 April 2021, <<https://www.sciencedirect.com/science/article/pii/S095006181000125X>>.
- Manalo, AC, Aravinthan, T & Karunasena, W 2013, 'Mechanical properties characterization of the skin and core of a novel composite sandwich structure', *Journal of composite materials*, vol. 47, no. 14, pp. 1785-800, viewed 7 April 2021, <<https://journals.sagepub.com/doi/full/10.1177/0021998312451607>>.
- Mao, C, Shen, Q, Shen, L & Tang, L 2013, 'Comparative study of greenhouse gas emissions between off-site prefabrication and conventional construction methods: Two case studies of residential projects', *Energy and Buildings*, vol. 66, pp. 165-76, viewed 1 March 2021, <<https://www.sciencedirect.com/science/article/pii/S0378778813004210>>.
- Mara, V, Haghani, R & Harryson, P 2014, 'Bridge decks of fibre reinforced polymer (FRP): A sustainable solution', *Construction & building materials*, vol. 50, pp. 190-9, viewed 5 March 2021, <<https://www.sciencedirect.com/science/article/pii/S0950061813008763>>.
- Memari, A & Solnosky, R 2014, 'In-Plane Shear Performance of Wood-Framed Drywall Sheathing Wall Systems under Cyclic Racking Loading', *Open Journal of Civil Engineering*, vol. 04, pp. 54-70, viewed 1 December 2020, <https://www.researchgate.net/publication/269791421_In-Plane_Shear_Performance_of_Wood-Framed_Drywall_Sheathing_Wall_Systems_under_Cyclic_Racking_Loading>.

- Mishnaevsky, L, Branner, K, Petersen, HN, Beauson, J, McGugan, M & Sørensen, BF 2017, 'Materials for Wind Turbine Blades: An Overview', *Materials (Basel, Switzerland)*, vol. 10, no. 11, p. 1285, viewed 10 May 2021, <<https://www.ncbi.nlm.nih.gov/pmc/articles/PMC5706232/>>.
- Oktavianus, Y, Kristombu Baduge, KS, Orlowski, K & Mendis, P 2018, 'Structural behaviour of prefabricated load bearing braced composite timber wall system', *Engineering structures*, vol. 176, pp. 555-68, viewed 30 November 2020, <<https://www.sciencedirect.com/science/article/pii/S0141029618320637>>.
- Peck, Q, Rogers, N & Serrette, R 2012, 'Cold-Formed Steel Framed Gypsum Shear Walls: In-Plane Response', *Journal of Structural Engineering*, vol. 138, no. 7, pp. 932-41, viewed 17 May 2021, <[https://doi.org/10.1061/\(ASCE\)ST.1943-541X.0000521](https://doi.org/10.1061/(ASCE)ST.1943-541X.0000521)>.
- PlasticsEurope n.d., 'Information Sheet 01 - Introduction to Fibre Reinforced Plastics (FRP)', fact sheet, PlasticsEurope, Belgium, viewed 7 May 2021, <<https://www.plasticseurope.org/en/resources/publications/431-information-sheet-1-introduction-fibre-reinforced-plastics-frp>>.
- Portland Cement Association 2002, *Types and Causes of Concrete Deterioration*, document serial no. 2617, Portland Cement Association, information sheet, <[https://www.cement.org/docs/default-source/fc_concrete_technology/durability/is536-types-and-causes-of-concrete-deterioration.pdf?sfvrsn=4#:~:text=Corrosion%20of%20reinforcing%20steel%20and,delamination%20C%20and%20spalling%20\(Figs.\)](https://www.cement.org/docs/default-source/fc_concrete_technology/durability/is536-types-and-causes-of-concrete-deterioration.pdf?sfvrsn=4#:~:text=Corrosion%20of%20reinforcing%20steel%20and,delamination%20C%20and%20spalling%20(Figs.))>.
- Rajak, D, Pagar, D, Menezes, P & Linul, E 2019, 'Fiber-Reinforced Polymer Composites: Manufacturing, Properties, and Applications', *Polymers*, vol. 11, p. 1667, viewed 10 May 2021, <https://www.researchgate.net/publication/336471171_Fiber-Reinforced_Polymer_Composites_Manufacturing_Properties_and_Applications>.
- Richard, N, Daudeville, L, Prion, H & Lam, F 2002, 'Timber shear walls with large openings: Experimental and numerical prediction of the structural behaviour', *Canadian Journal of Civil Engineering*, vol. 29, pp. 713-24, viewed 19 March 2021, <https://www.researchgate.net/publication/235580575_Timber_shear_walls_with_large_openings_Experimental_and_numerical_prediction_of_the_structural_behaviour>.
- Rubino, F, Nisticò, A, Tucci, F & Carlone, P 2020, 'Marine Application of Fiber Reinforced Composites: A Review', *Journal of Marine Science and Engineering*, vol. 8, p. 26, viewed 10 May 2021, <https://www.researchgate.net/publication/338411181_Marine_Application_of_Fiber_Reinforced_Composites_A_Review>.

- Sadeghi Marzaleh, A, Nerbano, S, Sebastiani Croce, A & Steiger, R 2018, 'OSB sheathed light-frame timber shear walls with strong anchorage subjected to vertical load, bending moment, and monotonic lateral load', *Engineering structures*, vol. 173, pp. 787-99, viewed 10 August 2021, <<https://www.sciencedirect.com/science/article/pii/S0141029617322630>>.
- Satasivam, S & Bai, Y 2014, 'Mechanical performance of bolted modular GFRP composite sandwich structures using standard and blind bolts', *Composite structures*, vol. 117, pp. 59-70, viewed 8 May 2021, <<https://www.sciencedirect.com/science/article/pii/S0263822314002803>>.
- Shahnewaz, I, Tannert, T, Shahria Alam, M & Popovski, M 2017, 'In-Plane Stiffness of Cross-Laminated Timber Panels with Openings', *Structural engineering international : journal of the International Association for Bridge and Structural Engineering (IABSE)*, vol. 27, no. 2, pp. 217-23, viewed 1 December 2020, <<https://www.tandfonline.com/doi/abs/10.2749/101686617X14881932436131>>.
- Shakir Abbood, I, Odaa, Sa, Hasan, KF & Jasim, MA 2021, 'Properties evaluation of fiber reinforced polymers and their constituent materials used in structures – A review', *Materials Today: Proceedings*, vol. 43, pp. 1003-8, viewed 6 May 2021, <<https://www.sciencedirect.com/science/article/pii/S2214785320357618>>.
- Sharda, A, Manalo, A, Ferdous, W, Bai, Y, Nicol, L, Mohammed, A & Benmokrane, B 2021, 'Axial compression behaviour of all-composite modular wall system', *Composite Structures - Pre-Proof Article*, p. 113986, viewed 19 April 2021, <<https://www.sciencedirect.com/science/article/pii/S0263822321004463>>.
- Soutis, C 2005, 'Fibre reinforced composites in aircraft construction', *Progress in Aerospace Sciences*, vol. 41, no. 2, pp. 143-51, viewed 10 May 2021, <<https://www.sciencedirect.com/science/article/pii/S0376042105000448>>.
- Standards Australia 2013, *Residential timber-framed construction - Part 2: Non-cyclonic areas*, AS 1684.2-2010, Standards Australia Ltd, Australia, viewed 6 May 2021, <<https://www.standards.org.au/standards-catalogue/others/sa/as--1684-dot-2-2010>>.
- Stewart, R 2011, 'Rebounding automotive industry welcome news for FRP', *Reinforced Plastics*, vol. 55, no. 1, pp. 38-44, viewed 10 May 2021, <<https://www.sciencedirect.com/science/article/pii/S0034361711700364>>.
- Strand7 n.d.-a, *Strand7 summary of features*, web page, Strand7, Sydney, Australia, viewed 26 July 2021, <<https://www.strand7.com/html/specsummary1.htm>>.
- Strand7 n.d.-b, *Strand7 Reference Manual*, Strand7, Sydney, Australia.

- Summerscales, J 2000, 'The bulk modulus of carbon fibers', *Journal of materials science letters*, vol. 19, no. 1, pp. 15-6, viewed 25 May 2021, <<https://link.springer.com/content/pdf/10.1023/A:1006731210592.pdf>>.
- Syngros, G, Balaras, CA & Koubogiannis, DG 2017, 'Embodied CO2 Emissions in Building Construction Materials of Hellenic Dwellings', *Procedia Environmental Sciences*, vol. 38, pp. 500-8, viewed 2017/01/01/, <<https://www.sciencedirect.com/science/article/pii/S1878029617301172>>.
- Szczepański, M & Migda, W 2020, 'Analysis of Validation and Simplification of Timber-Frame Structure Design Stage with PU-Foam Insulation', *Sustainability*, vol. 12, p. 5990, viewed 30 November 2020, <https://www.researchgate.net/publication/343235326_Analysis_of_Validation_and_Simplification_of_Timber-Frame_Structure_Design_Stage_with_PU-Foam_Insulation>.
- Tam, VWY, Tam, CM, Zeng, SX & Ng, WCY 2007, 'Towards adoption of prefabrication in construction', *Building and Environment*, vol. 42, no. 10, pp. 3642-54, viewed 1 March 2021, <<https://www.sciencedirect.com/science/article/pii/S0360132306002873>>.
- van de Lindt, JW 2004, 'Evolution of Wood Shear Wall Testing, Modeling, and Reliability Analysis: Bibliography', *Practice periodical on structural design and construction*, vol. 9, no. 1, pp. 44-53, viewed 29 January 2021, <<https://ascelibrary.org/doi/pdf/10.1061/%28ASCE%291084-0680%282004%299%3A1%2844%29>>.
- Van Den Einde, L, Zhao, L & Seible, F 2003, 'Use of FRP composites in civil structural applications', *Construction & building materials*, vol. 17, no. 6, pp. 389-403, viewed 20 February 2021, <<https://www.sciencedirect.com/science/article/pii/S0950061803000400>>.
- Vasconcelos, G, Poletti, E, Salavessa, E, Jesus, AMP, Lourenço, PB & Pilaon, P 2013, 'In-plane shear behaviour of traditional timber walls', *Engineering structures*, vol. 56, pp. 1028-48, viewed 1 December 2020, <<http://www.sciencedirect.com/science/article/pii/S0141029613002319>>.
- Wagners 2021, *Composite Fibre Technologies*, web page, Wagners, Australia, viewed 11 May 2021, <<https://www.wagner.com.au/main/what-we-do/composite-fibre-technologies/cft-home/>>.
- Wagners CFT Manufacturing Pty Ltd 2016, *Product Guide*, version 04, July 2016, product guide, <<https://www.wagner.com.au/media/1190/wagners-cft-product-guide.pdf>>.
- Wang, J, Hota, G, Liang, R & Liu, W 2015, 'Durability and prediction models of fiber-reinforced polymer composites under various environmental conditions: A critical review', *Journal of Reinforced Plastics and Composites*, vol. 35, viewed 10 May 2021,

<https://www.researchgate.net/publication/283537423_Durability_and_prediction_models_of_fiber-reinforced_polymer_composites_under_various_environmental_conditions_A_critical_review>.

Wang, Y, Han, Q, de Vries, B & Zuo, J 2016, 'How the public reacts to social impacts in construction projects? A structural equation modeling study', *International Journal of Project Management*, vol. 34, no. 8, pp. 1433-48, viewed 13 May 2021,

<<https://www.sciencedirect.com/science/article/pii/S026378631630059X>>.

Wu, YF 2009, 'The structural behavior and design methodology for a new building system consisting of glass fiber reinforced gypsum panels', *Construction and Building Materials*, vol. 23, no. 8, pp. 2905-13, viewed 11 March 2021,

<<https://www.sciencedirect.com/science/article/pii/S0950061809000671>>.

Xiao, Y, Li, Z & Wang, R 2015, 'Lateral Loading Behaviors of Lightweight Wood-Frame Shear Walls with Ply-Bamboo Sheathing Panels', *Journal of Structural Engineering*, vol. 141, p. B4014004, viewed 30 November 2020, <<https://ascelibrary.org/doi/full/10.1061/%28ASCE%29ST.1943-541X.0001033>>.

Zaman, A, Gutub, SA & Wafa, MA 2013, 'A review on FRP composites applications and durability concerns in the construction sector', *Journal of Reinforced Plastics and Composites*, vol. 32, no. 24, pp. 1966-88, viewed 8 May 2021, <<https://doi.org/10.1177/0731684413492868>>.

Appendix A: Project Specification

ENG4111/4112 Research Project

Project Specification

For: Saxon Xeros

Title: Comparative Evaluation of the In-Plane Shear Behaviour of GFRP Composite Wall Systems With and Without Window Openings

Major: Civil Engineering

Supervisors: Dr. Allan Manalo

Sponsorship: Wagners Composite Technologies Ltd.

Enrollment: ENG4111 – EXT S1, 2021
ENG4112 – EXT S2, 2021

Project Aim: To investigate the lateral behaviour of a composite wall system under in-plane shear loading, and to analyse the effects of the window openings.

Programme: Version 2, 13th March 2021

1. Undertake research to establish the potential benefits and limitations of using GFRP materials in civil applications such as composite walls and prefabricated construction
2. Establish the gap in research of GFRP wall behaviour when subject to in-plane shear by reviewing previous experimental work on in-plane shear testing of walls and the effect of openings on composite wall behaviour when subject to in-plane shear
3. Develop an experimental program to assess the in-plane shear behaviour of single-panel walls constructed of GFRP frame and sheathing and undertake testing
4. Process and analysis experimental data and draw conclusions by comparison with previous experimental work, noting aspects such as strength, stiffness, failure mode
5. Review previous work undertaken on finite-element modelling (FEM) of composite walls
6. Develop FEMs in Strand7 of the test walls with and without an opening, and calibrate the FEM by comparing the model to the experimental results
7. Undertake a parametric study using the FEM to analysis the effect of openings on panel behaviour by varying opening location and size
8. Review the FEM results and evaluate how openings affect the behaviour of the panel

If time and resource permit:

9. Develop additional FEMs by varying sheathing parameters such as thickness and strength characteristics
10. Evaluate FEM results and assess how these sheathing parameters affect walls in in-plane shear

Student

Saxon Xeros

Supervisor

Allan Manalo

Appendix B: Risk Assessment

This project consisted of experimental testing of full-size wall panels in an industrial shed environment. Additionally, the GFRP is a hazardous material and can cause serious harm if it gets into the eyes, mouth, or respiratory system. As such, there was inherent safety risks associated with this project and a risk assessment was required to assess and mitigate the hazards to ensure the project was completed safely. A Risk Management Plan (RMP) for the experimental work was undertaken and is provided below.

Safety Risk Management Plan	
 UNIVERSITY OF SOUTHERN QUEENSLAND	University of Southern Queensland USQ Safety Risk Management System
Print View	
Version 2.0	
Risk Management Plan ID: RMP_2021_5570	Status: <i>Draft</i>
Current User: i:0#.w usq\	Author: i:0#.w usq\
Supervisor: i:0#.w usq\crowellw	Approver: i:0#.w usq\manalo
Assessment Title: GFRP wall testing - In-plane shear - single panel - ENG4111/ENG4112	Assessment Date: 1/02/2021
Workplace (Division/Faculty/Section): 204060 - School of Civil Engineering and Surveying	Review Date: 24/05/2021 (5 years maximum)
Approver: Allan Manalo	Supervisor: (for notification of Risk Assessment only) Wayne Crowell
Context	
DESCRIPTION:	
What is the task/event/purchase/project/procedure?	Testing of GFRP walls in in-plane shear
Why is it being conducted?	Experimental component of research project
Where is it being conducted?	P11 - University of Southern Queensland, Toowoomba Campus
Course code (if applicable)	ENG4111/ENG4112 Chemical Name (if applicable)
WHAT ARE THE NOMINAL CONDITIONS?	
Personnel involved	Arvind Sharda, Alan Manalo
Equipment	Testing frame, Hydraulic jack (manual), Floor trolley, Hand tools, Glue, Acetone, Bolts and washers, Computer equipment, Strain gauges and wiring
Environment	P11, industrial shed
Other	
Briefly explain the procedure/process	Apply strain gauges to panel with glue, using acetone to clean beforehand. Lift wall panel into place and bolt down onto supporting beam, set up lateral supports. Apply lateral, in-plane load with manual hydraulic jack and take measurements. Load until failure. Unbolt wall and lift down. Repeat for other walls
Assessment Team - who is conducting the assessment?	
Assessor(S):	Allan Manalo
Others consulted: (eg elected health and safety representative, other personnel exposed to risks)	

Risk Matrix					
Probability	Consequence				
	Insignificant No Injury 0-\$5K	Minor First Aid \$5K-\$50K	Moderate Med Treatment \$50K-\$100K	Major Serious Injury \$100K-\$250K	Catastrophic Death More than \$250K
Almost Certain 1 in 2	M	H	E	E	E
Likely 1 in 100	M	H	H	E	E
Possible 1 in 1,000	L	M	H	H	H
Unlikely 1 in 10,000	L	L	M	M	M
Rare 1 in 1,000,000	L	L	L	L	L

Recommended Action Guide

Extreme:	E= Extreme Risk – Task MUST NOT proceed
High:	H = High Risk – Special Procedures Required (Contact USQSafe) Approval by VC only
Medium:	M= Medium Risk - A Risk Management Plan/Safe Work Method Statement is required
Low:	L= Low Risk - Manage by routine procedures.

Risk Register and Analysis												
Step 1	Step 2	Step 2a	Step 2b	Step 3			Step 4	Step 4				
Hazards: From step 1 or more if identified	The Risk: What can happen if exposed to the hazard without existing controls in place?	Consequence: What is the harm that can be caused by the hazard without existing controls in place?	Existing Controls: What are the existing controls that are already in place?	Risk Assessment: Consequence x Probability = Risk Level			Additional Controls: Enter additional controls if required to reduce the risk level	Risk assessment with additional controls: Has the consequence or probability changed?				
				Probability	Risk Level	ALARP		Consequence	Probability	Risk Level	ALARP	
<i>Example</i>	Working in temperatures over 33°C	Heat stress/heat stroke/exhaustion leading to serious personal injury/death	catastrophic	Regular breaks, chilled water available, loose clothing, fatigue management policy.	possible	high	No	temporary shade shelters, essential tasks only, close supervision, buddy system	catastrophic	unlikely	mod	Yes
1	Panel falling ...	Personal injury	Moderate	Panel weight approx 35kg PPE to be worn including steel cap boots, hard-hat, safety glasses, gloves, and long pants and sleeves.	Unlikely	Me...	<input checked="" type="checkbox"/>					<input type="checkbox"/>
2	Falling equip...	Personal injury	Moderate	Tools to be placed on benches when not in use. Personnel to avoid working beneath each other in case of dropping tools. PPE to be worn including steel cap boots, hard-hat, safety glasses, gloves, and long pants and sleeves.	Unlikely	Me...	<input checked="" type="checkbox"/>					<input type="checkbox"/>
3	Electrical haz...	Electrocution	Moderate	Ensure all equipment has current safety tags. Do not use damaged equipment, inspect before use. Do not leave leads or electrical equipment in areas that it may be damaged.	Rare	Low	<input checked="" type="checkbox"/>					<input type="checkbox"/>
4	GFRP dust m...	Eye or respiratory system injury	Minor	Wear mask and eye protection if dust or fibres present.	Rare	Low	<input checked="" type="checkbox"/>					<input type="checkbox"/>
5	Use of glue a...	Eye and skin injury	Minor	Wear eye protection and gloves. Clean hands after use	Rare	Low	<input checked="" type="checkbox"/>					<input type="checkbox"/>
6	COVID 19	Sickness	Moderate	Utilize appropriate social distancing, clean and sanitize hands regularly, do not attend if sick or feeling unwell.	Possible	High	<input type="checkbox"/>	Undertake precautions in accordance with government and University guidelines	Moderate	Unlikely	Me...	<input checked="" type="checkbox"/>
7	Handling of s...	Personal injury	Minor	Use appropriate manual lifting technique. Wear gloves, hard hat, steel cap boots, long pants and sleeves.	Unlikely	Low	<input checked="" type="checkbox"/>					<input type="checkbox"/>

8	Flying debris	Eye injury and cuts and bruises	Minor	PPE to be worn including steel cap boots, hard-hard, safety glasses, gloves, and long pants and sleeves.	Rare	Low	<input type="checkbox"/>								
9	Trips and falls	Personal injury	Minor	No working at heights. Use available step ladders if required. Keep work area clean and clear of equipment, cables, and tools.	Rare	Low	<input type="checkbox"/>								

Step 5 - Action Plan (for controls not already in place)					
	Additional Controls:	Exclude from Action Plan: (repeated control)	Resources:	Persons Responsible:	Proposed Implementation Date:
6	Undertake precautions in accordance with government and University guidelines	<input checked="" type="checkbox"/>			

Supporting Attachments
<input type="checkbox"/> No file attached

Step 6 – Request Approval	
Drafters Name: <input type="text" value="Saxon Xeros"/>	Draft Date: <input type="text" value="24/05/2021"/>
Drafters Comments: <input type="text"/>	
Assessment Approval: All risks are marked as ALARP	
Maximum Residual Risk Level: Medium - Cat 4 delegate or above Approval Required	
Document Status:	<input type="text" value="Draft"/>

Step 6 – Approval	
Approvers Name: <input type="text" value="Allan Manalo"/>	Approvers Position Title: <input type="text"/>
Approvers Comments: <input type="text"/>	
<i>I am satisfied that the risks are as low as reasonably practicable and that the resources required will be provided.</i>	
Approval Decision: <input type="text"/>	Approve / Reject Date: <input type="text"/>
Document Status: <input type="text" value="Draft"/>	

